Mercury in Till and Bedrock, Kejimkujik National Park Area, Nova Scotia

Belinda M. Culgin

Submitted in Partial Fulfillment of the Requirements
for the Degree of Bachelor of Science, Honours
Department of Earth Sciences
Dalhousie University, Halifax, Nova Scotia
April 2002

Dalhousie University

Department of Earth Sciences
Halifax, Nova Scotia
Canada B3H 3J5
(902) 494-2358
FAX (902) 494-6889

DATE May 7, 2002

AUTHOR Belinda M. Culgin

TITLE Mercury in Till and Bedrock, Kejimkujik National Park Area, Nova Scotia

Degree BSc Convocation May Year 2002

Permission is herewith granted to Dalhousie University to circulate and to have copied for non-commercial purposes, at its discretion, the above title upon the request of individuals or institutions.

Signature of Author

Abstract

Loons in Kejimkujik National Park (KNP), southwestern Nova Scotia, have the highest levels of mercury (Hg) concentration in blood of any loon population in North America. For the past several years, a multi-disciplinary team of research scientists has been attempting to identify the potential Hg source(s) and process(es) responsible for the anomalous Hg levels. This thesis is a geochemical component of this research involving the collection and geochemical analysis of till and bedrock samples to quantify the geogenic contribution of Hg from glacial sediments and bedrock sources of the Meguma Supergroup. Health Canada provided funding for the project through the Toxic Substance Research Initiative (TSRI).

A total of 32 C horizon till samples were collected at 100 to 200 m intervals from three NW-SE transects that cross the inferred contact between the Halifax and Goldenville Groups immediately south of the KNP boundary. Samples were collected at depths ranging from 70 to 120 cm. Geochemical results for the <63 microns size fraction were determined by Cetac CV-AA and indicate Hg ranges from 6.6 ppb to 151.5 ppb (mean = 37.7 ppb). Nine slate and greywacke bedrock samples were collected along the same transects. Geochemical results for the <105 microns size fraction of the bedrock samples, also determined by Cetac CV-AA, had Hg values ranging from 0.2 ppb to 3.4 ppb (mean = 2.37 ppb). Strict QA/QC protocols were followed in the collection, preparation, and analysis of all samples.

Results show that the Hg concentrations of slate till (mean = 40.8 ppb) and greywacke till (mean = 32.4 ppb) are quite comparable. Till Hg values are similar to reported values within the Park. Log-probability plots indicate there is only one geologic control affecting Hg values such as lithology or mineralogy. Mercury values in the bedrock samples are low but comparable to other values in KNP. There is no apparent correlation between Hg and the Goldenville - Halifax Transition Zone (GHT). Field mapping, clast identification and counts and total field magnetic survey indicate that the geologic boundary is 500m to 1000m further north and the areal extent of the Halifax Group is smaller than reported on recent geologic maps.

Table of Contents

Table of Figures

Table of Tables

Acknowledgements

I wish to thank my thesis advisor Don Fox for his constant support, guidance and laughter that made this thesis more enjoyable. Don was always there for assistance throughout the year despite his hectic schedule and made this year so much easier.

I would like to thank Terry Goodwin for the immeasurable support, attention to detail and enthusiasm for the project. I could not have asked for a better field partner whose great ability to teach has allowed me to gain valuable knowledge in geochemical techniques. He always took the time to explain and assist whenever it was needed. I would also like to thank Paul Smith for his financial support and assistance throughout this project.

Special thanks to Marcos Zentilli for his kindness, patience and encouragement that he extends to all his students. He genuinely cares and takes that extra step to provide support throughout this year.

Thank you to my friends and family for their support through this year as well as years past. Finally I would to thank Mike Pickett for his encouragement that instills confidence that I can accomplish anything.

Chapter 1: Introduction

1.1 Objective and General Statement

Mercury is a heavy metal that is easily transformed between liquid and gaseous forms. Mercury in the environment can originate from both naturally occurring and anthropogenic sources. It can methylate through biological processes to a particularly toxic organic form called methyl mercury that bioaccumulates in the food chain. Both methyl mercury and inorganic elemental mercury are readily taken into the blood stream through ingestion and inhalation and are capable of crossing the brain blood barrier allowing the toxins to accumulate in the nerve tissue (Nadakavukaren, 2000). This neurotoxin leads to deformations and reproduction problems in humans as well as wildlife (CCME, 1998, Krabbenhoft *et al.*, 1997, http). In the 1950's and 1960's the harmful effects of mercury became widely recognized. The most notable incident was in Minamata Bay, Japan where the mercury induced neurological disease, Minamata disease gained its name. In the 1950's thousands of people living around the bay developed methyl mercury poisoning through the consumption of contaminated fish and water. Mercury dumping by chemical companies surrounding the bay polluted the waters for years before the harmful effects were recognized and diagnosed (Nadakavukaren, 2000, Ebinghaus, *et al.*, 1999).

Kejimkujik National Park, in southwest Nova Scotia, is the focus of a multidisciplinary Toxic Substance Research Initiative (TSRI) program investigating possible Hg sources and processes in the Park area. Previous research by the Canadian Wildlife Services in 1995 determined heightened levels of Hg in the blood of the common loon (*Gavia immer*) (Burgess *et al.*, 1998). Burgess *et al.* (1996 and 1998, http)

has determined that the blood of loons in Kejimkujik National Park have levels of Hg almost three times higher than other loon populations tested across North America. In 1999 a multidisciplinary research group involving biologists, geologists, limnologists, chemists, and meteorologists began examining the interrelationship between the atmosphere, geosphere, hydrosphere, and biological communities to investigate the complex cycling of mercury in aquatic and terrestrial environments (Rencz, 1999). Part of the geochemical component of the project includes investigating mercury concentrations in the tills and rocks in and around the Kejimkujik National Park area. This thesis investigates the relationship of naturally occurring mercury concentrations in till and bedrock of the Meguma Supergroup including the Goldenville – Halifax Transition Zone (GHT) immediately south of Kejimkujik National Park.

1.2 Purpose and Scope

In order to better understand the relationships between mercury and geology within the Kejimkujik National Park area, this thesis examines mercury concentrations in the till and rocks over the Meguma Supergroup. In order to achieve this, the study was divided into three components: 1) till and rock geochemical sampling/analysis, 2) bedrock and surficial mapping identifying the stratigraphic units and 3) detailed ground magnetic survey to accurately locate the geological boundaries.

1.3 Study Area

The study area is located on N.T.S mapsheet 21A/06 immediately south of the Kejimkujik National Park boundary in the Low Landing area just north of Lake

Rossignol covering approximately 25 km^2 (Figure 1.1 and 1.2). Three NW-SE transects ranging from 2.3 km to 3.7 km in length follow along logging roads crossing the inferred Halifax-Goldenville Group contact. They were chosen on the basis of their location and accessibility. Mixed mature deciduous and coniferous forest dominate the area with minor recent clear cutting characterizing parts of the study area. The extensive till veneer is relatively thin (~3m thick) thus limiting outcrop exposure (<2%) to logging roads and stream sections. In addition to the logging companies, recreational campers, cottagers and boaters frequent the area.

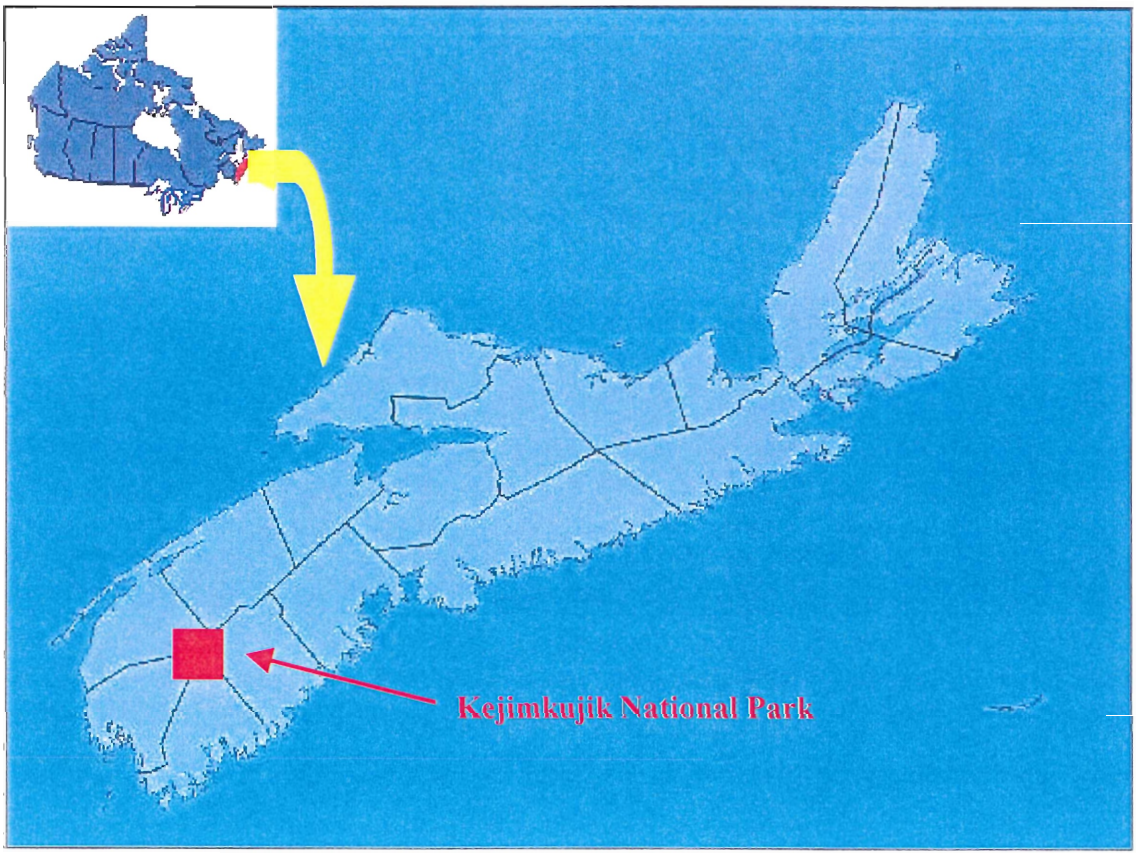

Figure 1.1 Kejimkujik National Park in Southwestern Nova Scotia.

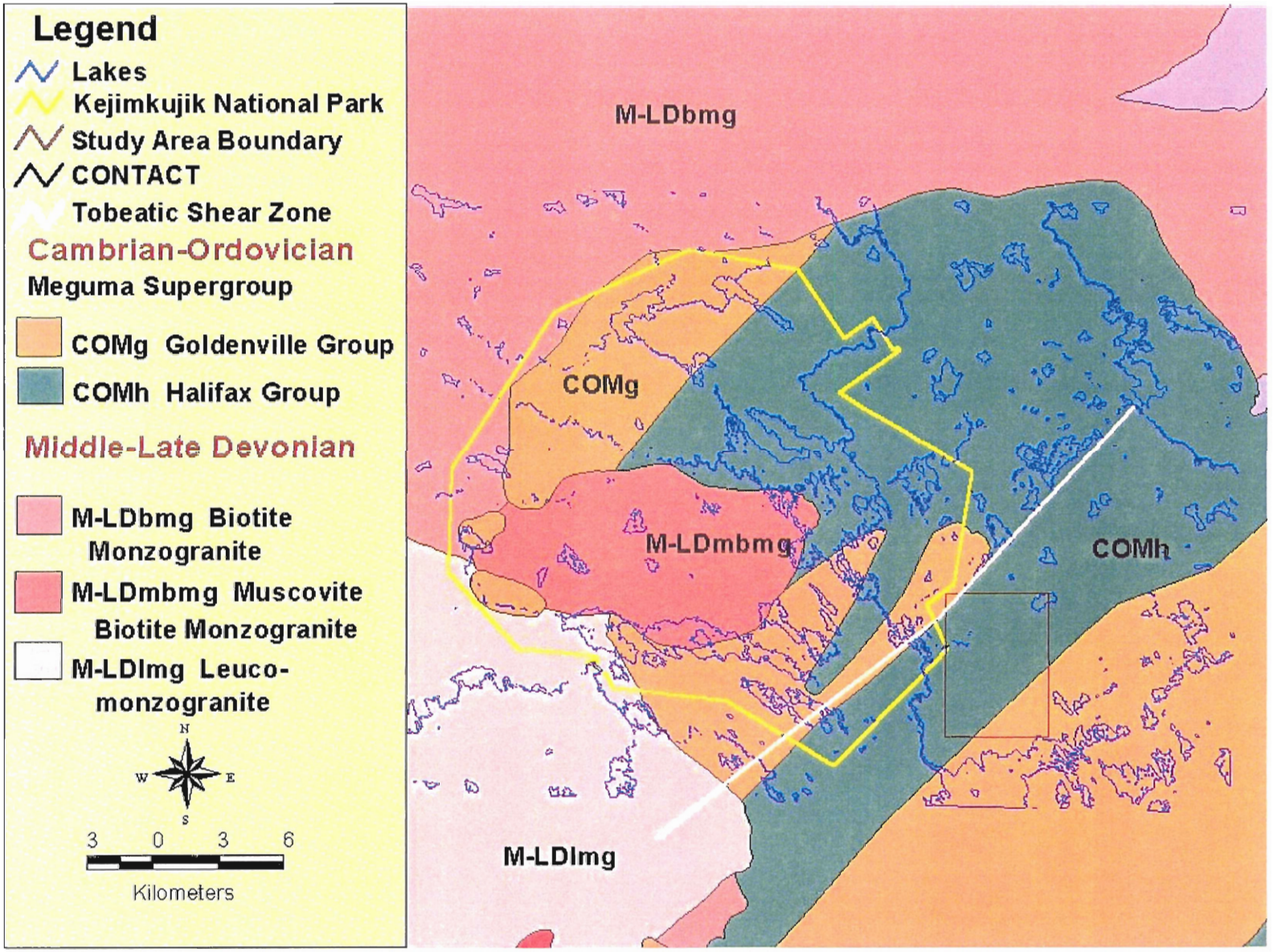

Figure 1.2 Kejimkujik National Park boundary (yellow) and study area south of park. (generated using ArcView 3.2)

1.4 Methodology

During the summer of 2001 under the supervision of Terry Goodwin, Project Geochemist for Nova Scotia Department of Natural Resources, a geochemical, geological and geophysical field program of the study area (Figure 1.2) was completed involving (1) till and bedrock sampling, (2) geological mapping and (3) total field ground magnetics. Thirty two C horizon till samples were collected every 100m to 200m from depths ranging from 70cm to 120cm along logging roads. In addition to the till samples 9 rock samples were collected from exposed slate and greywacke outcrops along the same transects. Total field magnetic readings were acquired at 12.5 m spacing along each of the three traverses crossing the inferred contact.

The till (<63 microns size fraction) and rock samples (<105 size fraction) were analyzed for Hg and 34 additional elements. Particular attention was given to quality control protocols including the insertion of certified standards, preparation splits and field duplicates during the collection, preparation and analysis of the till and rock samples.

1.5 Previous Work

Environment Canada Canadian Wildlife Services (CWS) began investigating mercury levels in 24 Common Loons on 12 lakes (including Kejimkujik National Park) across Nova Scotia and New Brunswick in August 1995 (Monitoring Mercury Levels, 1996, http). Previous monitoring by the CWS in 1988 concluded that reproductive success rates of the common loon were about half of what was required to maintain a growing population (Kerekes *et al.*, 1995). Results of the CWS study in 1995 showed that common loons in Kejimkujik National Park had the highest concentrations (5.7 ppm

Hg, wet wt.). Hg in blood samples from 23 other loons located in other areas of Nova Scotia and New Brunswick were as high as 2.3 ppm (Kerekes *et al.*, 1995). Loons migrate to sea coasts in the winter and rear their young on fresh water lakes in the spring where the young feed on the lake fish. Since similar concentrations of mercury were identified in the adult and their offspring, it was concluded that the nesting lakes in Kejimkujik National Park contained the fish with high mercury concentrations (Monitoring Mercury Levels, 1996, http). Comparing common loons throughout North America, Evers *et al.* (1998) and Burgess *et al.* (1998) concluded that the loons of Kejimkujik National Park have more than twice the Hg concentration in their blood than the other areas studied (Figure 1.3).

In 1997 Beaucamp *et al.* (1998) measured the total gaseous mercury (TGM) concentrations in ambient air and precipitation at sites across Canada including Kejimkujik National Park. The study concluded that the average TGM concentrations in the ambient air (1.49 ng/m^3) and the precipitation (9.4 ng/L) in the park compared similarly with the other study areas. Overall the study concluded that the atmospheric Hg levels of Kejimkujik Park are in the low to moderate range compared to other studied areas throughout North America (Beaucamp *et al.*, 1998). Figure 1.4 outlines equivalent units of measure.

A study by Clair *et al.* (1998) investigated Hg concentrations in lakes throughout the Atlantic region. The mean concentration for Kejimkujik National Park was 3.30 ng/L which was the average concentration of the areas studied. Rutherford *et al.* (1998) and d'Entremont *et al.* (1998) concluded that concentrations of Hg in the fish (Brook Trout,

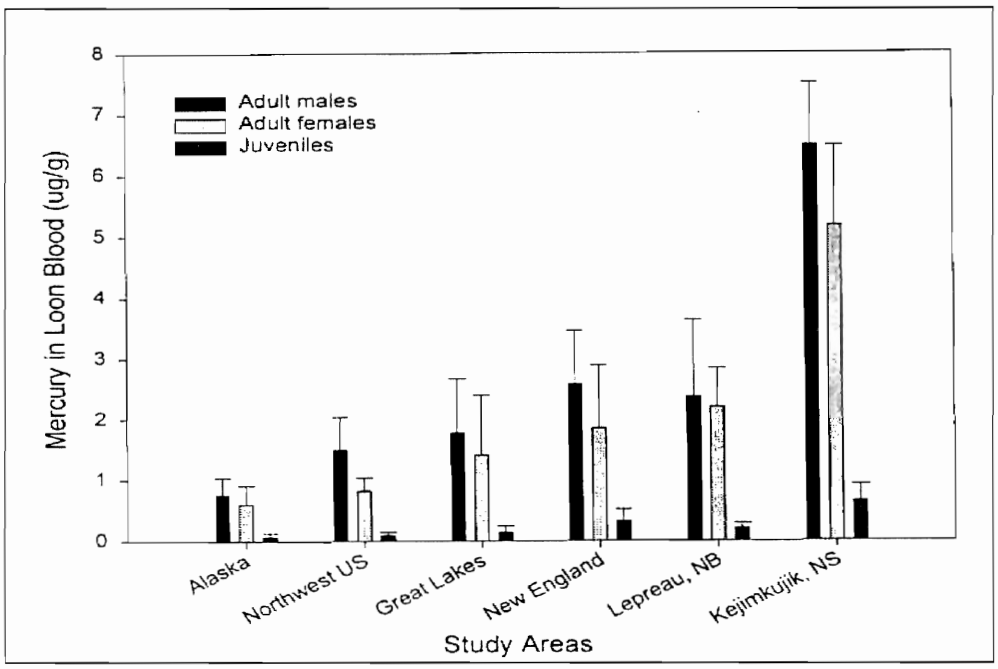

Figure 1.3 Mean mercury concentrations in the blood (+1 S.D.) of adult and juvenile loons within different regions of North America. North American data from Evers *et al.* (1998). (Burgess *et al.*, 1998)

Unit of Measure	Equivalent Unit of Measure
ug/l	parts per billion on weight to volume basis
mg/l	parts per million on weight to volume basis
ug/g	parts per million on weight to weight basis
mg/kg	parts per million on weight to weight basis

Figure 1.4 Conversion table of equivalent units of measure

White Perch and Yellow Perch) ranged from 0.05 ppm to 2.30 ppm and the majority of fish tested exceeded the Health Canada safe consumption guidelines of 0.5 ppm.

In 1999 a multidisciplinary team of researchers obtained three years of funding under the Toxic Substance Research Initiative (TSRI) program to investigate the origin and complex cycling of mercury in Kejimkujik National Park. The team of researchers compiled and organized existing information and targeted areas of importance to identify sources and processes in the park area that could contribute to the high mercury levels (Rencz, 2000). Table 1.1 indicates the range of Hg values determined in the most recent report published in 2000. These results indicate the majority of values in the vegetation, soils, rocks and water are not unusually high in Hg (Rencz, 2000). Figure 1.5 summarizes the previous and current work performed within the park. Smith (2000) investigated the relationship of Hg concentrations of various bedrock lithologies within the park and surrounding area (Figure 1.6). The average Hg concentration from the 146 bedrock samples is 3.3 ppb. Further studies by Page (2001) indicate high values in the biotite rich rocks (monzogranite) as high as 9.6 ppb but the average Hg values in the bedrock is 3.65 ppb quite similar to results found by Smith (2000). A study by Sangster *et al.* (2001) of 685 samples concludes average Hg concentrations of bedrock range from 0.80 ppb to 35.9 ppb (Figure 1.7).

1.6 Organization of the Thesis

The thesis is divided into 5 chapters. The introductory chapter outlines the importance of the project, general methodology, and a brief history of the research completed in the

Media	Number of Samples	Hg (total)
White Pine (leaf)	91	21 - 46 ppb
Red Maple (leaf)	104	7 – 85 ppb
Soils (Ao horizon)	28	123 – 388 ppm
Soils (Ah horizon) >63 u < 2mm	39	 56 – 460 ppm 76 – 466 ppm
Soil (C horizon) >63 u < 2mm	39	 15 – 304 ppm 6 – 184 ppm
Rocks	117	0.04 – 12.5 ppb
Water	50	22 – 10 ppt

Table 1.1 Mercury concentration of various media tested with in the Kejimkujik National Park (modified from Rencz *et al.*, 2000)

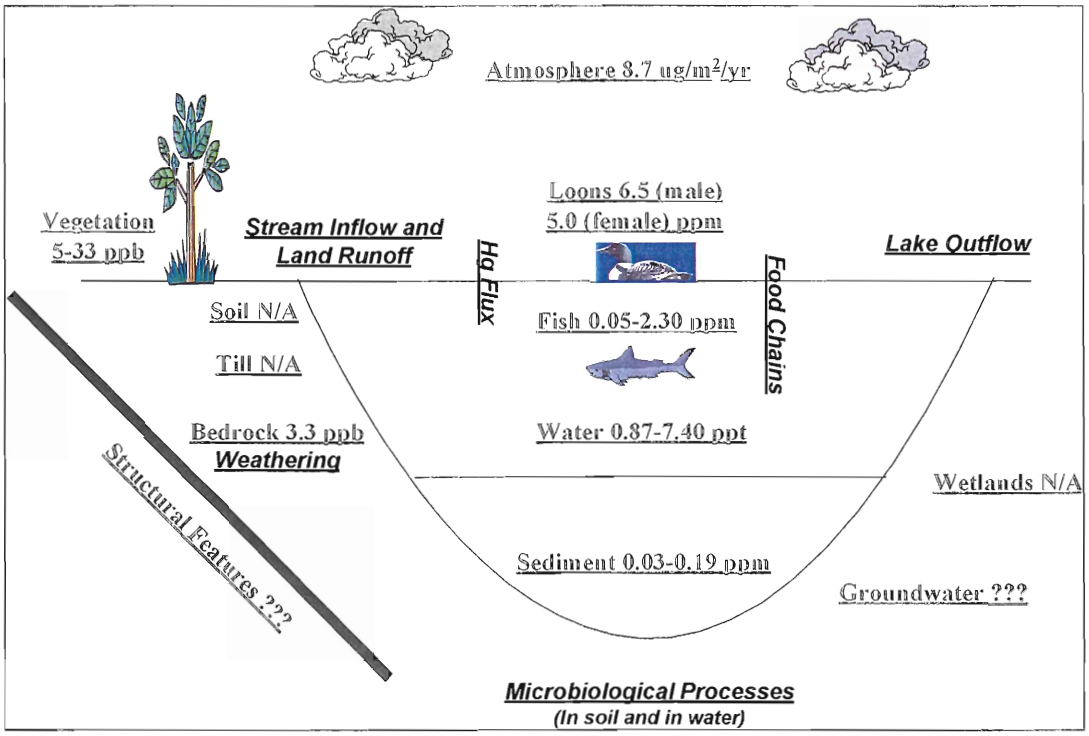

Figure 1.5 Summary of Hg concentrations in Kejimkujik National Park to date. Hg processes are italicized and sources are in Times New Roman (Figure taken from Page, 2001)

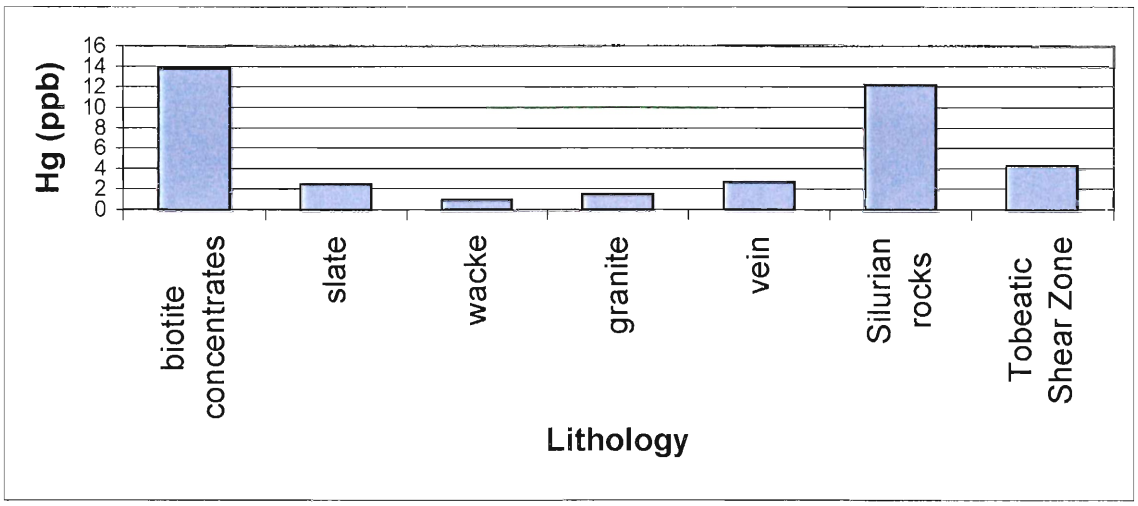

Figure 1.6 Average mercury concentrations of different lithologies in Kejimkujik National Park and surrounding areas (modified from Smith, 2000)

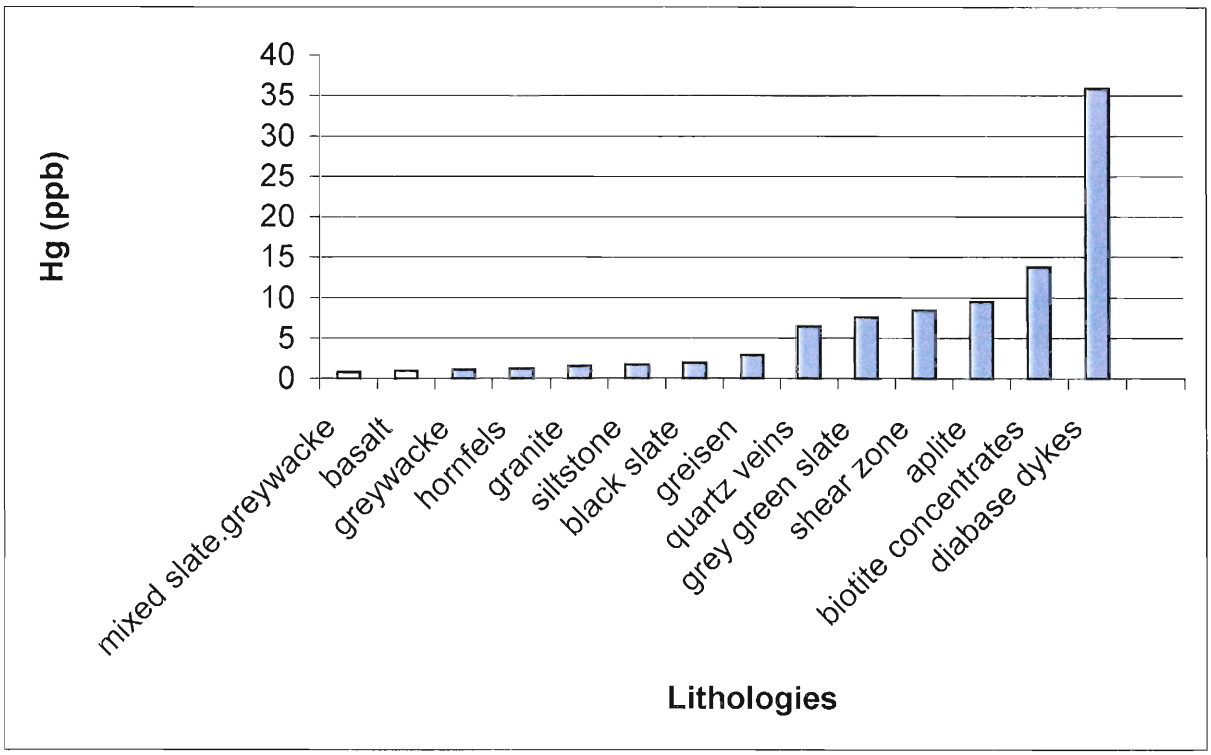

Figure 1.7 Average Hg concentrations of bedrock within KNP area. (modified from Sangster *et al.*, 2001)

area. Chapter 2 describes the various types and transformations of mercury and its relationship within the environment. The following chapters describe the local and regional surficial and bedrock geology, geological mapping and geophysical analysis of the area. Chapter 4 focuses on the till and rock sampling procedures and investigates analytical results. The chapter is divided into two sections emphasizing till and rock geochemistry, respectively. Each section summarizes the field methods, sampling/ analytical procedures, results and discussion. Chapter 5 integrates the four previous chapters drawing conclusions based on the results from the geological, geophysical and geochemical research. Recommendations are suggested for future work.

Chapter 2: Mercury in the Environment

2.1 Introduction

Mercury is found in natural sources such as rocks, biota, soils, and water but since industrialization, anthropogenic mercury far exceeds the presence of natural mercury (Ebinghaus *et al.*, 1999). About 930 tons of gaseous mercury is drifting in the world's atmosphere at any given time (Internationella Miljoinstitutet, 1997, http). It is estimated that since 1890, 200,000 tons of Hg has been emitted from anthropogenic sources (Ebinghaus *et al.*, 1999). All substances undergo cycling and transformations in the environment and this is especially important for mercury. Mercury exists in several physical states and chemical forms under normal environmental conditions and has the ability to undergo biological transformations. These characteristics contribute to the complexity of how Hg interacts within the environment. Thus, it is imperative to consider the physical changes, geochemical reactions and biochemical exchanges of Hg in order to fully understand transport and fate within the environment (Mercury: Chapter 2, 1996, http). This chapter outlines the different forms and interactions of mercury in the environment and its role in a geological context.

2.2 Mercury Forms: General Overview

Mercury is a heavy metal that is commonly found in three forms including uncharged elemental mercury (Hg^0), inorganic or divalent mercury (Hg^{2+}), and organic or methyl mercury (CH_3Hg^+ or abbrev. MeHg) which is most prevalent to processes within the environment (Ebinghaus *et al.*, 1999; Mercury: Chapter 2, 1996, http). Elemental

mercury is the most common form found in the atmosphere. It readily volatilizes at low temperatures (~ 40 °C) from its liquid state, it is very stable and can travel long distances in the atmosphere, although elemental Hg is not commonly found in the soil and water. Unlike elemental mercury, inorganic mercury (Hg^{2+}) is found quite regularly in the soil and surface waters. Inorganic Hg is more water-soluble than elemental mercury thus allowing it to persist in these areas. Inorganic mercury can be methylated by microorganisms in water, soils and sediments to form the toxic methyl mercury. Methyl mercury is most prevalent in the tissues of humans and animals. Methyl mercury has the ability when ingested to pass from the blood into the brain entering the tissues where it can eventually cause nerve damage (Toxicological Profile of Mercury, 2001). The accumulation of methyl mercury in the tissues of humans and animals magnifies in concentration (bioaccumulates) as it moves up the food chain (Mercury: Chapter 2, 1996, http). Figure 2.1 outlines the cycling of the three forms of mercury within a remote watershed. The three forms of mercury discussed above are the basis of mercury distribution within nature (Ebinghaus *et al.*, 1999).

2.3 Transformations and Cycling in the Environment: Oxidation and Reduction

There are two predominant types of chemical transformations that mercury undergoes. These include oxidation-reduction and methylation-demethylation (see Figure 2.2). These common mercury transformations involve changes in valence states. In oxidation the uncharged elemental mercury is converted to a higher valence state. Reduction is the reverse transformation where the addition of electrons form elemental

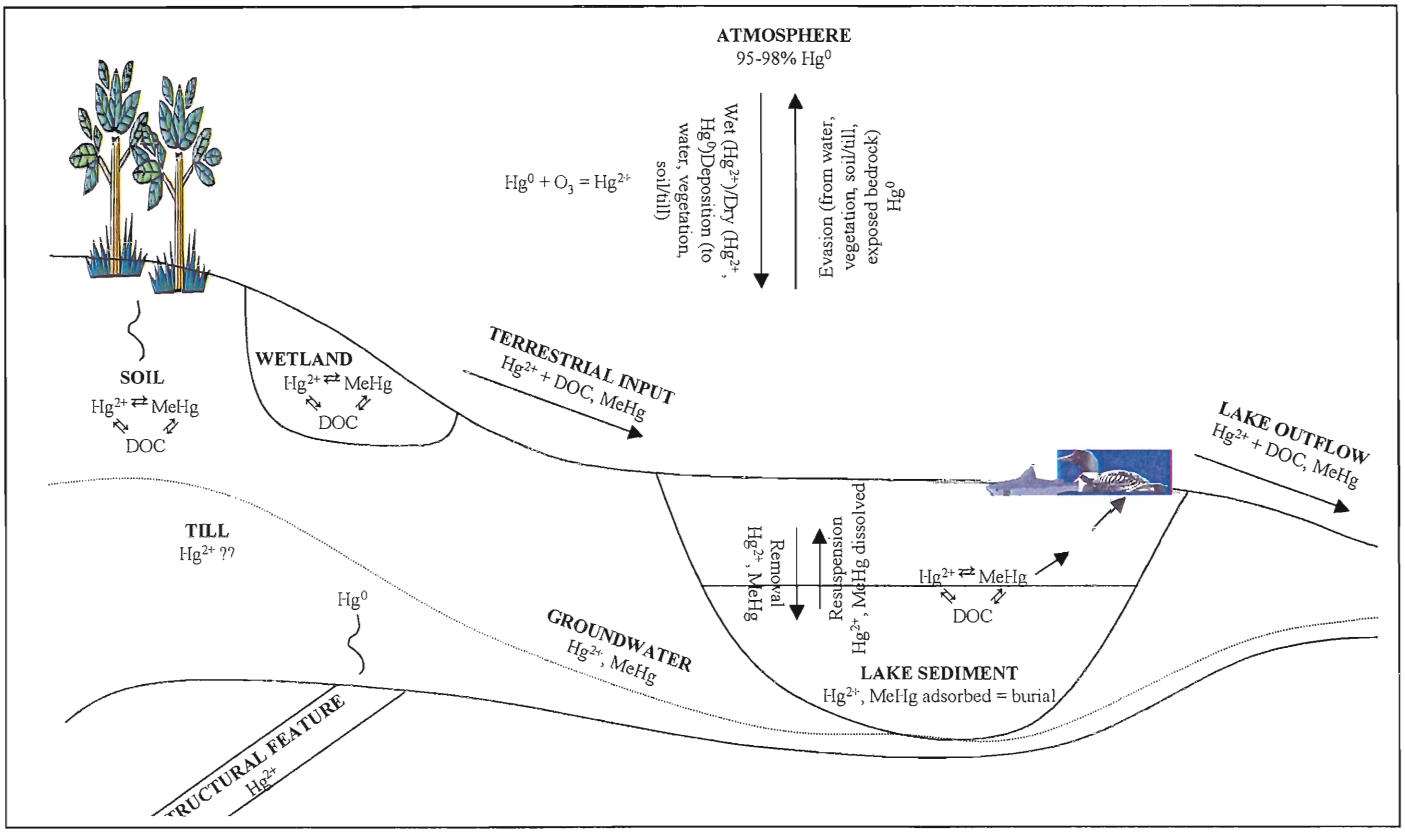

Figure 2.1 Overview of Hg cycling in a remote water shed (DOC - dissolved organic content). (Taken from Page, 2001)

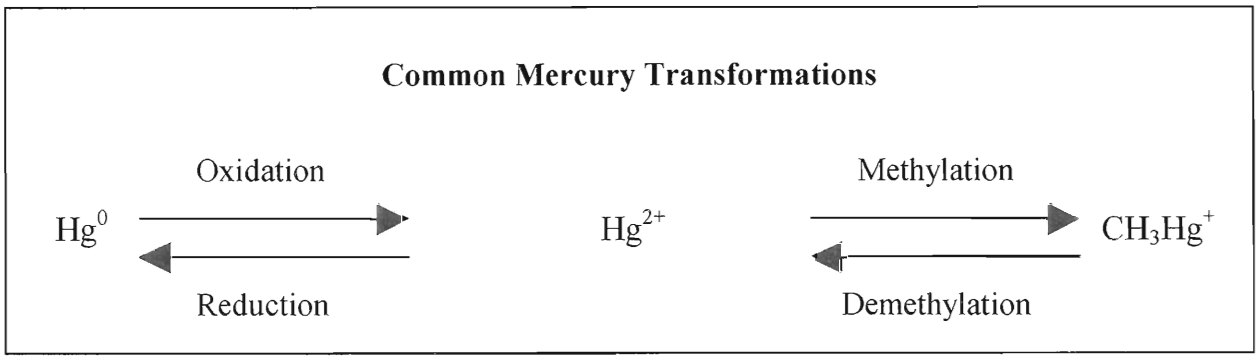

Figure 2.2 Common Hg transformations in the environment. (Mercury: Chapter 2, 1996, http.)

mercury (Mercury: Chapter 2, 1996, http). During methylation an organic "methyl group" (hydrocarbon group – CH_3) is added to elemental mercury forming methyl mercury (Figure 2.2). Demethylation is the reverse reaction where the methyl group is lost. Demethylation is poorly understood but methylation and demethylation can occur by biotic and abiotic processes (Mercury:Chapter 2, 1996, http; Parkman 1994). Methylation is the most significant transformation in living organisms and biotic processes (conversion by microorganisms) play an important role during the methylation process converting Hg^{2+} to $HgCH_3$.

Methylation in water and sediments is affected by the amount of dissolved oxygen present, the amount of sulfur present, the pH of the water and sediments, and the presence of clay and organic material (Mercury: Chapter 2, 1996). Sulphate reducing bacteria in soil, sediment and water are the main microorganisms involved during methylation (Branfireum *et al.*, 1999). Oxygen depleted areas of lakes including lake sediments are the most common environments for methylation to occur. Low pH is associated with an increase in methylation in both water and soil entering lakes, ponds, or oceans through erosion, rainfall and leaching (Mercury: Chapter 2, 1996, http; Page, 2001). Increased levels of elemental mercury in the environment can lead to an increase in levels of methyl mercury through methylation, which is taken up by organism through ingestion and absorption. Mercury is persistent and not biodegradable, hence accumulates in the environment. The combined qualities of environmental persistence, ability to bioaccumulate and toxicity make mercury very difficult to understand in the environment (Mercury: Chapter 2, 1996, http).

2.4 Sources: Natural and Anthropogenic

Mercury can originate from anthropogenic and natural sources. However, because of the interactions of Hg within the environment it is difficult to totally separate what is a natural Hg source or anthropogenic Hg source. Mercury released to the environment naturally is usually in the elemental form from several sources including: (1) the erosion and weathering of minerals and mineral deposits (2) volatilization from the ocean where the Hg source is from the mid ocean ridges and rift systems, (3) volcanic eruptions, and (4) degassing of geological and geothermal fractures (Mercury, Chapter 2, 1996, http).

Anthropogenic sources contribute mercury in the form of Hg^{2+} that is transported in the environment through the water system or in gaseous form. Once the Hg^{2+} has volatilized into the atmosphere it can travel long distances until it is deposited into the water and sediments through precipitation because of its solubility with water (Carpi, 1997). Anthropogenic sources include: (1) the burning of fossil fuels, (2) chemical processing plants, (3) waste incinerators and landfills, (4) metal smelting and refining, (5) mining that exposes Hg containing rock to weathering (6) Hg used in gold mining process, and (7) agriculture (pesticides) (Mercury, Chapter 2, 1996; Rasmussen *et al.*, 1998).

2.5 Geologic Role in Mercury Cycling

Mercury constitutes only 0.08 ppm to 0.5 ppm of the earth's crust making it scarcer than uranium but more plentiful than gold or silver (Mason, 1982; Rasmussen *et al.*, 1998). Several geologic sources such as rocks, soil and till can be important sources of Hg in the natural environment. Research has shown that chemical and physical

weathering along with erosion of bedrock, glacial deposits and soil enriched in mercury increases the methyl mercury concentrations in lake environments and waterways (Rasmussen *et al.*, 1998).

2.5.1 Soil

Mercury in soils is usually in the form of Hg^{2+}, however several forms can be found in the organic layer of soil (Godbold, 1994). Mercury can enter soil from the atmosphere via precipitation, contaminated sites (sewage sludge and landfills), and underlying bedrock and till (Mercury: Chapter 2, 1996, http.). Generally soils are divided up into individual layers referred to as soil horizons including the A horizon (organic litter, humus and leached zone), B horizon (zone of accumulation including clay, hydrous oxides, organic matter) and the C horizon (parent material including glacial sediments or weathering bedrock) (Figure 2.3) (Mason, 1982). The B horizon often has a red-brown to yellow-brown colour from an accumulation of iron oxides while the C horizon is generally gray to olive brown reflecting its unoxidized nature.

Table 2.1 illustrates typical mercury concentrations of soils. As noted above, soils in the A-horizon have increased concentrations relative to the other soil horizons because mercury is strongly bound to the organic matter in the A-horizon. Methyl mercury can be produced abiotically in the A-horizon. If there is a decrease in oxygen or pH or an increase in sulphur levels methyl mercury production will increase (Mercury: Chapter2, 1996, Rogers, 1976, Cocking *et.al.*, 1994). Mercury can remain in soils for a long time but can also be transported by ground and surface water. Studies have indicated that methyl mercury can be mobilized and transported more readily than Hg^{2+} due to weaker

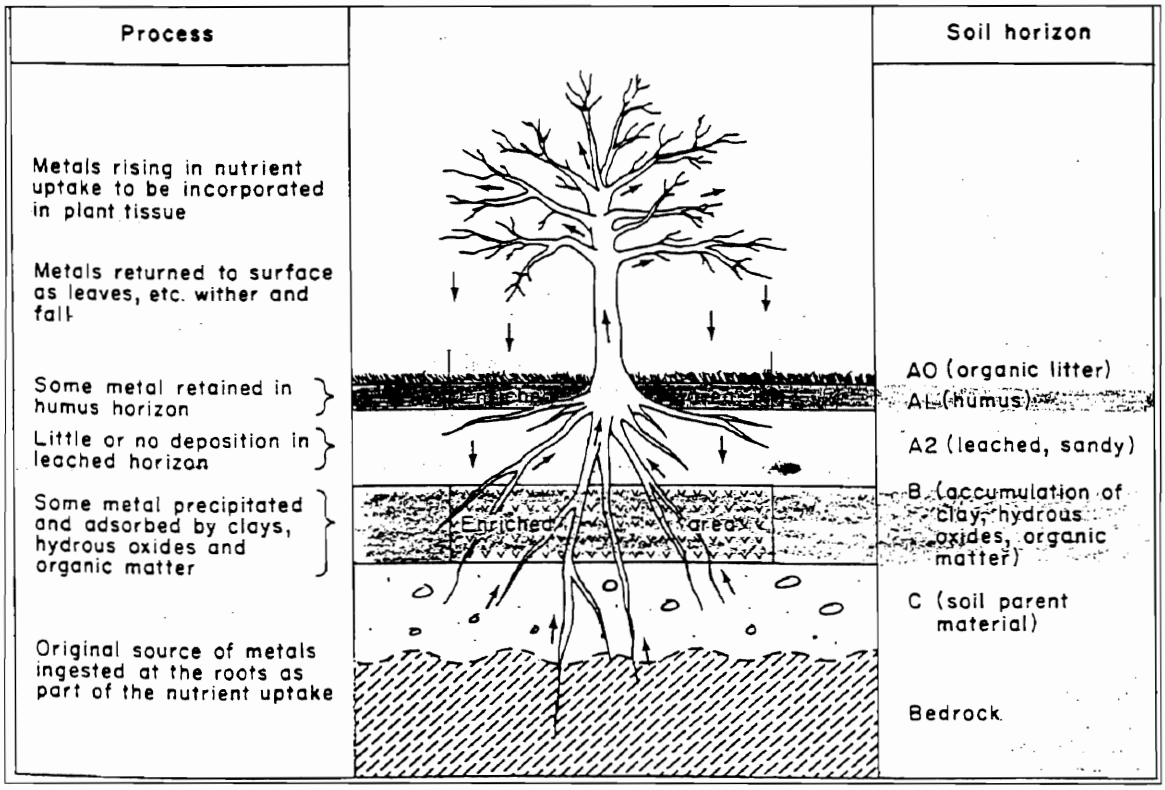

Figure 2.3 Overview of soil horizons A, B and C **(**Ramussen,1996**)**

Description	Range	Mean
(a) Waters (ppb)		
Rainwater	0.05 — 0.48	0.20
Snow	< 0.005 — 0.05	0.01
Stream, river and lake waters	0.01 — 0.10	0.03
Oceans and seas	0.03 — 5.0	0.20
Hot springs and certain mineral waters	< 0.01 — 2.5	0.10
Ground waters	0.01 — 0.10	0.05
Coal-mine, oil-field and other saline waters	0.1 — 230	....
(b) Soils (ppb)		
Soils (arctic, temperate, tropical)	20 — 150	70
Tills, glacial clay, sand, etc.	20 — 100	50
Soils in mineralized belts:		
A horizon	60 — 200	161
B horizon	30 — 140	89
C horizon	25 — 150	96
Weathered crusts (limonitic, lateritic, etc.)	50 — 200	100
(c) Air (ng per m³)*		
Atmosphere	0.2 — 10	....
Atmosphere over mercury deposits	30 — 1600	....
Soil air over mercury deposits	< 1 — 2000	....
Volcanic exhalations (USSR only)	100 — 9600	....
(d) Volcanic Condensates and Precipitates (ppb)		
Condensates	0.2 — 72	....
Precipitates	up to 0.2%	....

Table 2.1 Mercury content of normal waters, soils and air (ppb) (taken from Jonasson and Boyle, 1972)

bonds (Lee *et al.*, 1994 and Mercury: Chapter 2, 1996). Others factors contributing to mobilization include increase in pH, organic poor soils and microbial activity (Cockling, *et.al.*, 1994).

2.5.2 Till

Plouffe (1998) indicates that distribution of metals in surficial sediment is profoundly effected by glacial erosion, transport, and deposition. Glaciers erode the underlying mineralized bedrock resulting in diamicton enriched in metals that is transported in the direction of ice flow and deposited as till (Shilts, 1975; Plouffe, 1998). A zone of metal enrichment in the till is usually noted parallel to the ice flow direction known as a dispersal train (Shilts, 1979; DiLabio, 1990; Plouffe, 1998). The metal concentrations are anomalous near the source and consistently decrease in the direction of ice flow from dilution during glacial transport (Plouffe, 1998). The threshold is the boundary between the anomalous and background concentrations and concentrations above the threshold could be part of the metal dispersal train (Rose *et. al.*, 1976).

Mercury in till (C horizon) is generally considered to be from a geogenic source and not anthropogenic sources such as air borne pollution (Plouffe, 1995). Tills contain relatively little organic matter so methylation of mercury is not likely to occur. Therefore, mercury found in till is in the form of Hg^{2+}. Since Hg is adsorbed in the organic layer of the soil, mercury (Hg^{2+}) found in the till is generally originating from the underlying bedrock (Plouffe, 1998). Jonasson and Boyle (1972) indicate Hg in normal tills generally range from 20 – 100ppb (Table 2.1).

Elevated mercury levels in till are found in association with several types of bedrock mineralization mentioned in section 2.5.3 (Jonasson and Boyle, 1972; Boyle, 1970; Shilts and Coker, 1995). The nature of the bedrock is a determining factor of the amount of material transported during glaciation. For instance, if the bedrock is metamorphosed or faulted it is normally more brittle resulting in increased till with more metal accumulation that could be transported further i.e. a longer dispersal train (Plouffe, 1998). Natural mercury degassing along faults is also a possible source of mercury in the sediments and till (Rasmussen, 1993, Azzaria, 1992). The degassing occurs from high vapour pressure of native mercury that releases mercury gas during faulting (Jonasson and Boyle, 1971, Plouffe, 1998). However mercury in the gaseous state usually migrates and accumulates in the organic matter of the soil as mentioned above (Plouffe, 1998).

Studies by Shilts (1973, 1984, 1995), Nikkarinen *et al.* (1984) and Plouffe, (1995) investigated the partitioning of different grain size fractions of till. Generally it is concluded that the range in grain size of the bedrock mineralogy reflects the metal distribution in the different size fractions of till. For instance most base metals in unstable mineral phases (e.g. pyrite) are enriched in the clay-size material due to the primary enrichment of metals in phyllosilicates of bedrock (Plouffe, 1997). The metals adsorb on the clay particles during weathering of the bedrock (Plouffe, 1997). However, minerals more resistant to weathering and oxidation will show enrichment in clay as well as the larger size fractions (Dreimanis and Vagners, 1971; Plouffe, 1997; Shilts, 1984). Shilts, (1973, 1984, 1995), and Nikkarinen *et al.* (1984) concluded that metal partitioning could be related to a combination of factors including (1) resistance to weathering of primary mineral phase in the silt and sand sized ranges (i.e. 0.002-2mm) (2) the

enrichment of phyllosilicates or other minerals within bedrock that easily binds to clay during glaciation and (3) the adsorption of metals on clay during postglacial weathering (not as significant) (Plouffe, 1997). Plouffe (1997) concluded that the clay-sized fraction of the till yielded the highest Hg concentration, which is related to the highest adsorption capacity for Hg.

2.5.3 Rocks

Cinnabar (HgS) normally contains 86.22% Hg and 13.7% sulfur hence it is the most abundant mercury-bearing mineral found in sedimentary rocks (particularly sandstone and limestone) of Paleozoic and younger rocks throughout the world (Boyle and Jonasson, 1972). Cinnabar occurs in low temperature environments, near hot springs, or where there has been volcanic activity. It forms in epithermal veins associated with pyrite, quartz, calcite, opal, chalcedony, and dolomite (Chesterman, 1998). Cinnabar can form as a compact mass, in a vein or impregnated in quartz sandstone (Chesterman, 1998). A search of the Nova Scotia Department of Natural Resources mineral occurrence database indicates there are no known cinnabar occurrences in Nova Scotia.

It is important to consider bedrock lithology, age and abundance of sulphide mineralization when evaluating the natural distribution of mercury (Rasmussen *et al.*, 1998). Sulphides in base metal deposits contain variable amounts of mercury. For example pyrite can contain 0.1 ppm to 100 ppm mercury (Table 2.2) (Jonasson and Boyle, 1972). Studies have shown that black shales usually have elevated levels of mercury particularly when metals such as pyrite are present (Rogers and Berger, 1995;

Cameron and Jonasson, 1972). Mercury enrichment is found in carbonaceous sediments, sedimentary sulphides, barite and in the residual products of weathering, such as bauxites, iron and manganese oxides (Table 2.3) (Cameron and Jonasson, 1972). Figure 2.4 illustrates Hg concentrations in bedrock and stream sediments found in the Proterozoic Rove Formation (anomalous area) and Archean metavolcanics (background area) in the Thunder Bay region of Ontario (Rogers and Berger, 1995). The carbonaceous shales of the Rove Formation and stream sediment derived from it, show substantially elevated Hg levels compared to the background area. Black shale formations rich in carbon, sulphur and metals in Finland commonly contain 0.2 ppm of Hg (Loukola-Ruskeeniemi, 1990). Black shales can contain other elements of environmental interest including base metals, cadmium, chlorite, fluorine and selenium (Loukola-Ruskeeniemi, 1990).

The underlying bedrock can release mercury to the overlying soil and water. The degree of release to surface waters is influenced by the degree of acidity of the rock. The pH reducing effect of acid rain can enhance the weathering process by increasing Hg mobility and leaching capacity from the minerals (Burgess, *et.al.*, 1998) The physical (permeability and porosity) and chemical nature of the surrounding rock also affect the diffusive and capillary movement of mercury. For example, limestone can severely restrict the ionic movement of mercury resulting in a localized movement (Jonasson and Boyle, 1972). Table 2.3 illustrates mercury content of sedimentary, igneous and metamorphic rocks. The highest mean Hg rock values are in alkali-rich rocks (450 ppb) and carbonaceous shales (437 ppb). Other rock types elevated in Hg include hornfels (225 ppb) and ultrabasic rocks (168 ppb).

Mineral	Composition	*Normal Range (ppm) Limits	**Highest Reported Content (%)
tetrahedrite	$Cu_{12}Sb_4S_{13}$	10 — 1,000	17.6 ; 21
grey copper ores	$(Cu,As,Sb)_xS_y$	5.0 — 500	14
sphalerite	ZnS	0.1 — 200	1
wurtzite	ZnS	0.1 — 200	0.03
stibnite	Sb_2S_3	0.1 — 150	1.3
realgar	AsS	0.2 — 150	2.2
pyrite	FeS_2	0.1 — 100	2
galena	PbS	0.04 — 70	0.02
chalcopyrite	$CuFeS_2$	0.1 — 40	—
bornite	Cu_5FeS_4	0.1 — 30	—
bournonite	$PbCuSbS_3$	0.1 — 25	—
chalcocite	Cu_2S	0.1 — 25	—
marcasite	FeS_2	0.1 — 20	0.07
pyrrhotite	$Fe_{1-x}S$	0.1 — 5	—
molybdenite	MoS_2	0.1 — 5	—
arsenopyrite	FeAsS	0.1 — 3	—
orpiment	As_2S_3	0.1 — 3	—
native gold	Au	1.0 — 100	60
native silver	Ag	1.0 — 100	30
barite	$BaSO_4$	0.2 — 200	0.5
cerussite	$PbCO_3$	0.1 — 200	0.1
dolomite	$CaMg(CO_3)_2$	0.1 — 50	—
fluorite	CaF_2	0.01 — 50	0.01
calcite	$CaCO_3$	0.01 — 20	0.03
aragonite	$CaCO_3$	0.01 — 20	3.7
siderite	$FeCO_3$	0.01 — 10	0.01
chalcedony and opaline silicas	$SiO_2.nH_2O$	0.01 — 10	—
quartz	SiO_2	0.01 — 2	—
pyrolusite	MnO_2	1.0 — 1,000	2
hydrated iron oxides	$Fe_2O_3.nH_2O$	0.10 — 500	0.2
graphite	carbon	0.5 — 10	0.01
coal	—	0.05 — 10	2
gypsum	$CaSO_4.2H_2O$	0.01 — 4	—

Table 2.2 Mercury content of some common ore minerals (ppb) (taken from Jonasson and Boyle, 1972)

Rock Type	Range	Mean
(a) Igneous		
Ultrabasic (dunite, kimberlite, etc.)	7 — 250	168
Basic intrusives (gabbro, diabase, etc.)	5 — 84	28
Basic extrusives (basalt, etc.)	5 — 40	20
Intermediate intrusives (diorite, etc.)	13 — 64	38
Intermediate extrusives (andesite, etc.)	20 — 200	66
Acidic intrusives (granite, granodiorite, syenite)	7 — 200	62
Acidic extrusives (rhyolite, trachyte, etc.)	2 — 200	62
Alkali-rich rocks (nepheline, syenite, phonolite, etc.)	40 —1400	450
(b) Metamorphic		
Quartzites	10 — 100	53
Amphibolites	30 — 90	50
Hornfels	35 — 400	225
Schists	10 —1000	100
Gneisses	25 — 100	50
Marbles, crystalline dolomites	10 — 100	50
(c) Sedimentary		
Recent Sediments: stream and river	10 — 700	73
lake	10 — 700	73
ocean and sea	< 10 —2000	100
Sandstones, arkoses, conglomerates	< 10 — 300	55
Shales, argillites, mudstones	5 — 300	67
Carbonaceous shales, bituminous shales	100 —3250	437
Limestones, dolomites	< 10 — 220	40
Evaporites: gypsum, anhydrite	< 10 — 60	25
halite, sylvite, etc.	20 — 200	30
Rock phosphates (composite samples)	. . . . .	120

Table 2.3 Mercury content of rocks (ppb) (taken from Jonasson and Boyle, 1972)

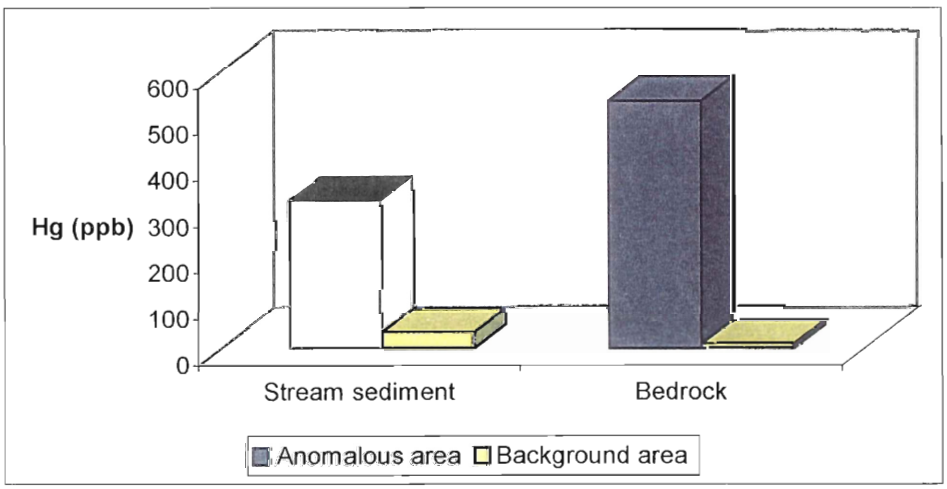

Figure 2.4 Concentrations of Hg in bedrock and stream sediments from the anomalous area (Proterozoic Rove Formation-black shale) and background area (Archean metavolcanics) in the Thunder Bay Area. (n = 7) (modified from Rogers and Berger, 1995)

As previously mentioned Smith (2000) found average Hg levels in southwest Nova Scotia of 3.3 ppb (n = 146 bedrock samples). Figure 1.6 summarizes the average Hg concentration in lithologies in the Kejimkujik National Park and surrounding area. The Hg content in the greywackes of the Goldenville Group is the lowest (1 ppb) along with the granites (1.5 ppb). The highest values are in the biotite separates from monzogranite (13.8 ppb) and the Silurian rocks from the Bear River area (12.2 ppb).

Sangster *et al.* (2001) summarize the Hg values found in different lithologies throughout Kejimkujik National Park including analysis of drill cores (Figure 1.7). The lowest Hg values are in the Goldenville Group (<0.5 ppb to 4.0 ppb; n = 47) and in the Kejimkujik monzogranite (<0.5 ppb to 5.8ppb; n = 31). The Halifax Group is slightly higher ranging from <0.5 ppb to 16.4 ppb (n = 100).

Sangster and Smith (2001) indicate that Goldenville and Halifax Group lithologies contain slightly elevated Hg concentrations. Goldenville Group samples from Eastville, Wire Lake and Molega Lake area contain Hg values ranging from <0.5 ppb to 13.2 ppb. Samples of drill cores from the Halifax Group from Clarksville, Eastville, and Lake Charlotte contain higher levels ranging from <0.5 ppb to 242 ppb. Eastville has the highest Hg levels, possibly related to sphalerite (ZnS) mineralization since sphalerite can contain up to 20 mole % of Hg in solid solution (Loukola-Ruskeeniemi, 1990).

Sangster and Smith (2001) conclude that Hg could be a transferred during the earliest weathering phases most pronounced in the porous well-cleaved sulphidic black slates that contain 5% pyrite and/or pyrrhotite increasing their acid generating capacity. Higher concentrations of Hg in the drill core could indicate that surface bedrock sampling is not an accurate account of Hg present in the bedrock (Sangster *et al.*, 2001).

Chapter 3 Bedrock and Surficial Geology

3.1 Introduction

The surficial geology and underlying bedrock geology influence the overlying soils. Southwest Nova Scotia is underlain by the Meguma Supergroup, the overlying Annapolis Supergroup which are both intruded by granite of the South Mountain Batholith (Figure 3.1)(Schenk, 1995b). Collectively these form the Meguma Terrane which is an Appalachian suspect terrane that accreted onto North America during the Early Devonian (Schenk, 1995b). The following outlines both regional and local bedrock and surficial geology.

3.2 Regional Geology

3.2.1 Meguma Terrane

A large portion of the following discussion is taken from Schenk (1995a,b) except where noted. The Meguma Terrane includes the Late Cambrian or older to Early Ordovician Meguma Supergroup, the overlying Early Ordovician to Early Devonian Annapolis Supergroup and the Devonian to Carboniferous granitoid intrusions (Figure 3.1) (Clarke *et al.*, 1985.) The contact between the Supergroups is assumed to be a paraconformity but locally is a disconformity or an angular unconformity. The Meguma Supergroup is composed of thick metamorphosed siliciclastic sequences occupying a portion of southern mainland Nova Scotia. The Meguma Supergroup is divided into two Groups (Figure 3.2) including the (1) Goldenville Group and (2) the Halifax Group. The Goldenville Group is composed of Cambrian age greywacke with minor slates that

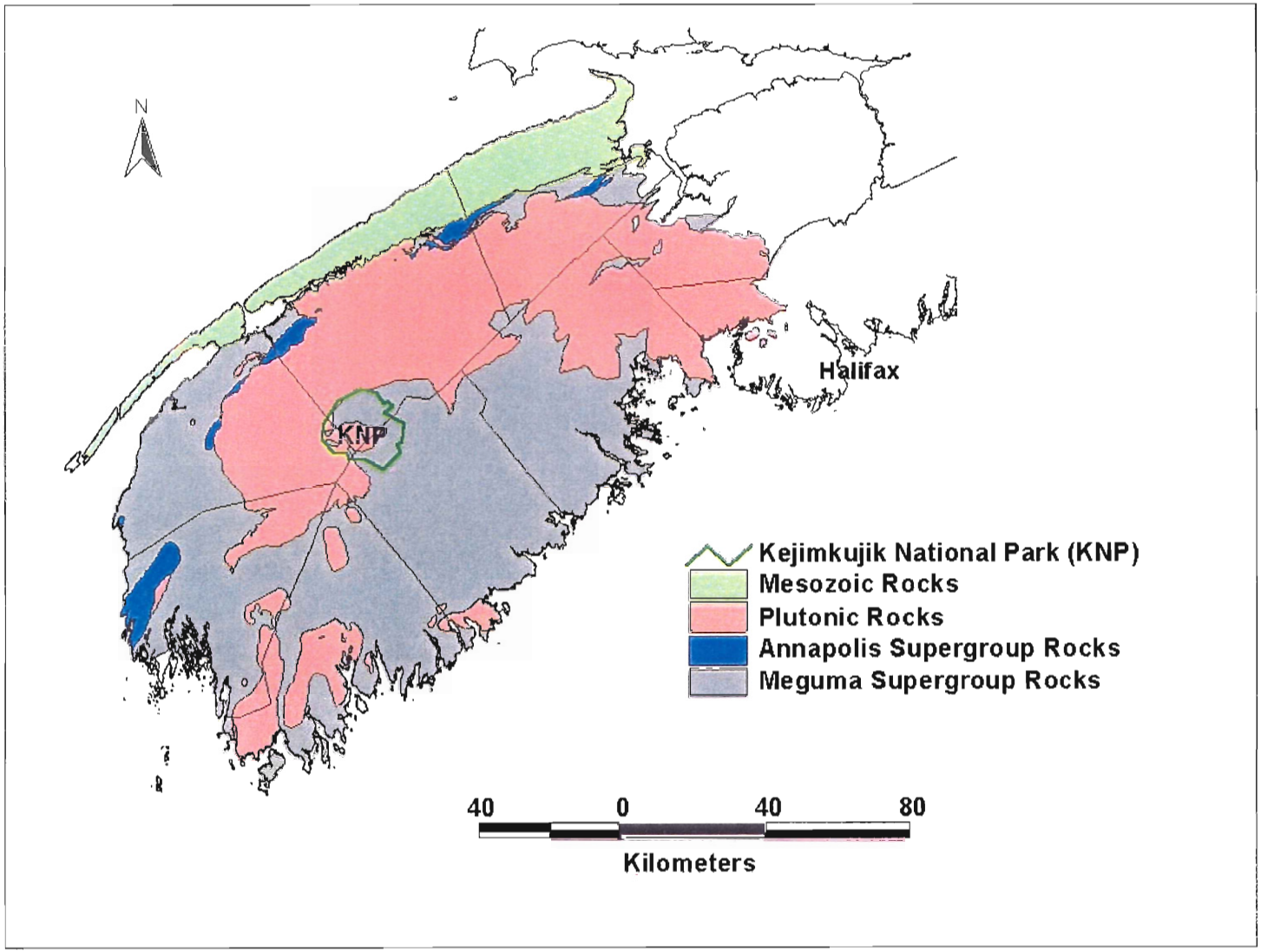

Figure 3.1 Four Rock Units of Southwest Nova Scotia. (Map modified from Keppie 2000, http; Page, 2001)

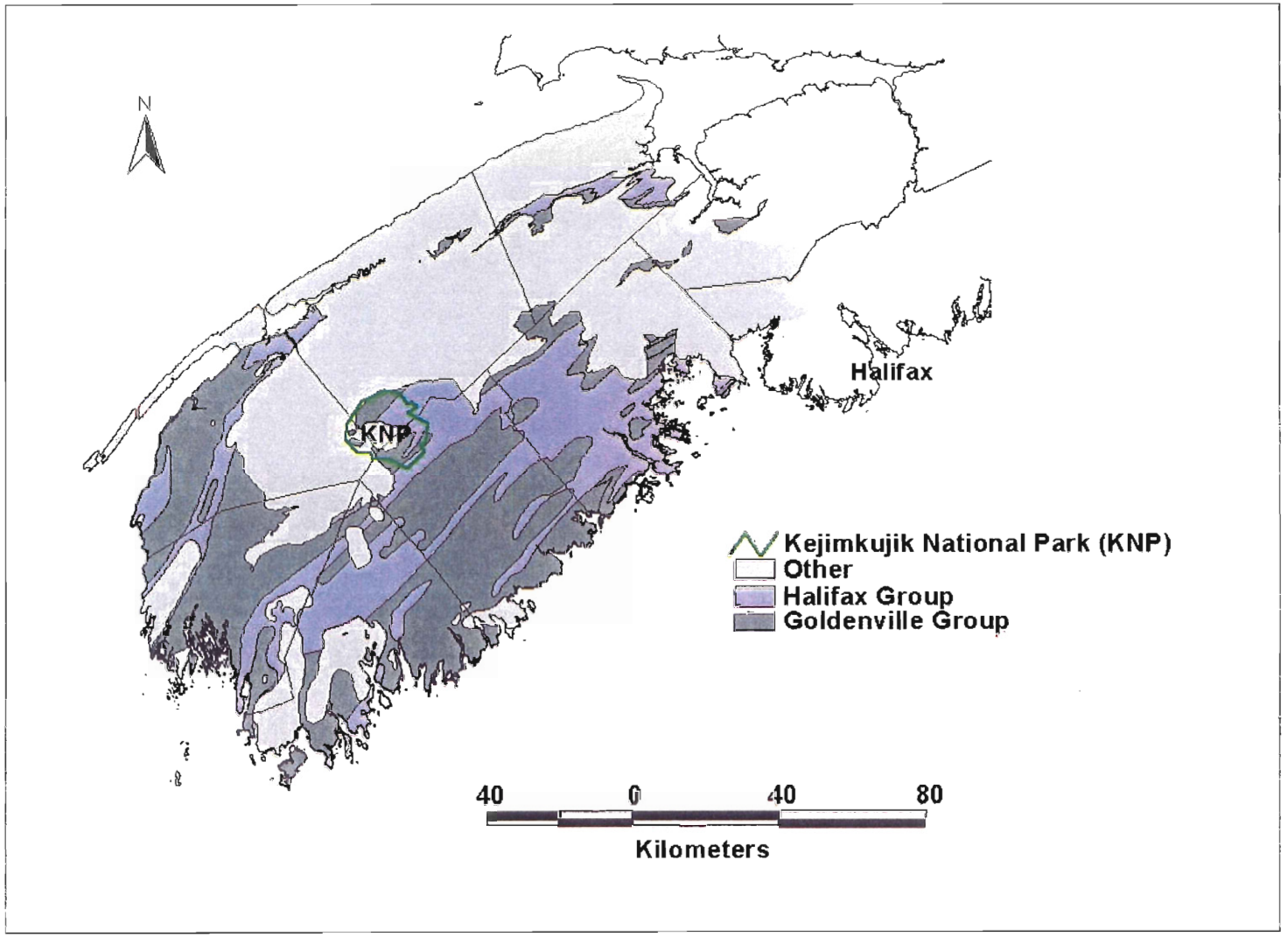

Figure 3.2. The Meguma Supergroup including the Goldenville Group and Halifax Group.(Map modified from Keppie, 2000, http; Page, 2001)

formed in an ancient abyssal plain fan. The Halifax Group is composed of the Early Ordovician age slates with minor greywacke that was formed in the mid to upper area of a deep sea fan.

There are three conformable and gradational Formations within the Goldenville Group in southwest Nova Scotia including (in ascending order); the New Harbour Formation, Risser's Beach Formation and West Dublin Formation. There are five conformable and gradational Formations in the Halifax Group including Mosher's Island, Cunard, Feltzen, Delancey's and Rockville Notch Formation. Schenk (1995a) describes each of these Formations in detail. Table 3.1 explains stratigraphic units and respective nomenclature from several studies of the Meguma Supergroup.

The stratigraphic region between the coarser-grained Goldenville Group and finer-grained Halifax Group is termed the Goldenville Halifax Transition Zone (GHT) known for its distinct lithologies typified by interstratified slate and greywacke as well as heavy metals including Mn, Ba, Pb, Zn, Cu, Mo, W, and Au (Zentilli and Graves, 1988). The GHT is a sedimentary transition zone typically composed of a finely laminated manganese-rich unit that is locally rich in calcareous or calc-silicate nodules, spessartine-rich quartzite and sulphide minerals (Graves and Zentilli, 1988). Generally the contact is sharp in the eastern areas of the Meguma Terrane and more gradational in the central and western area (Graves and Zentilli, 1988). The GHT is characterized by pyrite and pyrrhotite rich layers that may play an important role in mercury cycling when sulphide mineral oxidation allows the release of heavy metals in the environment (Fox *et al.*, 1997)

Meguma Supergroup Southwestern Meguma Terrane (Schenk, 1995b)		Meguma Group Mahone Bay area, Southwestern Meguma Terrane (O'Brien, 1986)		Meguma Group Central Meguma Terrane (Ryan *et al.*, 1995)		
Units		Units		Units		
Halifax Group	Rockville Notch Formation					
	Delanceys Formation					
	Feltzen Formation	Halifax Formation	Feltzen Member	Halifax Formation	Glen Brook Unit	?
	Cunard Formation		Cunard Member		Rawdon Unit	
	Moshers Island Formation	Green Bay Formation	Moshers Island Member		Beaverbank Unit	GHT
Goldenville Group	West Dublin (Green Bay area) andTancook (Mahone Bay area) Formations		West Dublin (Green Bay area) andTancook (Mahone Bay area) Members	Goldenville Formation	Steve's Road Unit	
	Tancook (Mahone Bay area) Rissers Beach (Green Bay area) Formations		Rissers Beach Member (Green Bay area)			
	New Harbour Formation	Goldenville Formation	New Harbour Member		Lewis Lake Unit Long Lake unit Mt. Uniacke Unit	?

Table 3.1 Organization chart of Meguma Supergroup stratigraphic units and respective nomenclature from several recent studies and location of Goldenville Halifax Transition Zone (GHTZ) (modified from Burns, 1997)

The Early Ordovician to Early Devonian Annapolis Supergroup is composed of thick sequences of fine-grained shallow marine siliciclastic sedimentary rocks and volcaniclastic rocks. The Annapolis Supergroup is an erosional remnant and quite possibly covered the entire Meguma Terrane at one time (Figure 3.1). The three groups within the Annapolis Supergroup include the Late Ordovician White Rock Group, the Silurian Kentville Group and the Devonian Torbrook Group described in detail in Schenk (1995b) (Figure 3.3). In southwest Nova Scotia the three Formations of the White Rock Group include the Nictaux Volcanics, the Fales River and the Deep Hollow. The two Formations of the Kentville Group are the Elderkin and Tremont. The Torbrook is divided into five informal formations known as 1-5 formations. Each of these formations are described in detail in Schenk (1995b).

3.2.2 Mesozoic Rocks

Mesozoic rocks in western Nova Scotia include Triassic to Jurassic redbeds, tholeiitic basalts and mafic dykes of the Fundy Group. These rocks are located on the northwest area along the Bay of Fundy (Figure 3.4) (Keppie, 1979). These Mesozoic rocks are related to the opening and closing of the Atlantic Ocean (Keen *et al.*, 1991). Three Formations overlie the Meguma Terrane in southwest Nova Scotia include the Triassic Wolfville Formation, Upper Triassic Blomidon Formation and Early – Middle Jurassic North Mountain Basalt shown in Figure 3.4 (Keppie, 1979). There are no known outcrops of Cretaceous rocks in western Nova Scotia.

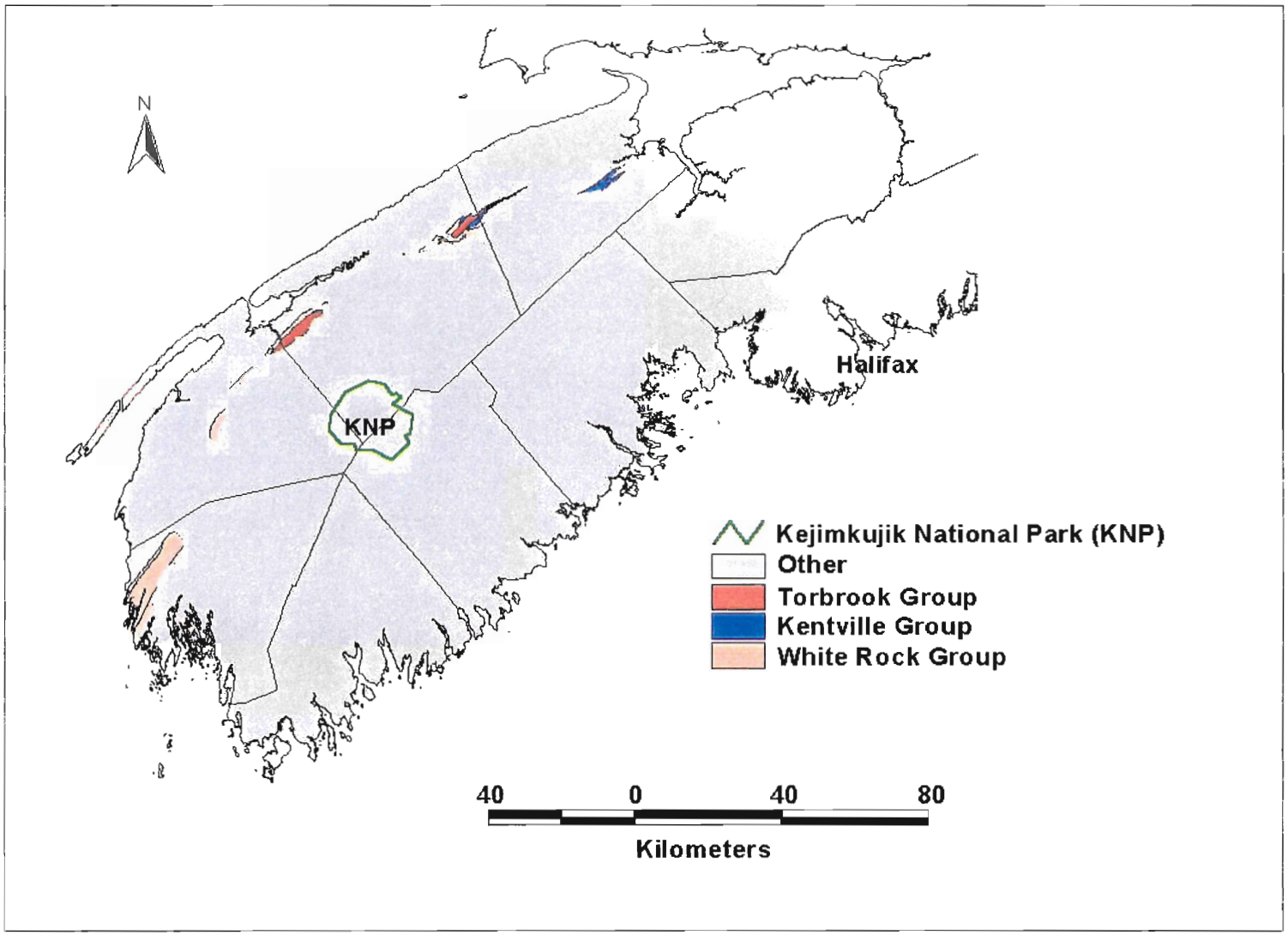

Figure 3.3. The Annapolis Supergroup includes the White Rock Group, Kentville Group, and Torbrook Group. (Map modified from Keppie 2000, http; Page, 2001).

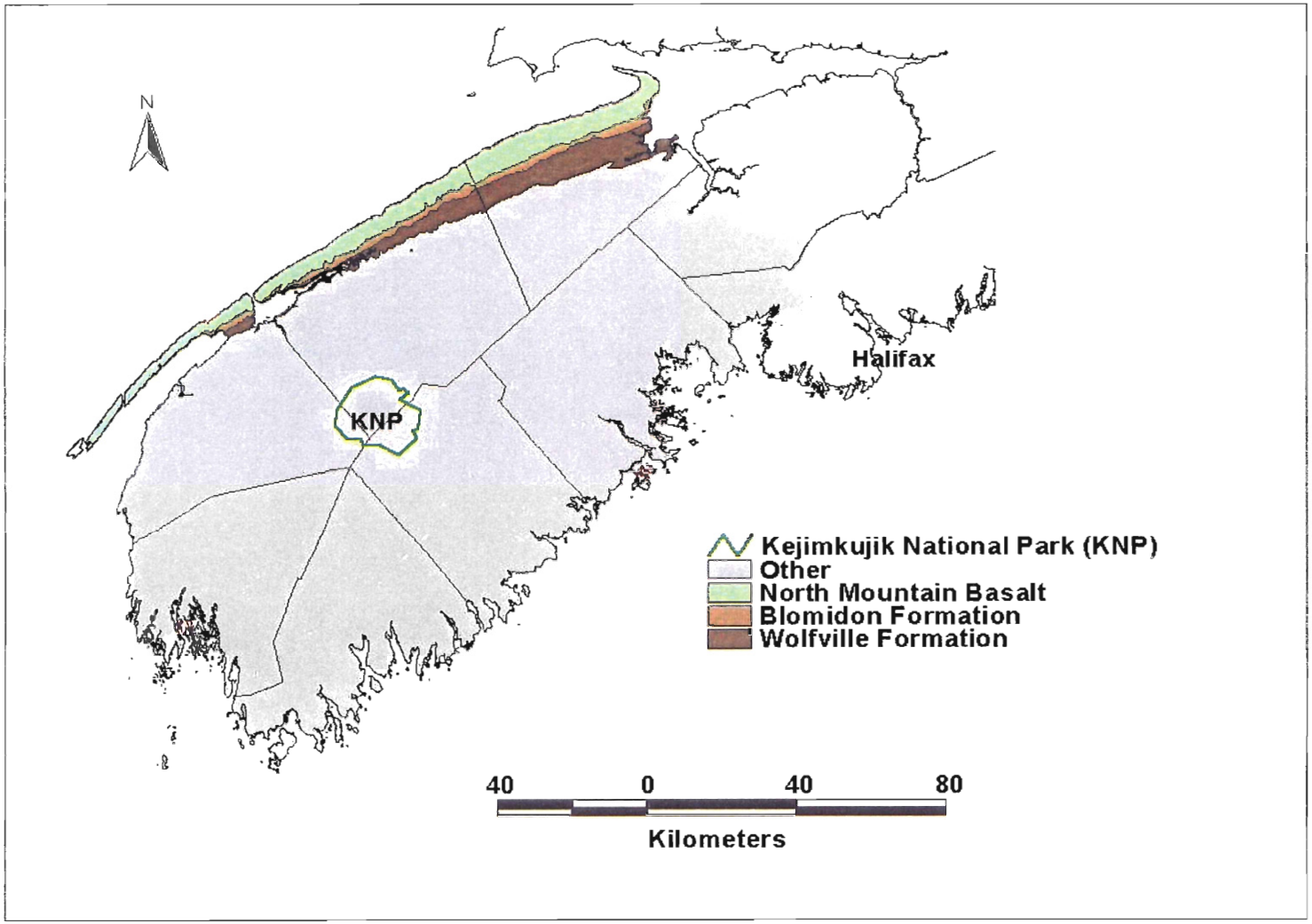

Figure 3.4. The Mesozoic rocks of southwest Nova Scotia include the Wolfville Formation, Blomidon Formation, and North Mountain Basalt. (Map modified from Keppie , 2000, http; Page, 2001).

3.2.3 Tectonics, Structure and Metamorphism

During the middle to Late Devonian Acadian Orogeny the Meguma Terrane was deformed, metamorphosed and intruded by voluminous granitoid bodies (Schenk, 1995b). The main structural consequence of the Acadian Orogeny is the extensive large-scale north trending, upright and low plunging folds in the southwest Nova Scotia. Second generation north/northeast trending steep cross- folds in the Halifax Group and third generation northwest trending kink folds/bands are evident over most of the Meguma Terrane (Schenk, 1995b). In Southwest Nova Scotia there are two mineralized northeast-trending shear zones including the East Kemptville that runs through the northern part of Kejimkujik National Park (O'Reilly, 1988) and Tobeatic Shear Zone that runs through the southern part of Kejimkujik National Park (Corey, 1994). Regional metamorphism occurred in the Late Silurian to Early Devonian ranging from greenschist facies in the central and eastern parts of the terrane to amphibolite facies in the southern most parts (Schenk, 1995b; Taylor and Schiller, 1966). Regional metamorphism predates the granitoid intrusions and contact aureoles (Schenk, 1995b; Reynolds and Muecke, 1978). The Meguma Supergroup exhibits both regional and contact metamorphism (Taylor and Schiller, 1966).

The Meguma Terrane is intruded by the Devonian South Mountain Batholith and its associated plutons (Clarke *et al.* 1980). The South Mountain Batholith outcrops over 10,000 km^2 in the Meguma Terrane (McKenzie and Clarke, 1975). Hornblende-hornfel facies contact metamorphism overprints the regional metamorphic assemblages (greenschist) in areas intruded, resulting in rocks usually appearing darker and harder

than rocks elsewhere (Taylor and Schiller, 1966). The composition of the plutons ranges from a muscovite leucogranite to mafic porphyry (MacDonald, 1994).

3.2.4 Surficial Geology

The following discussion was mainly taken from Stea *et al.* (1998) and Stea (2000, http) except where noted. The Maritime Provinces are located at the southeast margin of the Pleistocene Laurentide and Appalachian Ice Sheets. The Wisconsinan glacial history within the Maritimes is a record of the interaction of land-based glaciers with the sea. During Wisconsinan time the ice divides shifted over different terranes, forming variable sequences of till sheets with distinct origins.

There were four glacial phases over the last 75 thousand years ranging from the Early to Late Wisconsinan. These include the Caledonia Phase (Phase 1), Escuminac Phase (Phase 2), the Scotian Phase (Phase 3) and the Chignecto Phase (Phase 4) shown in (Figure 3.5a-d). Distinct till assemblages were deposited with each advance and retreat of the four phases. The Early to Mid-Wisconsinan Caledonia Phase (75-40 Ka) is the oldest ice flow that crossed in an eastward and then changed to a southeastward direction (Stea and Grant, 1988). A late stage large ice dome known as the Gaspereau Ice Centre developed later in northern New Brunswick producing the striation patterns visible today in Southern New Brunswick and Nova Scotia (Stea and Grant, 1988). The over consolidated, matrix rich tills deposited during the Caledonia Phase found in Nova Scotia include McCarron Brook Till, Hartlen Till, East Milford Till and Richmond Till. Figure 3.6 outlines till and ice flow phase correlations in Nova Scotia.

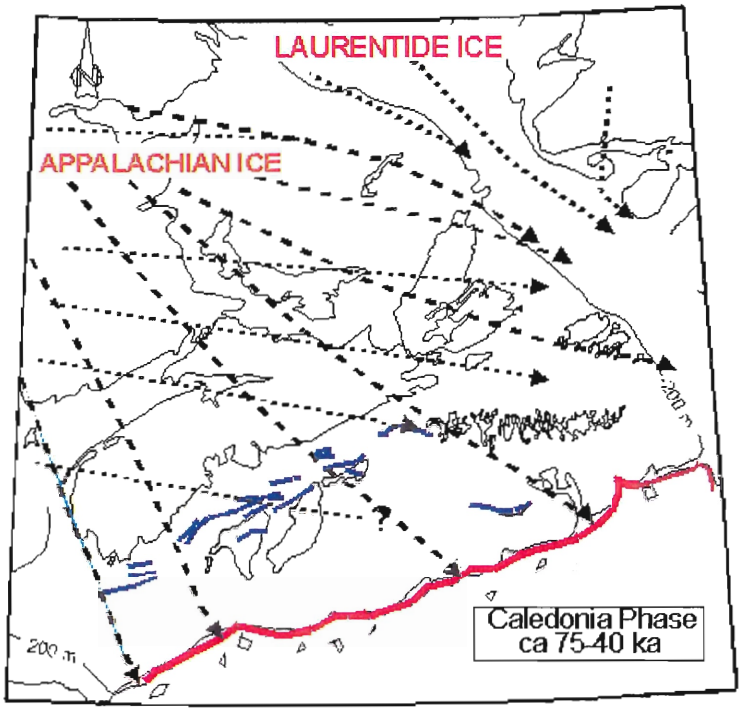

Figure 3.5a Phase 1: Caledonia Phase (Early to Mid-Wisconsinan Ice Flow Phase, 75-40 ka) (modified from Stea, 2000, http)

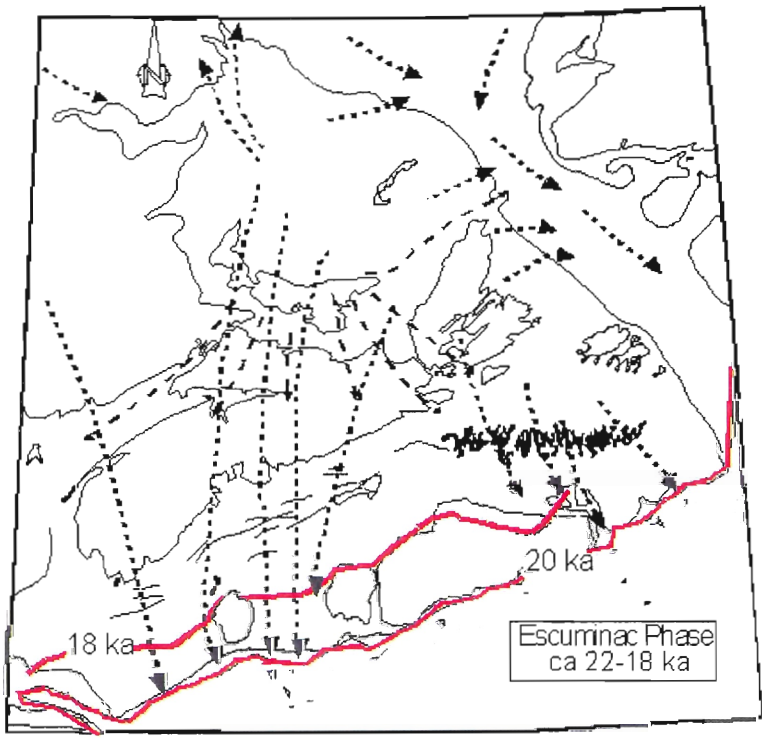

Figure 3.5b Phase 2: Escuminac Phase (Late Wisconsinan Ice Flow Phase, 22-18 ka) (modified from Stea, 2000, http).

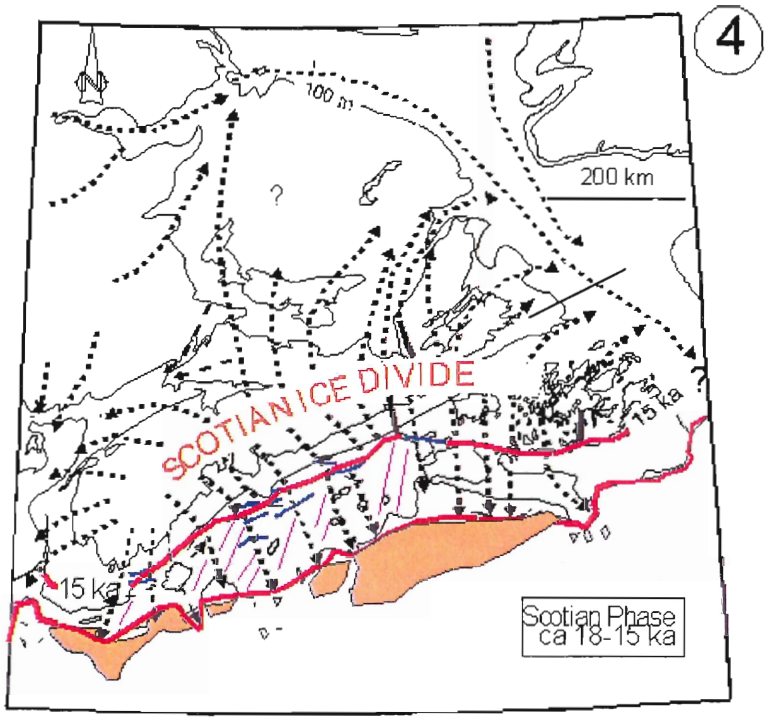

Figure 3.5c Phase 3: Scotian Phase (Late Wisconsinan Ice Flow Phase, 18-15 ka) (modified from Stea, 2000, http).

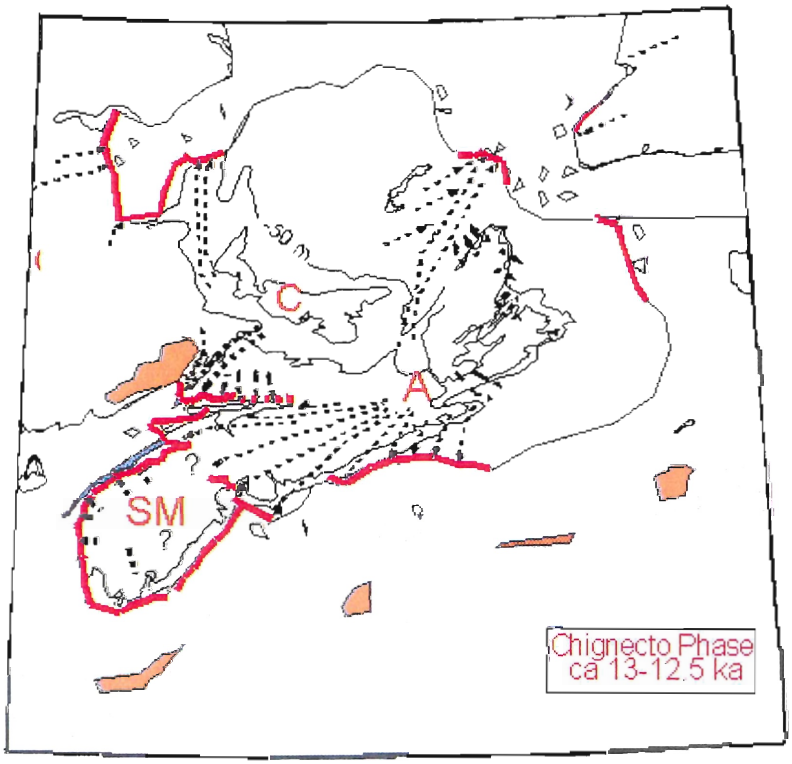

Figure 3.5d Phase 4: Chignecto Phase (SM-South Mountain Ice Cap) (C-Chignecto Glacier) (A- Antigonish-Chedabucto Bay Glacier Complex), (Late Wisconsinan Ice Flow Phase,13-12.5 ka)

The Late Wisconsinan Escuminac Phase (22-18 ka) crossed in a south to southwest direction with an ice dome (Escuminac Ice Center) on the Magdalen Shelf just north of Prince Edward Island that left directional evidence of striated outcrops in Nova Scotia and Prince Edward Island (Figure 3.5b) (Stea and Grant, 1988). During this phase the Lawrencetown Till was formed by the red hematitic sediments from the shelf. Figure 3.6 illustrates a complete list of tills formed during the Escuminac Phase.

During the Late Wisconsinan Scotian Phase (18-15 ka) ice retreated rapidly in seaward directions from the Scotian Ice Divide that formed in the center along the axis of Nova Scotia (Figure 3.5c). The rise in sea level cut off Nova Scotia from outlying ice sources (Escuminac and Gaspereau). The ice margin was close to the current Nova Scotia coastline 14 Ka years ago and remained there for at least 1500 years except for the coast along the Bay of Fundy- Gulf of Maine where ice was cleared by vigorous ice streams leaving raised beaches, deltas and marine deposits along the Bay of Fundy. During this phase a stoney (angular to subangular cobbles and boulders), sandy Beaver River Till formed almost exclusively derived from local bedrock. The Beaver River Till overlies the Lawrencetown and Hartlen Tills forming a till plain over most of the Atlantic coast. Figure 3.6 outlines till and ice flow phase correlations in Nova Scotia.

The Late Wisconsinan Chignecto Phase (13-12.5 ka) resulted from the generation of two small ice caps located over the South Mountain Batholith and over the Antigonish highland after the Scotian Phase retreat during a late- glacial climatic reversal. Cross-striated bedrock illustrate a directional change from northeastward flow (during the Scotian Phase), to northwestward and westward along the Bay of Fundy and southwest

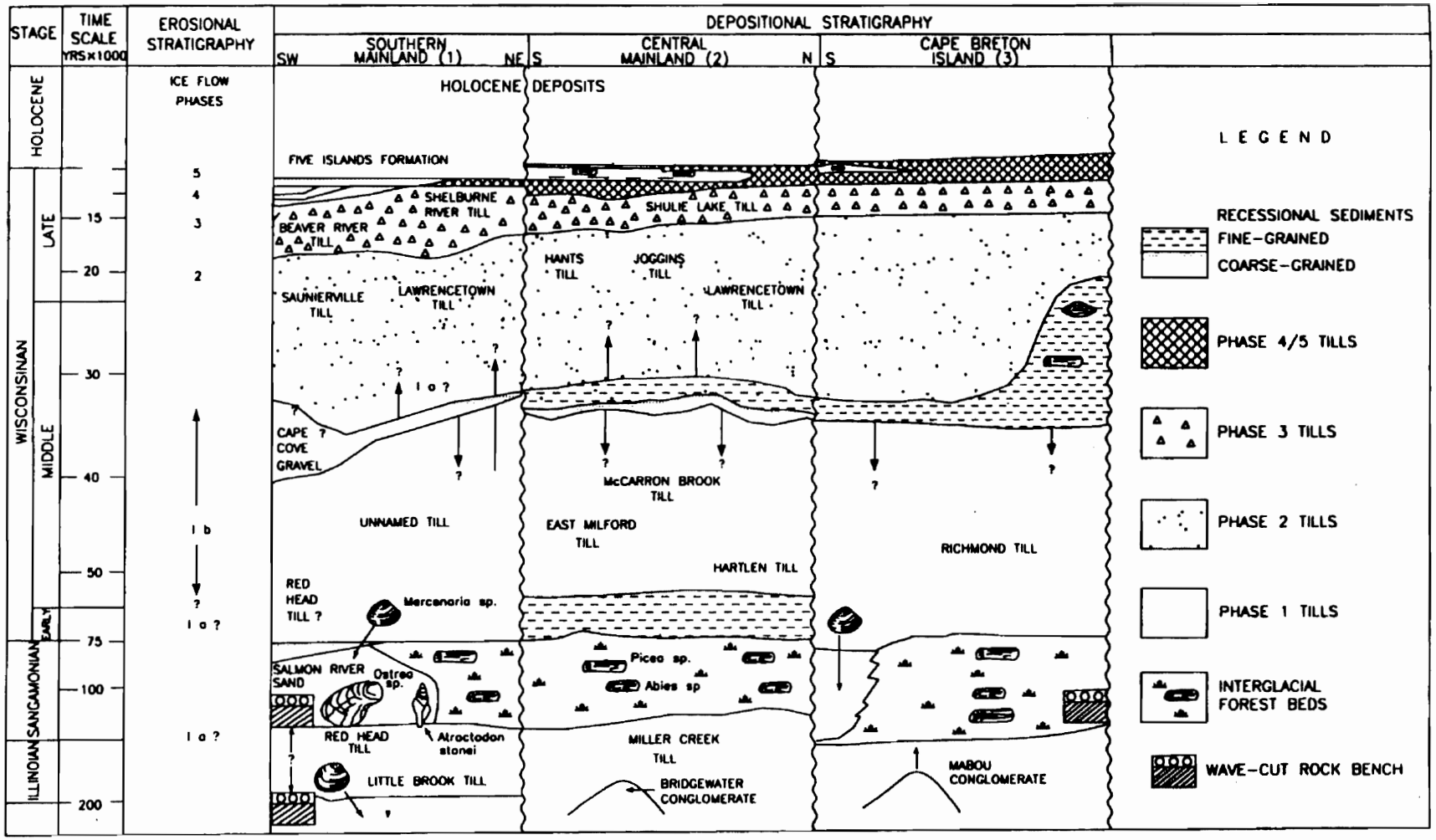

Figure 3.6 Correlation in time and space of erosional and depositional lithographic units and Quaternary stage names in Nova Scotia (Stea *et al.*, 1998; Stea *et al.*, 1992).

flow along the Atlantic coast of Nova Scotia during the Chignecto Phase (Figure 3.5d). Figure 3.6 indicates till stratigraphic location but no exact names are assigned to date.

Following this phase the climate warmed and most of the glaciers disappeared except for an interruption during the Younger Dryas event (Collins Pond Phase-11 ka) where a cold period reinvigorated glaciers with cold periods possibly continuing year round. As a result a distinctive sediment layer useful as a climate signature in lakes was deposited. By 10 ka the climate returned to a warming trend.

3.3 Local Geology

3.3.1 Bedrock Geology

The study area just south of Kejimkujik National Park is underlain by rocks of the Meguma Supergroup (Figure 1.2). The rocks consist of massive grey to greenish grey metawacke and minor laminated grey to black metasiltstone of the Goldenville Group. These are overlain by finely laminated greenish grey to black slate and metasiltstone of the Halifax Group (Horne and Corey, 1994; Williams *et al.*, 1985). North of the study area there are areas intruded by granitoid rocks of the South Mountain Batholith. These consist of three types: (1) leucomonzograntie (southwest Kejimkujik National Park) (2) muscovite-biotite monzogranite (central west Kejimkujik National Park) and (3) biotite monzogranite (north and west Kejimkujik National Park).

3.3.2a Geology of Study Area

Throughout the study area there is less than 2% outcrop most of which can be found along ditches and streams. The contact between the Halifax and Goldenville Group is not exposed. Along the 3 transects sulphide minerals are visible in the slate exposures of the Halifax Group on the south end of transect 3 (Figure 3.7). Sulphide mineral abundance decrease in the slate outcrops further north of the inferred contact. On the southern end of transect 2 and on nearby logging roads green to gray-green meta-siltstone outcrops of the Goldenville Group are exposed. These outcrops indicate a general location of the GHT. Based on this information detailed ground magnetics were completed along three transects crossing the area of the GHT discussed later in this chapter.

3.3.2b Surficial Geology

The following discussion is largely taken from Finck *et al.* (1994) except where noted. The study area contains Late to Middle Wisconsinan greywacke-slate Beaver River Till shown in Figure 3.8. During field mapping, ice flow indicators such as striations were mapped indicating a northeast-southwest and a southeast-northwest ice flow direction. The major transport direction for the Beaver River Till is southeastward over the South Mountain Batholith with a short renewal distance (< 1 km) resulting in a locally derived stoney till varying in thickness from 1 to 6 m.

Slate outcrop
Transect 3
(1m x 1m)

Sulphide mineral
casts

Oxidized sulphide
minerals

Figure 3.7 Sulphide rich slate outcrop on transect 3 illustrating casts of weathered sulphide minerals at the top of the picture.

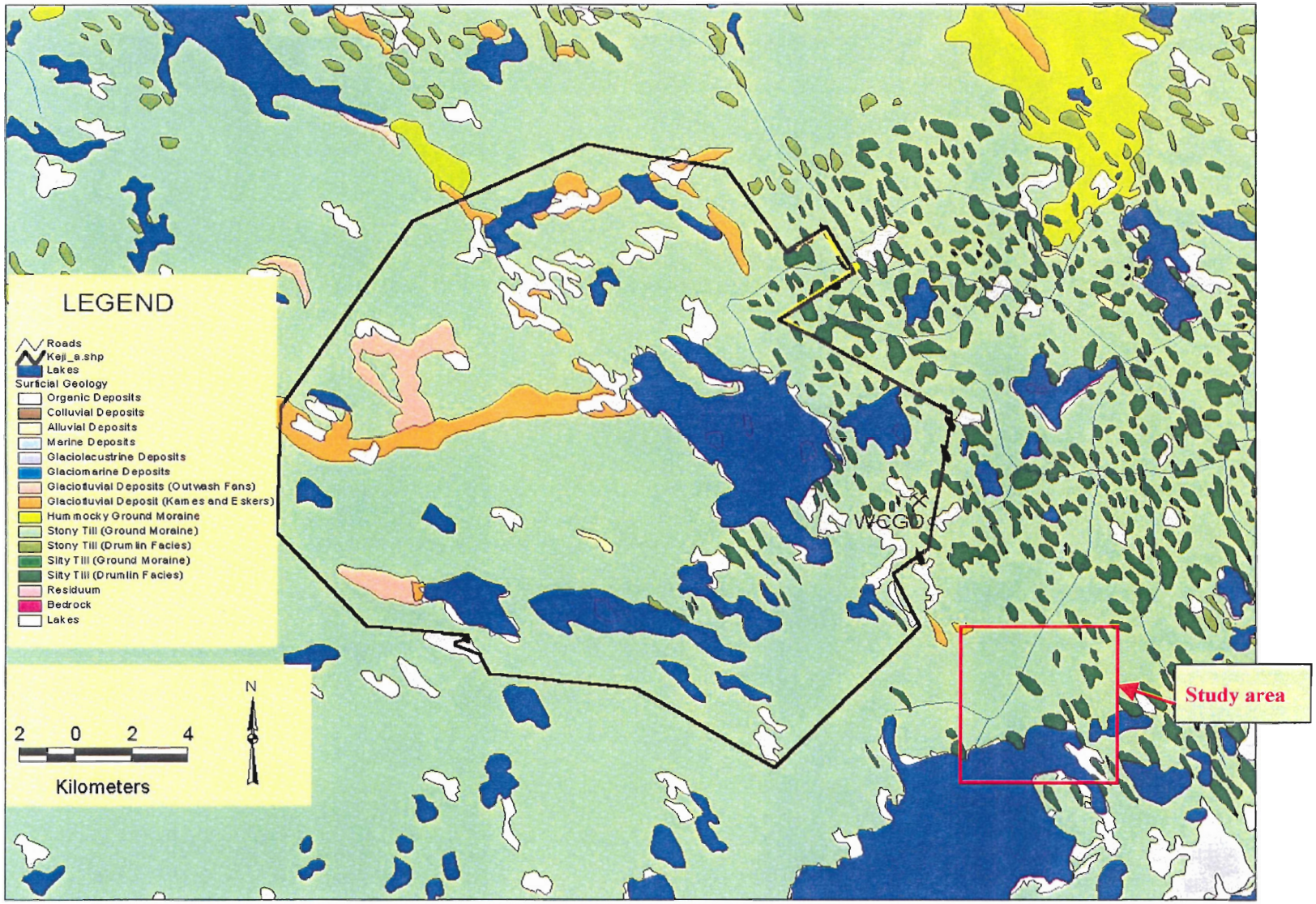

Figure 3.8 Surficial geology map of study area. Slate and greywacke Beaver River Till comprise the stoney till within the study area. For a more detailed map refer to Finck *et al*, (1994) ((**WCGD**) West Caledonia Gold District) (map generated using ArcView 3.2).

3.3.3 Gold Districts

Almost all of the gold mined in Nova Scotia came from south of the Glooscap Fault predominately from the Meguma Supergroup (Ryan and Smith, 1998). The greenschist grade regional metamorphism in the Rocks of the Meguma Supergroup can account for the mobilization and concentration of mesothermal gold bearing quartz veins (Ryan and Smith, 1998). There are 2 abandoned gold districts proximal to the study area. One, the Whiteburn Gold District, located 3 km to the east of the study area while the west Caledonia Gold District is located approximately 5 km to the NW. Historically mercury was used in the extraction process of gold leaving behind Hg as a waste product. However, since a small amount of gold was mined from the West Caledonia Gold District and Whiteburn Gold District and the closest abandoned is 3 to 5 km away Hg contamination of the till as a result of the gold extraction process is not an issue in this study.

3.4 Geophysics: Ground Magnetic Survey

3.4.1 Introduction

Previous studies by Goodwin *et al.* (2000) and Page (2001) indicate that there could be a spatial correlation between elevated Hg in soil gas and the Goldenville-Halifax Transition Zone (GHT). Identifying the precise location of the GHT is an integral component in interpreting the Hg geochemistry of the till. The GHT is characterized by sulphide mineral rich Units and as mentioned in section 3.2.1 sulphide minerals (e.g. pyrrhotite, pyrite) play a role in heavy metal release possibly increasing Hg concentrations in the till (Figure 3.9)(Graves and Zentilli, 1988; Fox *et al.*, 1997). In

detailed mapping the ferromagnetic minerals generally produce the largest secondary magnetic fields including minerals such as magnetite and pyrrhotite (King, 1995; Telford *et al.*, 1990). Paramagnetism produces a smaller magnetic field responsible for more subtle phenomena including magnetic fabrics in minerals such as biotite, ilmenite and garnet (King, 1995; Telford *et al.*, 1990). The GHT is also characterized by a significant increase in magnetic susceptibility compared to the Halifax and Goldenville Groups (Figure 3.9) (King, 1997). Therefore, the combination of an increase in ferromagnetic and paramagnetic minerals in the GHT plus increased magnetic susceptibility associated with the GHT makes the zone an attractive magnetic marker horizon.

3.4.2 Previous Work

With the use of thermal magnetic experiments, Schwartz and McGrath (1974) concluded that ferromagnetic pyrrhotite and hexagonal pyrrhotite were the main magnetic mineral in the Halifax Group slates. Cameron and Hood (1975) also concluded that there was at least 5% pyrrhotite in the Halifax Group. The black sulphide mineral rich basal slate unit of the Halifax Group contains pyrrhotite, pyrite and minor ilmenite. The overlying Unit contains little sulphides and only trace amounts of hematite.

In the Goldenville Group, Stern and Henderson (1983) determined with the use of X-ray diffraction that magnetite was the principle magnetic phase with minor amounts of hematite in the Goldenville Group. King (1995) also identifies magnetite with trace amounts of hematite in the Goldenville Group along with minor amounts of ilmenite and pyrite. King (1997) concludes that pyrrhotite and ilmenite are magnetic components of the GHT.

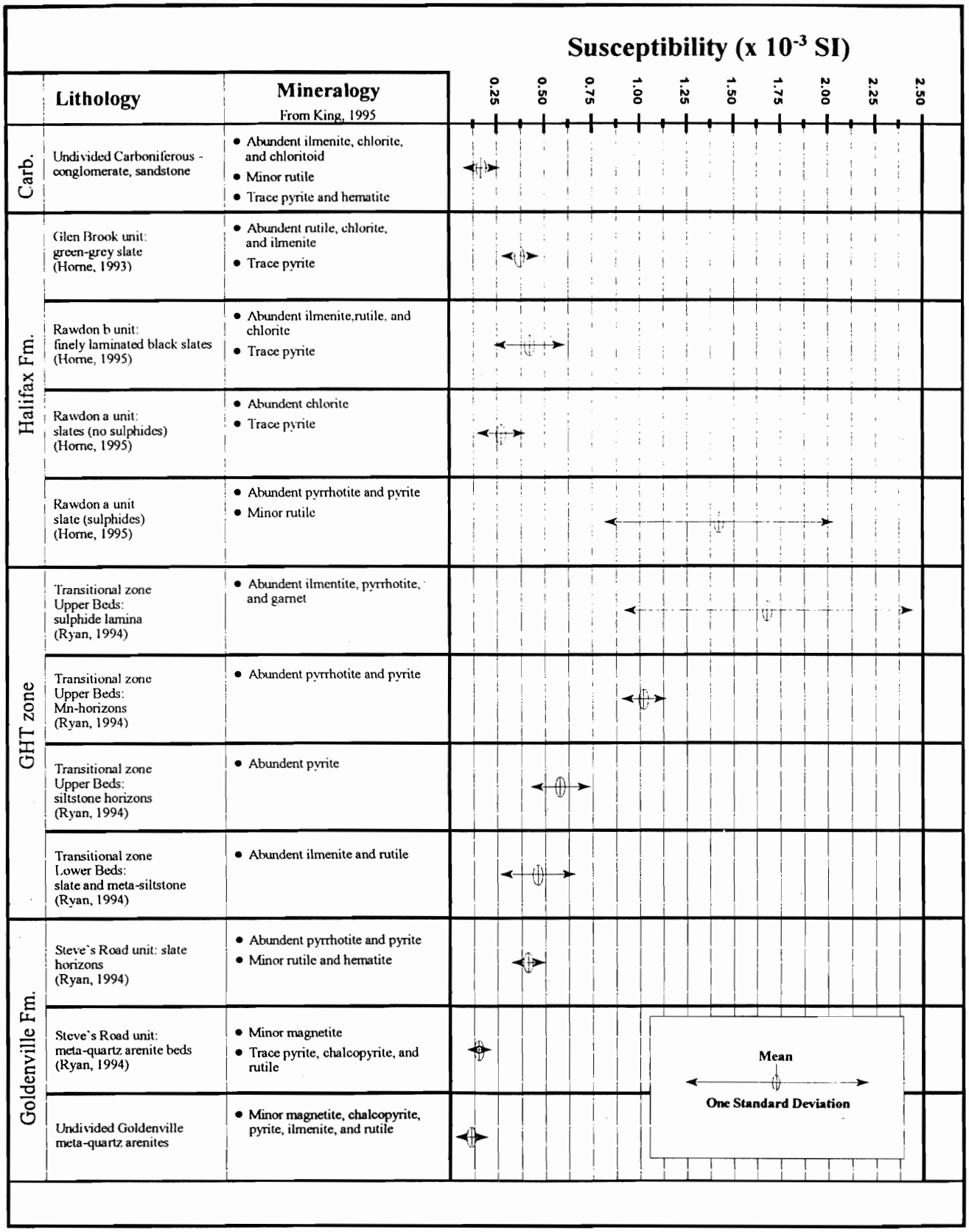

Figure 3.9 Magnetic susceptibility readings from the Central Meguma correlated with geology and stratigraphy. Refer to Table 3.1 for related stratigraphic nomenclature from previous studies. (King, 1997)

Drill cores from stratigraphic horizons within the GHT contain numerous sulphide and oxide phases (Binnet *et al.*, 1986). Ryan (1994) identified a correlation between lithology and magnetic mineralogy in the GHT with abundant pyrrhotite and ilmenite. King (1994b) identified a definite relationship between magnetic susceptibility and stratigraphy through the GHT and identifies a magnetic signature with a magnetic low, then high amplitude anomaly and parallel low (Figure 3.10). King (1997) reinforced his earlier findings with additional correlations of magnetic susceptibility and stratigraphy from readings in the central Meguma that identify a similar magnetic low, high amplitude anomaly and parallel low over the GHT (Figure 3.9). See Table 3.1 for correlating stratigraphic nomenclature and GHT correlations in other studies. On account of the strict regulations over National parks the most recent aeromagnetic map for Kejimkujik National Park is from 1957 published by the Nova Scotia Department of Natural Resources (NSDNR, 1957).

3.4.3 Field Methods

A detailed ground magnetics survey was completed along the three NW-SE transects that cross the inferred contact between the Halifax and Goldenville Groups. A Scintrex MP-2 portable proton – precession magnetometer was used to collect the total field magnetic readings at 12.5 m intervals (Figure 3.11). Base station readings and time of day were recorded at the beginning and end of each transect to provide corrections for diurnal drift (Telford *et. al.*, 1990). The operator (Terry Goodwin) removed all magnetic material from his person during the course of the survey. Universal Transverse

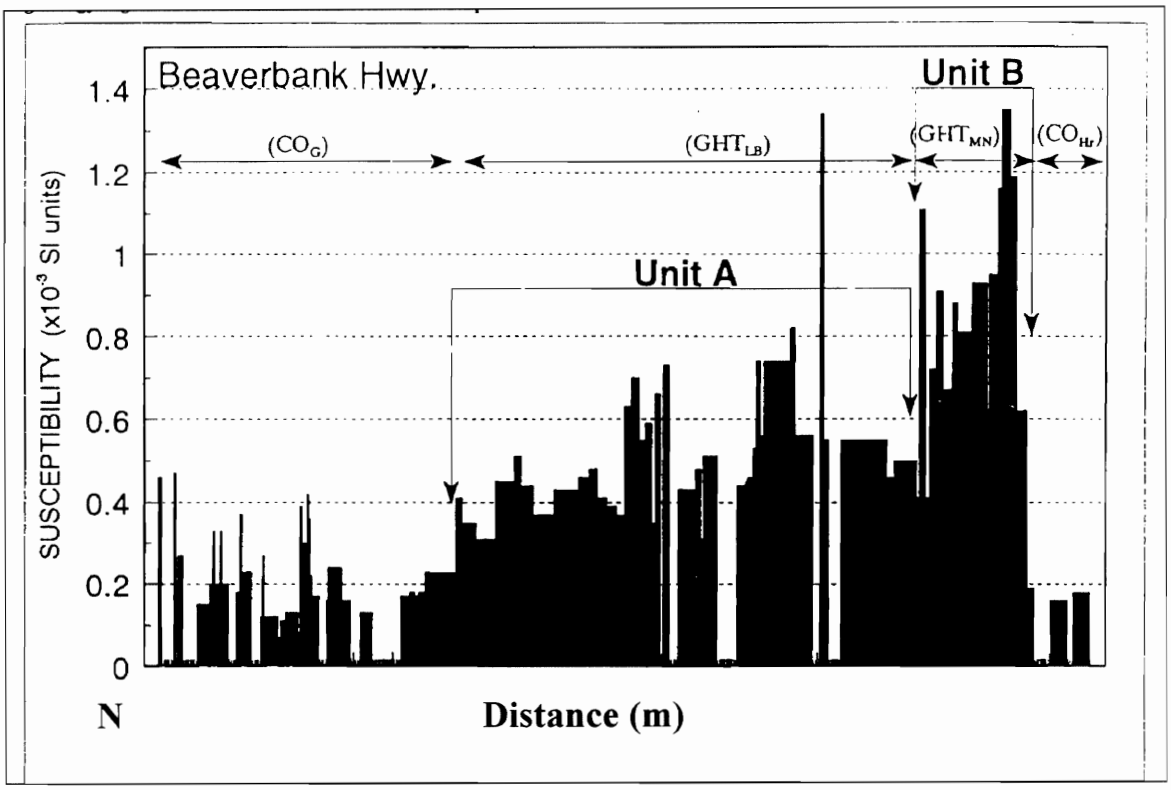

Figure 3.10 Magnetic susceptibility profile of area studied on the Beaverbank Hwy with geology and magnetostratigraphic units. Profile identifies a magnetic signature with a magnetic low, then high amplitude anomaly and parallel low (**CO_G** Goldenville Group, **GHT_{LB}** Goldenville-Halifax Transition lower beds, **GHT_{MN}** Goldenville-Halifax Transition upper beds, **CO_{HR}** Halifax Group-Rawdon unit) (King, 1994b)

Mercator (UTM) coordinates (NAD 27) were recorded with a Garmin GPS 12 at each reading for plotting purposes and correlation with till and rock sample locations (Appendix A-1). Corrections were subsequently performed on the raw data for diurnal drift.

3.4.4 Results and Discussion

The total field ground magnetic survey revealed from North to South a magnetic low characterized by the Goldenville Group, followed by a high magnetic anomaly (~400 nT) representing the GHT and a second magnetic low of similar amplitude that characterizes the Halifax Group (Figure 3.12). This low-high-low magnetic pattern was consistent throughout the three transects and confirms the GHT as a magnetic marker horizon. The profiles compare closely to the magnetic susceptibility data presented in Figure 3.9 and 3.10. Figure 3.13 indicates the location of the contact on the most recent published map by Horne and Corey (1994) and the location of the inferred contact within the GHT based on the interpreted magnetic anomaly. The magnetic anomaly may be associated with the upper beds of the transition zone that contain abundant pyrrhotite and minor ilmenite. Results of bedrock and surficial mapping constrain the geological boundaries between the Goldenville and Halifax Groups but the actual contact is not exposed within the study area. The position of the magnetic anomaly combined with the results of geological mapping in the field confirm the actual contact is 500 to 1000m north of the mapped contact shown by Horne *et al.* (1994). Outcrops mapped in the field confirm the inferred contact is 500 to 1000m north of the mapped contact shown by Horne and Corey (1994). The estimated thickness of the GHT is approximately 800 m based on the averaged thickness of the high magnetic anomaly from the 3 transects.

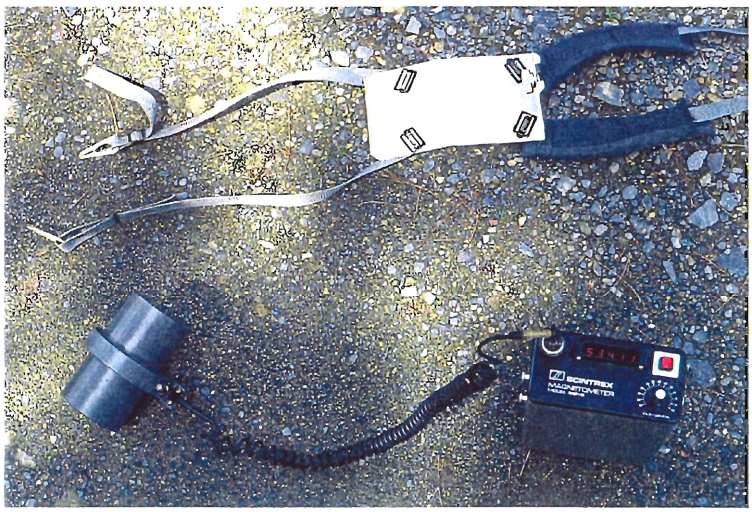

Figure 3.11 Scintrex MP-2 portable proton – precession magnetometer

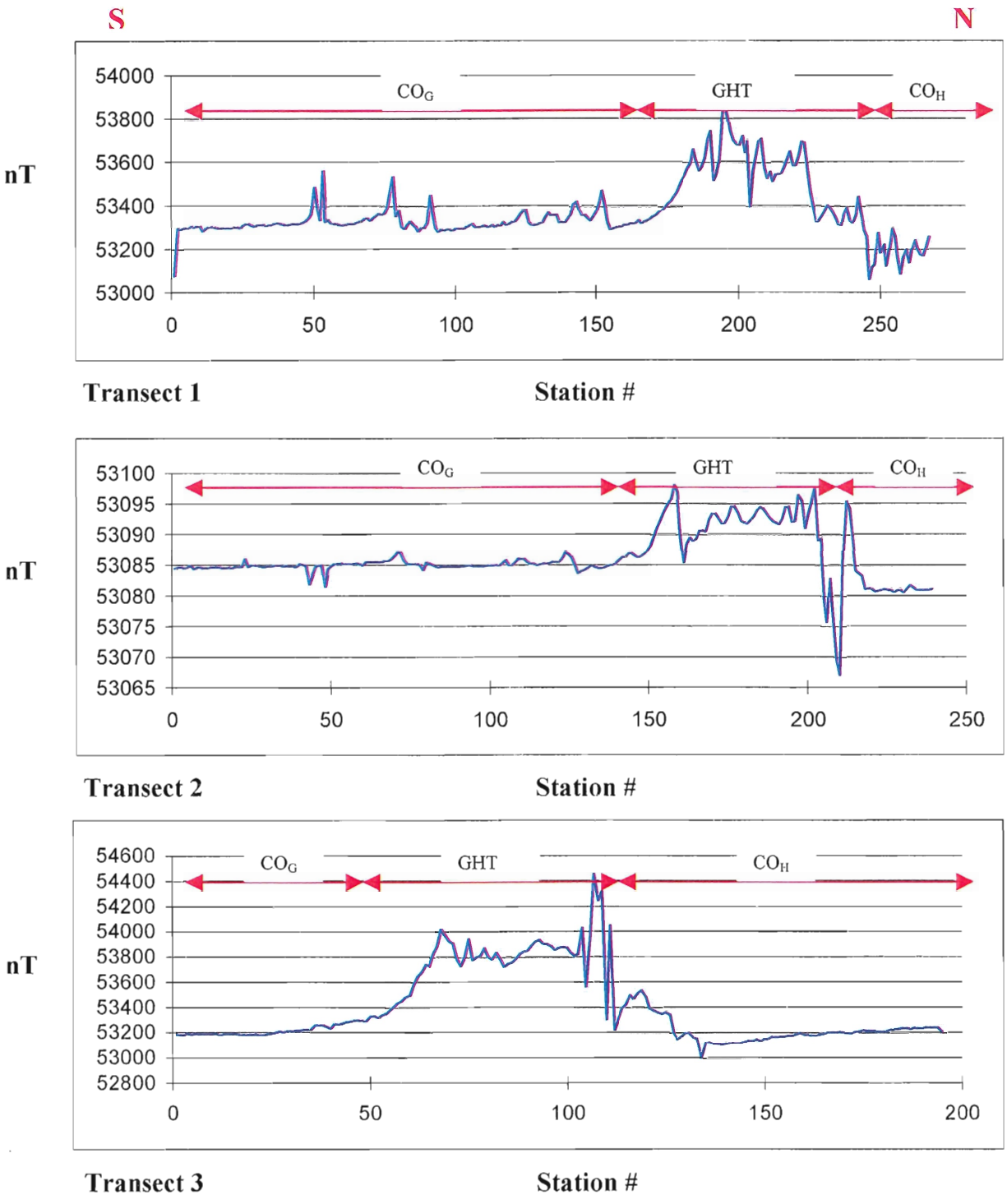

Figure 3.12 Total field magnetic survey profiles along the three transects with interpreted Goldenville Halifax Transition Zone ~800m (GHT), Goldenville Group (CO_G), and Halifax Group (CO_H). Stations are at 12.5m spacing. GHT positioned based on previous reports by King (1994a,b, 1995 and 1997) (Refer to Figure 3.13 for location map of inferred GHT. (Graphs generated using excel)

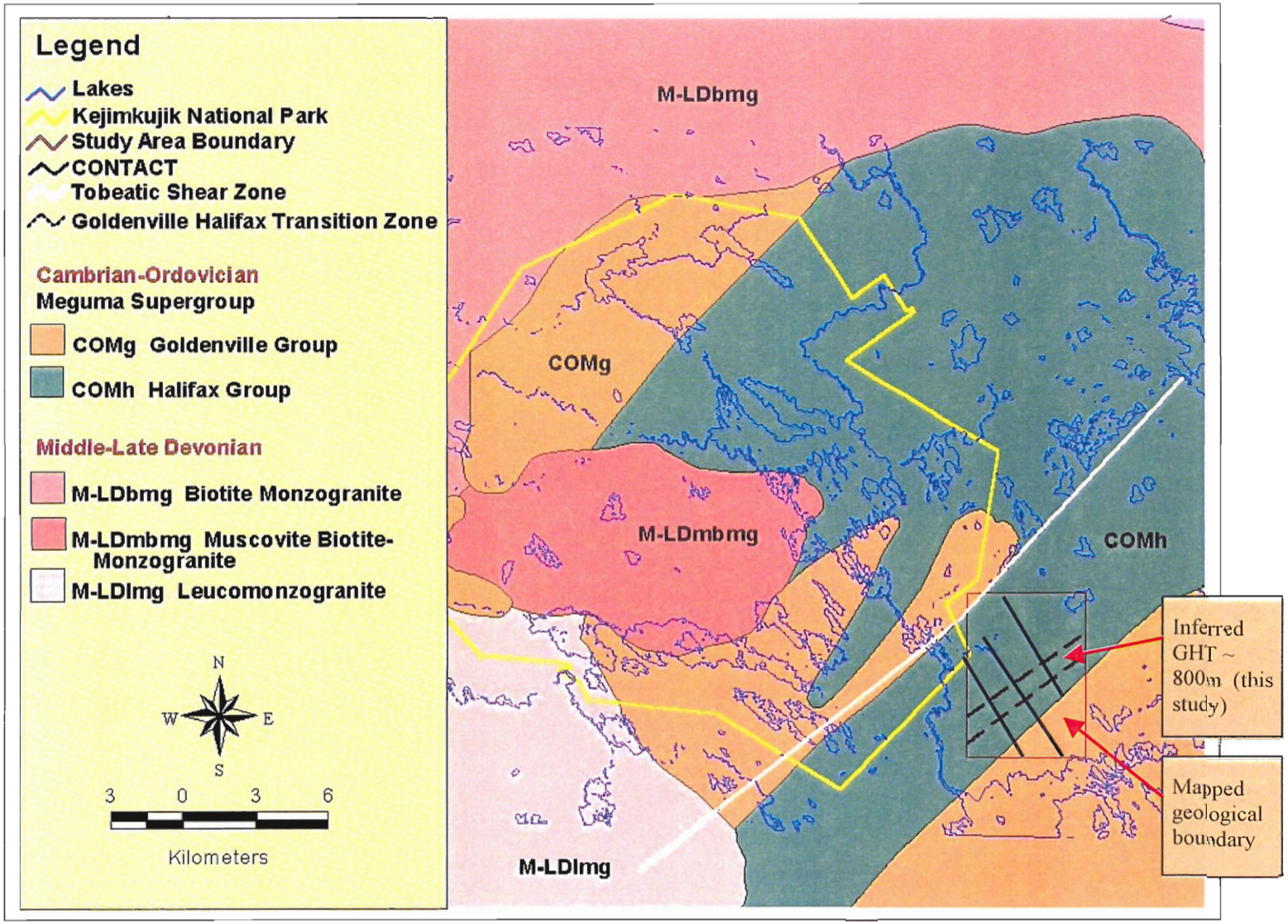

Figure 3.13 Geology map of inferred GHT and mapped contact within the study area. Solid black lines are transects (Horne *a*nd Corey,1994*)* (map generated using ArcView 3.2)

3.5 Summary

The study area is characterized by relatively few outcrops (< 2%) of the Goldenville and Halifax Groups. Geological mapping located the approximate location of the Goldenville-Halifax contact. However, interpreted results from detailed magnetic survey identified the Goldenville Group, the GHT and the Halifax Group. The actual contact between the two Groups is approximately 500 m to 1000 m north of the contact on recent published maps. Previous studies by Goodwin *et al.* (2000) indicate a possible spatial correlation between Hg in soil gas and the GHT. Therefore, identifying the exact location of the GHT is an important factor in interpreting the Hg geochemistry of the till.

Chapter 4 Till and Rock Geochemistry

4.1 Introduction: Till Geochemistry

Till sampling in Kejimkujik National Park is an integral component of the TSRI project. Understanding the levels of Hg in till will lead to better understanding of its role in Hg cycling. This study performed till sampling over the Halifax and Goldenville Groups including the GHT to investigate Hg concentrations related to till derived from each rock type and associated rock types including the GHT.

Two previous till geochemical surveys were completed in the Kejimkujik National Park. Boner *et al.* (1990) focused on tills associated with the South Mountain Batholith. Stea and Grant completed a study in 1988 sampling till over mainland Nova Scotia (Stea, 1982 and 1983; Stea and Grant, 1982). Both till sampling programs did not include Hg analysis. Goodwin *et al.* (in progress, 2002) are sampling tills for Hg in the Kejimkujik National Park area as well as throughout mainland Nova Scotia. Current studies by Goodwin *et al.* (in progress, 2002) indicate the highest Hg till values within Kejimkujik National Park are in the greywacke till (mean = 99.3 ppb, n= 6) over the Tobeatic Shear Zone. Next highest are the granite till (mean = 67.3 ppb, n=31), greywacke till (mean = 50.3 ppb, n = 11) and slate till (mean = 41.4 ppb, n = 49).

All fieldwork for this study was based on surficial mapping by Finck *et al.*, (1994). Although the surficial map indicated that Beaver River Till and Shelburne River Till are in the study area all till samples were collected from the Beaver River Till and Shelburne River Till was not encountered during till sampling.

4.2 Field Methodology: Till Samples

Thirty-two C horizon till samples were collected on three NW-SE trending transects from logging roads and woods trails (Figure 3.7). The samples were collected at an average depth of 1 m using a combination of a shovel and auger. Till samples for geochemical analysis were collected in kraft size sample bags (~ 500g) and immediately stored in coolers for transport to the laboratory for analysis (Figure 4.1). At each sample site GPS locations (NAD 27) and detailed site observations (color, till type, location descriptions etc.) were recorded (Appendix B-1). Five Kg till samples used for clast identification and counts were collected at each sample site along transect 2 and 3 by Terry Goodwin, Project Geochemist for Nova Scotia Department of Natural Resources during the 2000 field season (Figure 4.1).

4.3 Analytical Methodology: Till Samples

Till samples were dried at 35 °C and sieved (<63 microns) at the DalTech Minerals Engineering Centre in Halifax. Three sets of samples were prepared from the 32 till samples (1) 10g samples for Hg analysis (2) 50 g samples for Au and multi-element analysis (3) duplicate 50 g samples for archival purposes. Each of the three sample sets were placed in clean vials and stored at room temperature for analysis.

The 10g sample set was analyzed for Hg at ACME Analytical Laboratories in Vancouver, British Columbia. Samples for Hg analysis were digested in an aqua regia mixture of 1:1:1 H_2O-HCL-HNO_3 and analyzed by Cetac Cold Vapour - Atomic Absorption (Cetac CV-AA). The 50 g sample set was analyzed for trace elements (Au-

Figure 4.1 (Top Photo) Large plastic bags were used to collect 5 Kg till samples for clast identification and counts. The smaller kraft size sample bag was used to collect a ~ 500 g sample for geochemical analysis. (Lower Photo) Till samples used for this study come from the relatively unoxidized tan coloured till from the c-horizon on the right. The red brown till on the left overlies the unoxidized till and was not sampled.

Ag-Cu-Pb-Zn-Mo-Ni-Co-Cd-Bi-As-Sb-Fe-Mn-Te-Ba-Cr-V-Sn-W-La-Al-Mg-Ca-Na-K-Sr-Y-Ga-Li-Nb-Sc-Ta-Ti-Zr-S) at Bondar Clegg in Val d'Or, Quebec. For trace elements analysis (excluding Au) samples were digested in an aqua regia mixture of HCL and HNO_3 and analyzed by Inductively Coupled Plasma/Atomic Emission Spectroscopy (ICP/AES). Au was analyzed by Fire Assay/Atomic Emission Spectroscopy (FA/AES). Appendix B-2 outlines the complete techniques and lower/upper detection limits used during analysis.

The clast identification and counts were completed on 11 samples collected from transect 2 and 3 during the 2000 field season. Each 5 kg sample was sieved (> 4 mm) at the DalTech Minerals Engineering Centre in Halifax. Each sample was separated into groups of similar pebble types, counted and significant characteristics were noted (Appendix B-3)

4.4 Quality Assurance/Quality Control (QA/QC)

To ensure accuracy in the data set strict QA/QC protocols and procedures were followed during sample collection, preparation and analysis. Two certified standards, two field duplicates and one analytical replicate were included with the 32 till samples. ACME laboratories inserted analytical replicate and internal standards during Hg analysis. As a check on analytical precision for the multi-elements, random samples were sent to ACME and compared to results reported by Bondar Clegg.

4.5 Results: Till Samples

4.5.1 Hg Levels in Till

The highest reported Hg value for all the samples were found in till derived from the Halifax Group slates ranging from 13.2 ppb to 151.5 ppb (n = 20, mean 40.8 ppb, sd = 31.12) (Figure 4.2). Till derived from the Goldenville Group meta-sandstone contain Hg values ranging from 6.6 ppb to 71.2 ppb (n = 12, mean 32.4 ppb, sd = 19.21) (Figure 4.3). Figure 4.4 illustrates the study area and sample locations with proportional symbol plots representing Hg concentrations in relation to geological contacts (full data sheet in appendix B-4). Sample locations and Hg values are represented in Figure 4.4. Analytical results are presented in appendix B-4.

4.5.2 Frequency Histograms

A frequency histogram is a useful preliminary statistical representation to show (1) the symmetry of the data, (2) the total range and range of greatest abundance (mode) and (3) to distinguish between background and anomalous values (Sinclair, 1976). The areas of the bars are proportional to the relative frequencies. A smooth curve called a density curve of distribution is fitted to the histogram to describe the shape of the curve. Smaller sample sizes are more prone to be skewed where larger sample sizes often conform to a normal distribution. Positive skewed data is commonly encountered in earth science related variables such as minor elements in geochemical mineral exploration, geophysical variables and sediment size data (Sinclair, 1976).

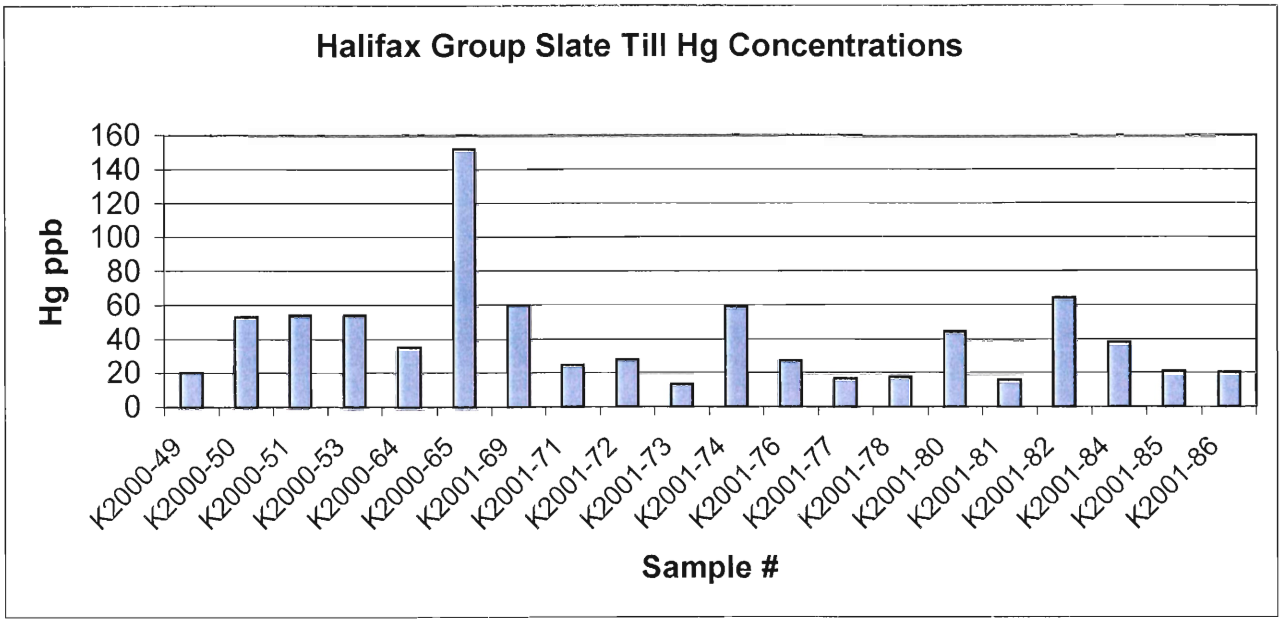

Figure 4.2 Halifax Group slate till Hg concentrations ranging from 13.2 ppb to 151.5 ppb (n = 20, mean 40.8 ppb, sd =31.12) (graph generated using excel)

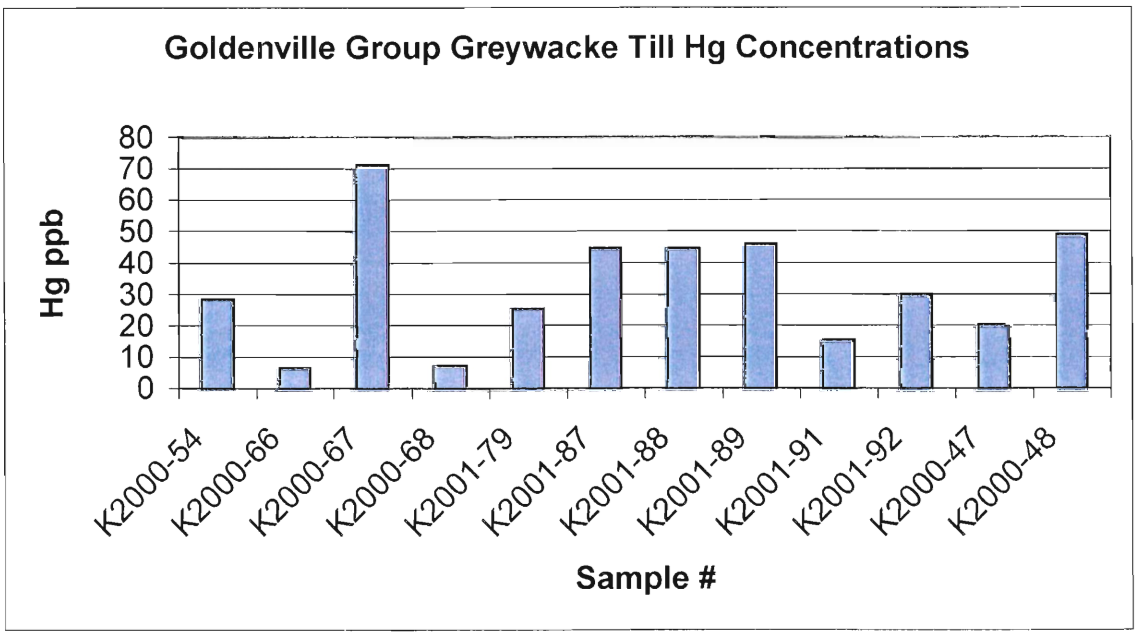

Figure 4.3 Goldenville Group greywacke till Hg concentrations ranging from 6.6 ppb to 71.2 ppb (n = 12, mean 32.4, sd = 19.21) (graph generated using excel)

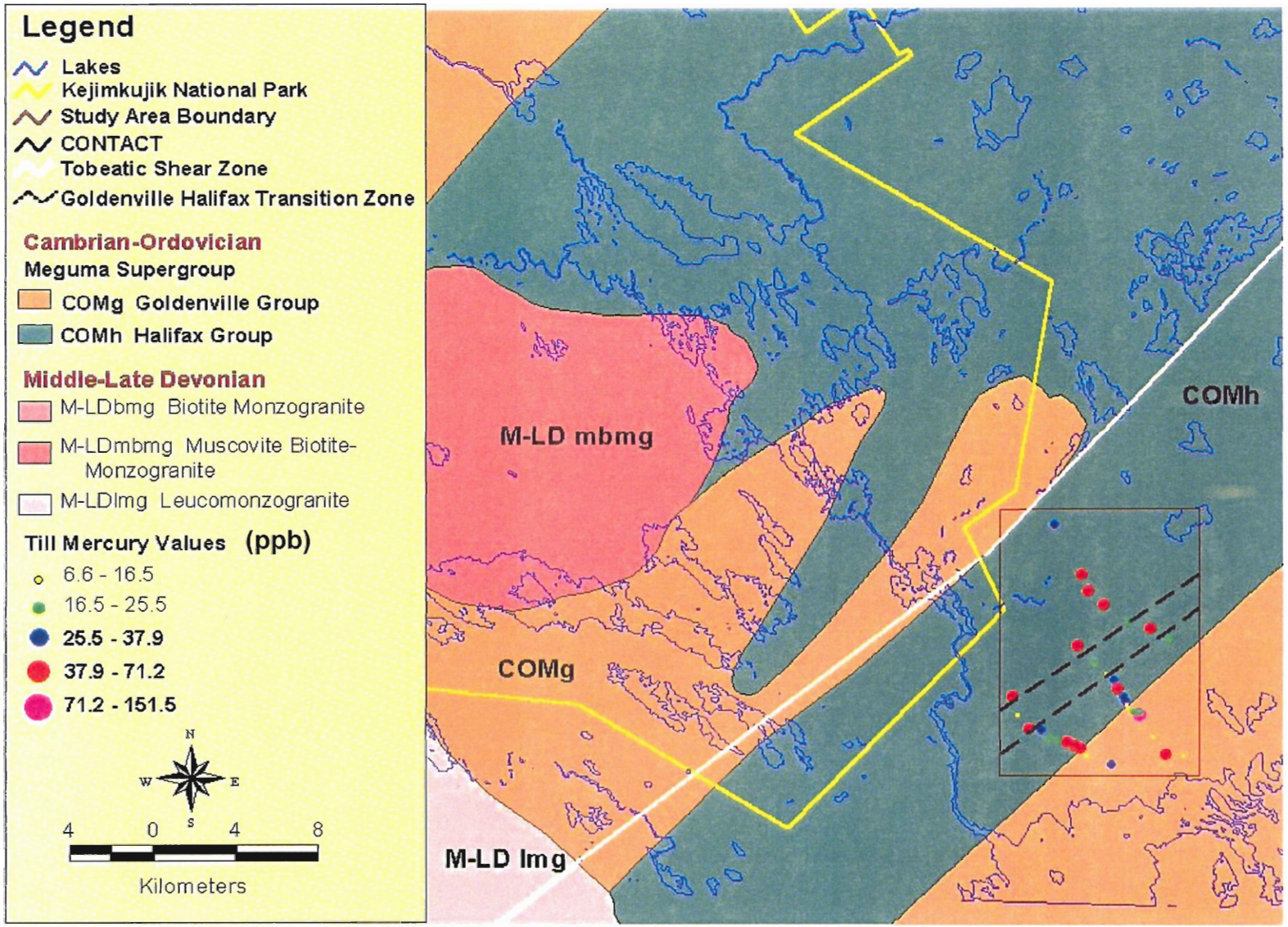

Figure 4.4 Sample locations and associated Hg (ppb)results (Horne *et al.* 1994) (map generated using ArcView 3.2)

Outliers are deviations from the overall pattern and can amplify the skewed shape. In some cases the outliers could be removed before further statistical analysis (Moore and McCabe, 1993).

The 32 Hg till samples plotted in a frequency histogram are positively skewed with only one peak (Figure 4.5). If the outlier (151.5) is removed the Hg data conforms to a bimodal distribution (Figure 4.6). The single peak on the histogram of all Hg data (outlier included) indicates that there is only one population or geological control. Although, with the outlier removed the distribution could be interpreted as bimodal, this study will analyze the data with the outlier included. To further illustrate, the till samples are separated into slate till and greywacke till (Figure 4.7 and 4.8). Figure 4.7 shows the positive skewed frequency histogram of the slate till and the effect on the histogram after the outlier is removed. Once the outlier is removed the histogram bimodal distribution. The mean of the slate till with the outlier removed (35.0 ppb) is very similar to the mean of the greywacke till (32.4 ppb) (Figure 4.8).

4.5.3 Probability Plot

In the case of a skewed frequency distribution the data must be transformed to follow a normal distribution for statistical analysis (Wheater and Cook, 2000). Data transformation can be done in several ways but the most common method in positive skewed geochemical data is log transformation (Lepeltier, 1969; Sinclair, 1976; 1990; Wheater and Cook, 2000)). In geochemical surveys lognormal distribution curves are the most commonly used to view the results of geochemical data (Lepeltier, 1969 and Sinclair, 1976; 1990).

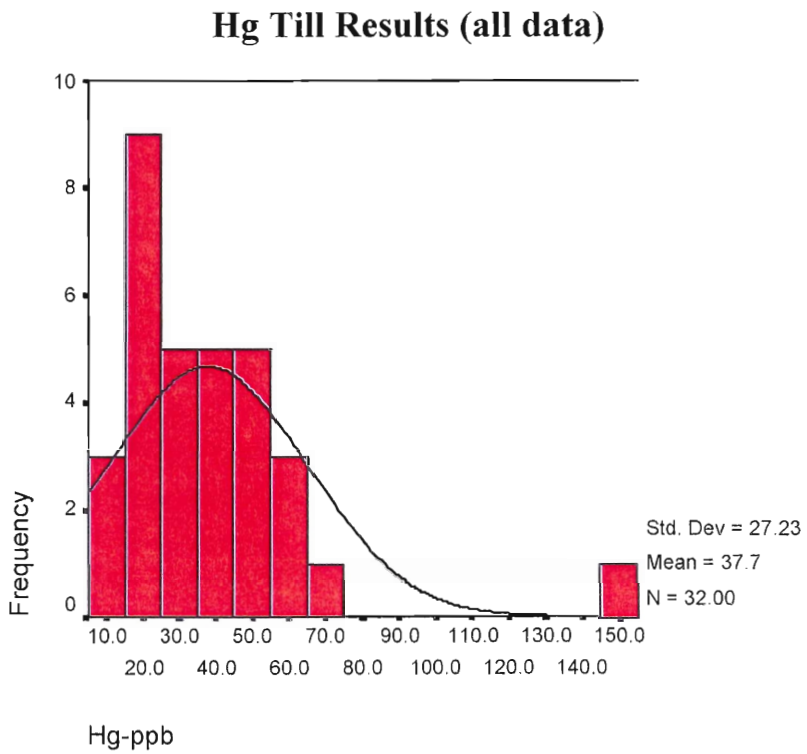

Figure 4.5: Slightly positive skewed frequency distribution for all Hg values (generated using SPSS).

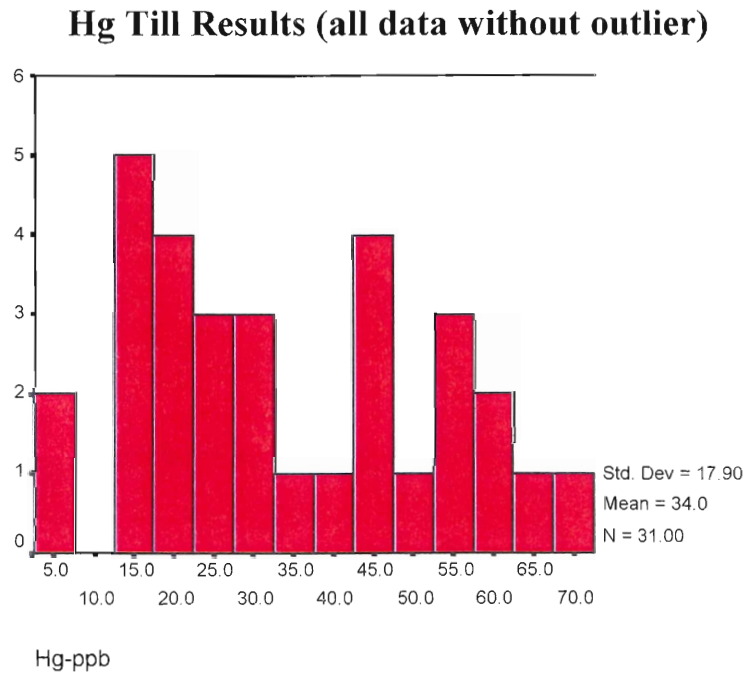

Figure 4.6: Bimodal frequency distribution once the outlier (151.5 ppb) is removed. (Generated using SPSS).

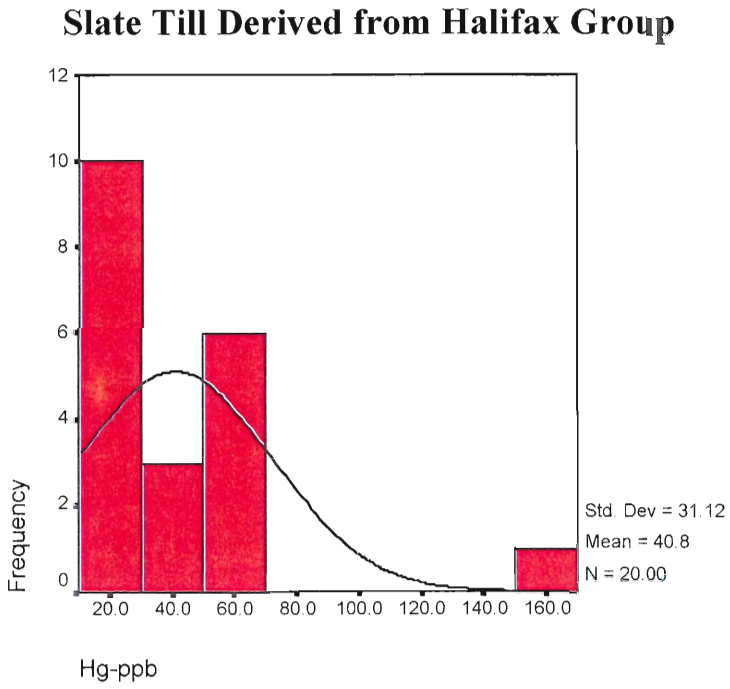

Figure 4.7 Comparison of frequency distribution of Hg values in slate till. Frequency histogram on the bottom with the outlier (151.5 ppb) removed has bimodal distribution and mean similar to the meta-sandstone samples. (Generated using SPSS).

Greywacke Till Derived from Goldenville Group

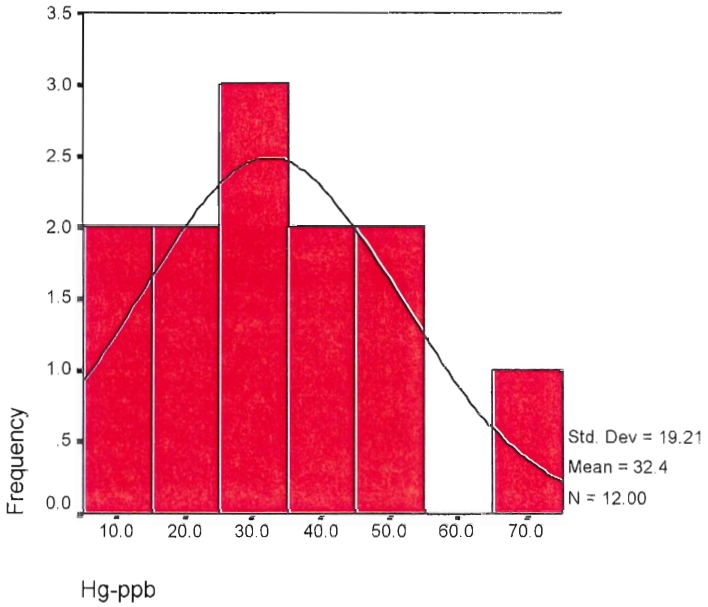

Figure 4.8 Greywacke till derived from Goldenville Group displaying normal distribution (Generated using SPSS).

Because of the nature of the probability scale a single, cumulative, normal population plotted over the full probability range would plot as a straight line with some scatter produced by sampling error. Different populations or geological controls within the data sampled can be identified using this graphical method (Sinclair 1976; 1990).

The lognormal probability plot was generated using an interactive website Statpoint (http, 2002) and accuracy rechecked on a hand plotted graph (Appendix B5). The 32 Hg values are transformed by plotting values on the x-axis log scale (Figure 4.9). On the y-axis the cumulative percent is calculated using Blom's method of proportion estimation (p) and plotted on the probability scale (Figure 4.9).

Blom's Method:

$$p = 100(i-0.375)/(n+0.25)$$

Where: p = cumulative percent
i = Hg values rated from 1 to 32 (sorted smallest to largest)
n = number of samples

The log probability plot of Hg for all 32 samples basically indicates one population of Hg as the data values fit to a straight line (Figure 4.9). If there were more than one population there would be a set of data points that another line could be fitted through (Sinclair 1976, 1990). The minimal scatter is usually more prominent in small data sets like this and is more pronounced at the end of the graph.

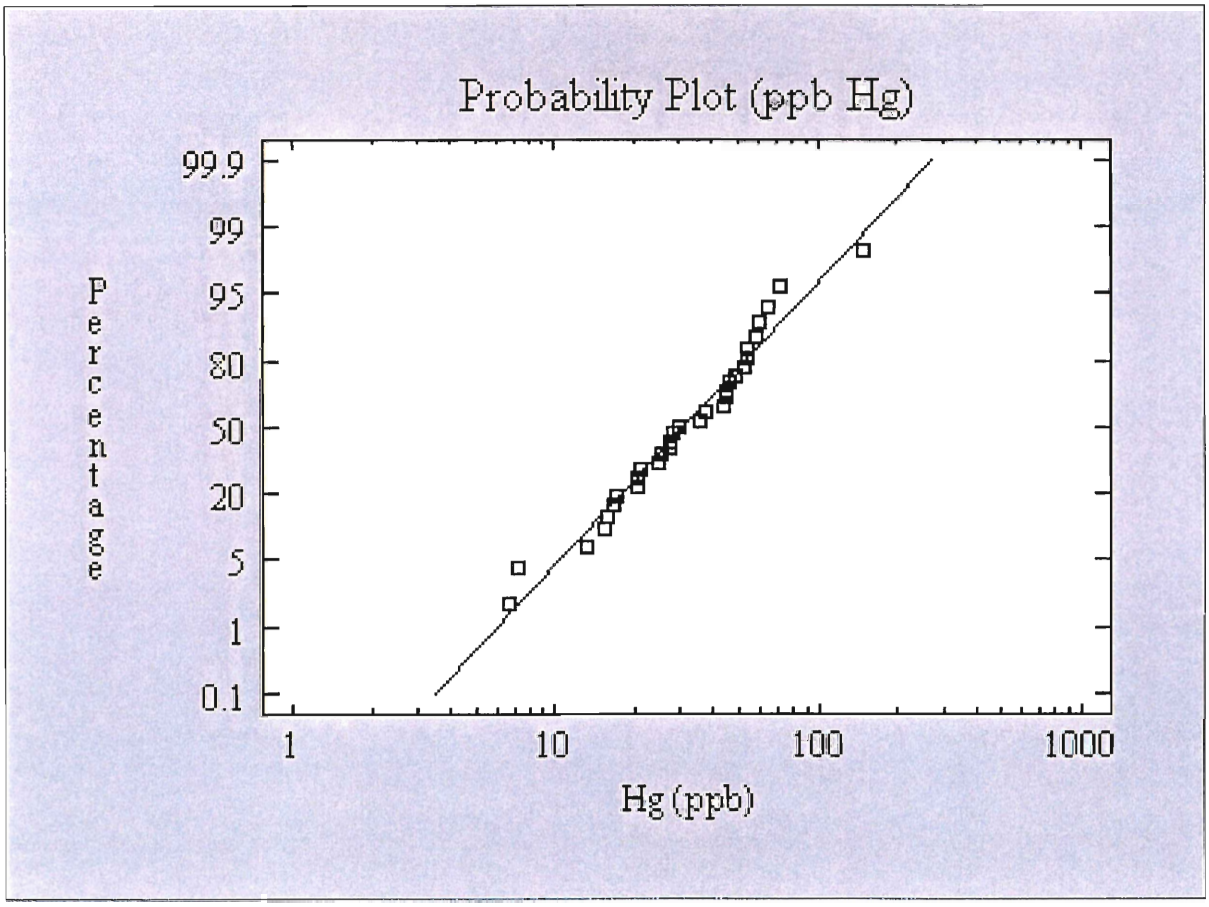

Figure 4.9 Log probability plot of Hg (ppb) in till samples using the procedures of Lepeltier (1969), Sinclair (1976, 1990). The data is fitted to a single line therefore illustrating a normal distribution. Log probability plot generated on interactive software site http://www.sgcorp.com/probability_plots.htm and accuracy rechecked using hand drawn graph (Appendix B5).

4.5.4 Clast Identification and Counts

The clast identification and counts from the >4mm pebble fraction of the till samples from transect 2 and 3 reveal a distinct difference in till types (Figure 4.10). The slate till derived from the Halifax Group and the greywacke till derived from the Goldenville Group are most prevalent. Figure 4.11 illustrates how glaciers erode the underlying bedrock distributing till down ice from its source. Clast identification and counts are a direct reflection of the underlying bedrock and how far glacier transport is in the area (i.e. renewal distance). The general SE direction of ice flow is confirmed from the renewal distance (~ 900m) of the greywacke clasts down ice from the geologic contact (near sample 48) of the Halifax/Goldenville Groups interpreted from the total field magnetic survey (section 3.4). The graph also indicates the relative width of the bedrock type (slate) scoured by the base of the glacier (Figure 4.10). Based on this it is determined that the areal extent of the bedrock is smaller than reported on recent published maps.

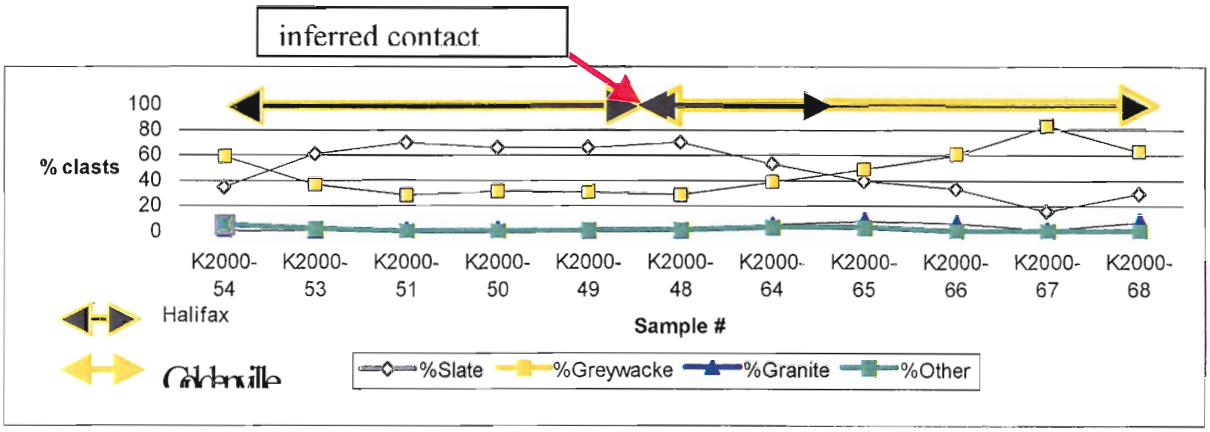

Figure 4.10: Clast counts from samples collected along transect 2 and 3 and incorporated into the same plane. The clast counts distinguish between the two main till types, Halifax Group (slate till) in grey and Goldenville Group (greywacke till) in yellow. The black arrow indicates the greywacke renewal distance (~900m). (Generated using Microsoft Excel)

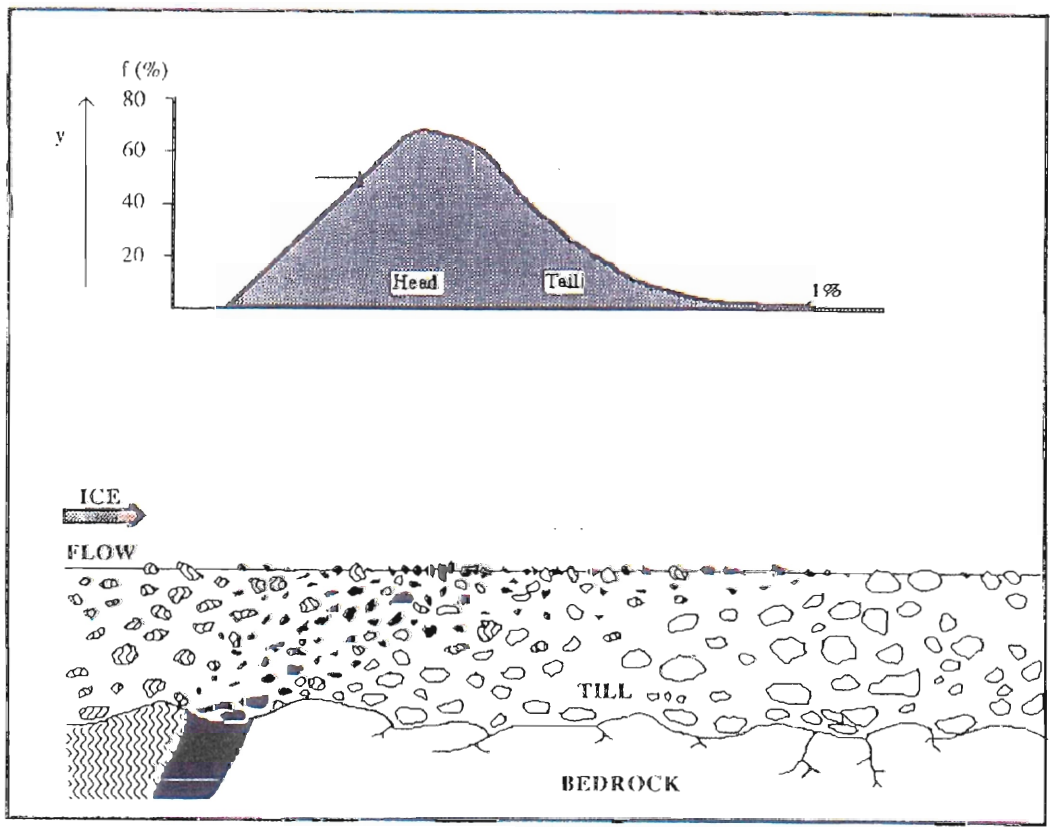

Figure 4.11 Till scoured from the underlying bedrock and is transported down ice during glacier movement (Kujansuu and Saarnisto, 1990).

4.5.5 Correlation Matrix

Correlation coefficients are used to measure the degree that two variables vary together or the strength of a relationship between two variables (Wheater and Cook, 2000). In this thesis, the relationship between Hg and 34 other elements is investigated through a correlation matrix. The correlation matrix is useful for a preliminary look at data to determine relationships with sources providing direction for further studies (Wheater and Cook, 2000). To ensure statistical accuracy, correlation matrices were plotted in Quattro Pro, Excel and SPSS. Each program generated identical (r) coefficient values. The correlation matrix in Table 4.1 was generated using Quattro Pro.

The Pearson's product moment correlation coefficient is used to calculate the (r) correlation coefficient. The Pearson formula is a measure of linear association between two variables therefore is only useful when two parameters have a linear relationship. Values of the correlation coefficient range from -1 to 1. The sign of the coefficient indicates the direction of the relationship (positive sign is a positive relationship and negative sign is a negative relationship), and its absolute value indicates the strength, with larger absolute values indicating stronger relationships. There is less correlation between variables as they near zero. The formula for the Pearson's product moment correlation is:

$$r = \frac{n\sum xy - \sum x \sum y}{([n\sum x^2 - (\sum x)^2][n\sum y^2 - (\sum y)^2])^{1/2}}$$

Where: r = correlation coefficient
n = number of data pairs
x = data point for one parameter
y = data point for the other parameter

	Hg-ppb	Au-ppb	Cu-ppm	Pb-ppm	Zn-ppm	Mo-ppm	Ni-ppm	Co-ppm	Cd-ppm	As-ppm	Fe-pct	Mn-ppm	Ba-ppm
Hg-ppb	1												
Au-ppb	-0.200	1											
Ag-ppm	0.000	0.000											
Cu-ppm	-0.064	-0.121	1										
Pb-ppm	0.243	-0.072	**0.464**	1									
Zn-ppm	0.334	0.030	**0.496**	**0.842**	1								
Mo-ppm	-0.086	0.002	**0.351**	-0.014	0.103	1							
Ni-ppm	-0.068	0.087	**0.596**	**0.562**	**0.752**	0.156	1						
Co-ppm	-0.254	-0.004	**0.891**	**0.421**	**0.438**	0.333	**0.661**	1					
Cd-ppm	-0.037	-0.053	**0.423**	0.026	-0.158	**0.495**	-0.068	**0.399**	1				
As-ppm	-0.087	0.179	**0.757**	**0.548**	**0.643**	**0.465**	**0.704**	**0.763**	0.334	1			
Fe-pct	-0.154	0.036	**0.675**	0.049	0.321	**0.737**	**0.456**	**0.634**	0.413	**0.715**	1		
Mn-ppm	-0.287	0.199	**0.373**	0.108	0.480	0.205	**0.734**	**0.459**	-0.325	**0.547**	**0.559**	1	
Ba-ppm	-0.288	0.358	0.312	0.129	**0.438**	0.293	**0.466**	**0.366**	-0.242	**0.368**	**0.515**	**0.690**	
Cr-ppm	-0.061	0.134	**0.484**	0.222	**0.495**	**0.647**	**0.679**	**0.565**	0.210	**0.622**	**0.788**	**0.632**	**0.57**
V-ppm	**0.484**	0.063	0.344	0.181	**0.628**	0.304	**0.441**	0.258	-0.098	**0.403**	**0.563**	**0.490**	**0.55**
La-ppm	-0.372	0.559	0.269	0.064	0.263	0.218	**0.464**	**0.436**	-0.101	0.345	**0.407**	**0.631**	**0.72**
Al-pct	**0.793**	-0.025	0.063	0.161	**0.484**	-0.004	0.105	-0.087	-0.194	0.053	0.157	0.070	0.20
Mg-pct	-0.333	0.233	**0.411**	0.222	**0.558**	**0.424**	**0.779**	**0.504**	-0.163	**0.621**	**0.672**	**0.917**	**0.75**
Ca-pct	-0.021	-0.071	0.152	**0.526**	**0.453**	-0.361	**0.414**	0.298	-0.177	0.180	-0.223	0.114	0.06
Na-pct	-0.161	**0.417**	0.048	-0.096	0.303	0.158	0.347	-0.033	-0.460	0.256	**0.372**	**0.707**	**0.68**
K-pct	-0.264	0.247	0.226	0.042	**0.431**	0.243	**0.437**	0.261	-0.359	0.325	**0.490**	**0.720**	**0.91**
Sr-ppm	-0.439	**0.473**	-0.032	-0.137	-0.055	0.113	0.034	0.145	-0.109	-0.003	0.165	0.297	**0.63**
Y-ppm	-0.196	0.329	**0.473**	**0.488**	**0.554**	0.070	**0.605**	**0.596**	-0.041	**0.524**	0.275	0.450	**0.55**
Ga-ppm	**0.786**	-0.044	-0.084	0.098	0.363	-0.214	-0.077	-0.273	-0.289	-0.124	-0.059	-0.081	0.04
Li-ppm	0.106	0.194	**0.350**	0.127	**0.594**	**0.365**	**0.684**	0.377	-0.201	**0.503**	**0.666**	**0.835**	**0.67**
Nb-ppm	**0.664**	-0.133	-0.196	0.045	-0.001	-0.243	-0.212	-0.273	0.004	-0.375	-0.327	-0.516	-0.32
Ti-pct	0.092	-0.115	**0.369**	**0.832**	**0.643**	-0.253	**0.445**	0.325	-0.070	0.344	-0.171	0.019	0.05
Zr-ppm	-0.206	0.181	0.241	0.025	0.366	**0.553**	**0.459**	0.274	-0.138	0.416	**0.659**	**0.659**	**0.68**
S-pct	0.250	**0.376**	-0.059	-0.036	0.041	-0.003	-0.188	-0.060	0.038	-0.031	0.076	-0.108	0.31

Table 4.1 Correlation matrix of till Hg with trace elements continued on next page. Significant (r) values are > 0.349 (P = 0.05) and in bolded text for easy identification (Matrix generated using Quattro Pro).

Cr-ppm	V-ppm	La-ppm	Al-pct	Mg-pct	Ca-pct	Na-pct	K-pct	Sr-ppm	Y-ppm	Ga-ppm	Li-ppm	Nb-ppm	Ti-pct	Zr-ppm	S-pct
1															
0.589	1														
0.469	0.255	1													
0.175	**0.835**	-0.040	1												
0.815	**0.514**	**0.639**	0.037	1											
-0.106	0.004	0.206	0.007	0.086	1										
0.326	**0.467**	**0.544**	0.206	**0.667**	-0.034	1									
0.532	**0.611**	**0.549**	0.247	**0.774**	0.062	**0.745**	1								
0.192	0.022	**0.808**	-0.142	0.326	0.137	0.390	**0.463**	1							
0.318	0.299	**0.683**	0.032	**0.477**	**0.588**	0.310	**0.454**	**0.452**	1						
-0.082	**0.690**	-0.182	**0.941**	-0.156	0.011	0.145	0.138	-0.200	-0.040	1					
0.818	**0.820**	**0.538**	**0.475**	**0.859**	-0.024	**0.647**	**0.718**	0.199	0.347	0.279	1				
-0.206	0.160	-0.216	**0.494**	-0.503	0.092	-0.354	-0.418	-0.176	-0.052	**0.551**	-0.182	1			
-0.113	0.003	0.030	0.060	0.053	**0.726**	-0.100	0.008	-0.076	**0.505**	0.078	-0.107	0.024	1		
0.690	**0.535**	**0.553**	0.194	**0.784**	-0.135	**0.619**	**0.730**	**0.382**	0.325	0.030	**0.747**	-0.385	-0.075	1	
0.012	0.291	**0.380**	**0.448**	-0.110	-0.044	0.137	0.145	**0.596**	0.182	0.420	0.085	0.334	-0.005	0.190	1

Table 4.1 Correlation matrix (continued) of till Hg with trace elements. Significant (r) values are > 0.349 (P = 0.05) and in bolded text for easy identification (Matrix generated using Quattro Pro).

The significance of (r) value correlation depends on (1) the number of data pairs and (2) the probability of the computed (r) values being obtained by chance (Wheater and Cook, 2000). To determine the importance of the correlation, the coefficient of determination is measured. The coefficient of determination is the proportion of the variation that the two variables have in common simply calculated by finding the square of the (r) value and representing it as a percentage multiplying by 100.

In this situation in order for the (r) correlation values to be significant using a sample number (n) of 32 and a 95% probability that the values are not obtained by chance (P=0.05), (r) values must be ≥ 0.349 (Wheater and Cook, 2000). Before the correlation matrix was generated any elements that reported below the lower detection limit for all samples were removed. These elements include Ag, Bi, Sb, Te, Sn, W, Sc, and Ta. Significant values (≥ 0.349) are highlighted in bold in Table 4.1. There is a significant positive relationship between Hg and Al (0.793), Ga (0.786), Nb (0.664) and V (0.484). To explain this more clearly, in the case of Hg and Al there is a highly significant positive relationship with the two elements having 63% of the variation in common (coefficient of determination; $0.793^2 = .6288 \times 100 = 63\%$).

4.6 Discussion: Till Samples

The highest amount of Hg is found in the Halifax Group slate till although both greywacke and slate till Hg values are quite comparable. Based on the correlation matrix the highest correlation with Al could be associated with the Al bearing phyllosilicates in the fine silts and clay size fraction (<63 microns) where Hg is predominately found. For

example Plouffe (1997) indicates that most base metals in unstable mineral phases (e.g. pyrite) are enriched in the clay-size material due to the primary enrichment of metals in phyllosilicates of bedrock and that the metals usually absorb on the clay particles during weathering of the bedrock. There is no significant correlation with sulphur possibly indicating that cinnabar or other sulphide bearing minerals such as pyrite or pyrrhotite are not related to Hg concentrations. In sphalerite (ZnS) there can be up to 20 mole % of HgS in solid solution, but there is no significant relationship between Hg, Zn and S indicated by the correlation matrix (Loukola-Ruskeeniemi, 1990). There is only one geological control affecting Hg values for examples lithology or mineralogy based on the single straight line on the probability plot. The majority of the till Hg values are well within the range of normal till reported by Jonasson and Boyle (1972) outlined in Table 2.1.

Figure 4.4 indicates that there is no direct correlation of increased Hg values with the GHT. Clast identification and counts identify the location of the dominant till types (slate and greywacke) and the relationship to the underlying bedrock. Analysis of the field mapping, clast identification and counts, total field magnetic survey and interpretation from a 1957 aeromagnetic map of the area indicate that the actual size of the Halifax Group is smaller than reported on the most recent maps.

4.7 Introduction: Rock Geochemistry

In addition to the till sampling in the study area, rock samples were collected in order to investigate a link between till and rock Hg values associated with the GHT. Several rock sampling studies by Smith (2000), Sangster *et.al.* (2001) and Page (2001)

(Results noted in section 2.5.3) investigated Hg content in rocks throughout the Kejimkujik National Park area but limited sampling concentrated on the GHT as a possible source of Hg. The pyrite and pyrrhotite rich layers of the GHT could be an important component with respect to the release of Hg into the environment. Fox *et al.*, (1997) indicate that sulphide mineral oxidation allows the release of heavy metals possibly releasing Hg into the environment.

4.8 Field Methodology: Rock Samples

Nine rock samples were collected from outcrops in ditches located along the three NW-SE transects in the study area. Fieldwork was based on bedrock mapping by Horne and Corey (1994). Although outcrops were rare, an attempt was made to collect samples free from dirt and excessive weathering. At each sample site, rock descriptions and location details were recorded as well as GPS locations (Appendix B-6). Rock samples were placed in labeled plastic bags and stored at room temperature for Hg and multi-element analysis (Figure 4.12).

4.9 Analytical Methodology: Rock Samples

The rock samples were crushed and pulverized to <105 micron size fractions at the DalTech Minerals Engineering Centre in Halifax. Two samples sets were prepared (1) for Hg analysis and (2) for Au and trace element analysis (listed in section 4.3).

Analytical procedures for sample analysis are identical to the analytical methods for till described above in section 4.3. Similar to the till samples, strict QA/QC

procedures were followed during the collection, preparation and analysis of the rock samples.

Figure 4.12 Rock sample from slate outcrop on north end of transect 2.

4.10 Results/Discussion: Rock Samples

The 9 rock samples contained low Hg values ranging from 0.2 ppb to 3.4 ppb (mean 2.37 ppb, n= 9, sd = 0.91) shown in Figure 4.13 (full description and data sheet in Appendix B-6 and B-7). A correlation matrix yielded no significant correlations (r = 0.602 at P = 0.05) (Table 4.2). Polished thin sections were prepared for each sample examined for sulphide mineral content (Appendix B-8). Only sample 8 and 9 had significant amounts of sulphide minerals including pyrite, pyrrhotite, chalcopyrite and possibly marcasite.

Rock samples 8 and 9 contain significant amount of sulphide minerals but Hg values are low. Therefore, a correlation between the sulphidic black slates and

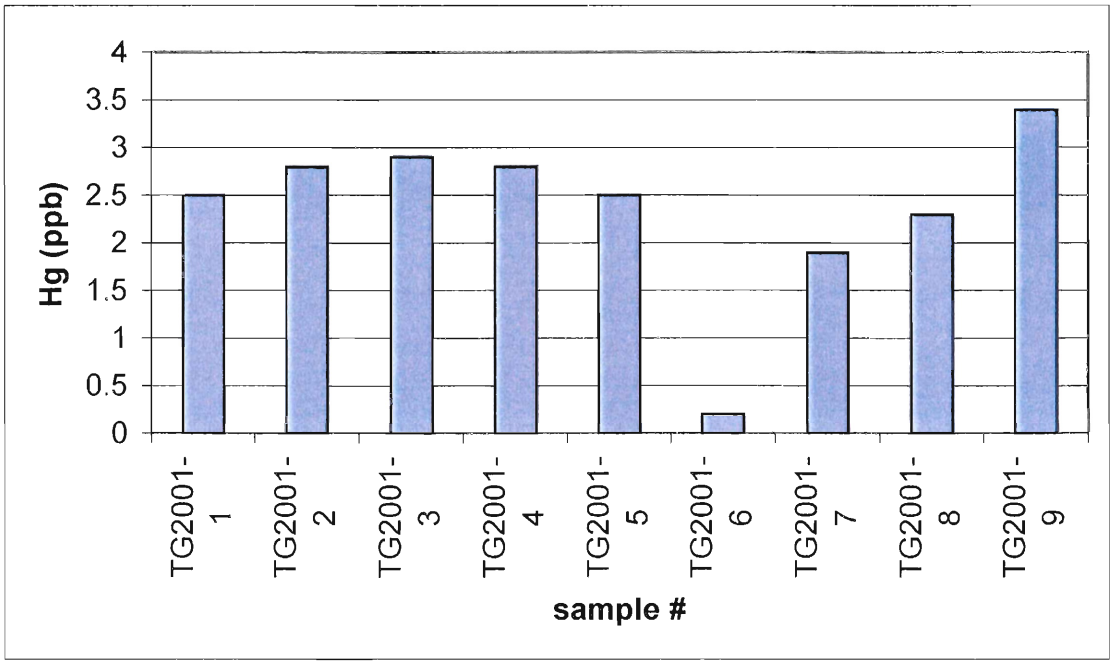

Figure 4.13 Rock samples Hg values ranging from 0.2ppb to 3.4 ppb (mean 2.37 ppb, n= 9, sd = 0.91). Sample 4 is greywacke all others are slate samples.

Hg is not evident. Hg values for the 9 rock samples are below the average Hg values for rock listed in Table 2.2. Smith (2000) reported a slightly higher mean Hg value of 3.3 ppb for a broader suite of rock types. The low number of rock samples requires a high correlation coefficient to be significant causing there to be no significant correlations between Hg and other elements. Previous study by Smith (2000) have significant correlations with Ca, Cd, Co, Cr, Fe, Mg, Ni, Sb, Sr, and V. Page (2001) found significant correlations between Hg and Ca, Co, Fe, Ga, Mg, Mn, Mo, S, Sr, Te, and V.

	Hg-ppb	AU	Cu	Pb	Zn	Mo	Ni	Co	Cd	As	Fe	Mn
Hg-ppb	1.00											
AU	0.14	1.00										
Cu	0.42	0.43	1.00									
Pb	0.20	0.55	0.84	1.00								
Zn	-0.50	-0.86	-0.46	-0.59	1.00							
Mo	0.20	0.28	0.35	0.63	-0.43	1.00						
Ni	-0.44	-0.54	-0.72	-0.70	0.56	-0.62	1.00					
Co	-0.65	-0.75	-0.69	-0.63	0.81	-0.43	0.87	1.00				
Cd	0.22	0.08	0.21	0.09	0.09	0.24	-0.28	-0.30	1.00			
As	0.04	-0.16	0.44	0.48	0.19	0.46	-0.19	-0.05	0.66	1.00		
Fe	-0.44	-0.79	-0.32	-0.51	0.94	-0.35	0.31	0.65	0.09	0.11	1.00	
Mn	-0.26	-0.72	-0.38	-0.67	0.84	-0.45	0.45	0.60	0.26	0.07	0.86	1.00
Ba	0.51	0.55	0.30	0.30	-0.75	0.25	-0.18	-0.51	0.01	-0.10	-0.76	-0.38
Cr	0.34	0.20	-0.19	-0.23	-0.42	-0.15	0.19	-0.12	-0.32	-0.56	-0.43	-0.06
V	0.11	0.22	-0.21	-0.20	-0.31	-0.14	0.27	-0.01	-0.16	-0.38	-0.36	0.06
La	-0.58	-0.61	-0.46	-0.48	0.67	-0.57	0.84	0.90	-0.47	-0.11	0.50	0.40
Al	-0.40	-0.86	-0.46	-0.61	0.98	-0.37	0.56	0.78	0.23	0.26	0.91	0.89
Mg	-0.36	-0.69	-0.24	-0.27	0.82	0.10	0.18	0.52	0.48	0.57	0.81	0.71
Ca	0.10	0.31	-0.41	-0.35	-0.38	-0.26	0.36	-0.01	-0.23	-0.58	-0.47	-0.08
Na	0.54	0.09	0.64	0.63	-0.34	0.67	-0.70	-0.54	0.12	0.41	-0.22	-0.45
K	0.31	0.49	0.01	0.02	-0.61	-0.03	0.10	-0.28	-0.11	-0.33	-0.66	-0.25
Sr	0.24	0.44	-0.03	-0.02	-0.58	-0.09	0.20	-0.18	-0.31	-0.43	-0.64	-0.27
Y	0.24	-0.21	-0.19	-0.18	-0.18	0.00	0.33	0.23	-0.71	-0.43	-0.22	-0.17
Ga	-0.54	-0.38	-0.22	-0.25	0.60	-0.07	0.11	0.42	0.14	0.09	0.71	0.74
Li	-0.45	-0.82	-0.43	-0.49	0.93	-0.22	0.49	0.75	0.22	0.37	0.84	0.70
Nb	0.18	0.50	-0.14	-0.07	-0.59	-0.12	0.19	-0.20	-0.25	-0.49	-0.65	-0.28
Ti	-0.01	0.09	-0.42	-0.48	-0.09	-0.50	0.53	0.19	-0.16	-0.49	-0.19	0.22
Zr	-0.36	-0.64	-0.15	-0.17	0.77	0.05	0.00	0.41	0.25	0.39	0.83	0.52
S	0.36	0.14	0.50	0.72	-0.39	0.90	-0.51	-0.39	0.21	0.64	-0.39	-0.50

Table 4.2 Correlation matrix of Hg in rock with trace elements continued on next page. There are no significant correlations where (r) values must be > 0.602 (P = 0.05) determined from Wheater and Cook (2000) (Matrix generated using Quattro Pro)

Ba	Cr	V	La	Al	Mg	Ca	Na	K	Sr	Y	Ga	Li	Nb	Ti	Zr	S
1.00																
0.79	1.00															
0.78	0.93	1.00														
-0.48	-0.17	-0.12	1.00													
-0.65	-0.36	-0.24	0.59	1.00												
-0.64	-0.60	-0.44	0.27	0.87	1.00											
0.69	0.91	0.91	-0.08	-0.32	-0.57	1.00										
-0.02	-0.39	-0.57	-0.43	-0.33	0.01	-0.63	1.00									
0.93	0.90	0.92	-0.27	-0.53	-0.67	0.90	-0.36	1.00								
0.88	0.90	0.89	-0.11	-0.53	-0.72	0.89	-0.36	0.97	1.00							
0.33	0.53	0.33	0.34	-0.18	-0.39	0.36	0.09	0.36	0.52	1.00						
-0.27	-0.05	0.16	0.14	0.61	0.61	-0.08	-0.42	-0.18	-0.23	-0.34	1.00					
-0.80	-0.61	-0.51	0.61	0.93	0.89	-0.52	-0.13	-0.72	-0.70	-0.20	0.41	1.00				
0.84	0.90	0.91	-0.19	-0.54	-0.72	0.95	-0.47	0.97	0.97	0.37	-0.19	-0.71	1.00			
0.56	0.84	0.91	0.12	-0.04	-0.38	0.93	-0.80	0.81	0.79	0.25	0.13	-0.31	0.85	1.00		
-0.89	-0.79	-0.74	0.26	0.74	0.87	-0.79	0.19	-0.93	-0.94	-0.41	0.47	0.84	-0.92	-0.64	1.00	
0.24	-0.23	-0.25	-0.41	-0.33	0.08	-0.39	0.80	-0.09	-0.13	0.10	-0.29	-0.15	-0.21	-0.57	0.04	1.00

Table 4.2 (Continued) Correlation matrix of Hg in rock with trace elements. There are no significant correlations where (r) values must be > 0.602 (P = 0.05) determined from Wheater and Cook (2000) (Matrix generated using Quattro Pro)

Chapter 5: Conclusions

5.1 Conclusions

Geochemical results indicate the highest mercury concentrations are in the slate till (mean = 40.8 ppb) compared to the greywacke till (mean = 32.4 ppb) but Hg values are quite similar. Mercury has no apparent correlation with sulphur possibly indicating the Hg is not associated with Hg bearing sulphides such as cinnabar. There is no correlation with Hg and any significant elements that could indicate what the Hg source(s) are. It still remains unclear whether there is a correlation to increased Hg to the GHT. This study shows there is no a direct relationship with increasing Hg concentrations and the GHT. Till values are within the range reported by Jonasson and Boyle (1972).

The slate and greywacke bedrock Hg concentrations (mean = 2.37 ppb) are low but similar to previously reported values within the park. The low values in the rock could be caused by weathering during early stages of exposure, possibly releasing Hg into the till and surrounding environment. Recent studies have indicated that Hg values are higher in bedrock from drill cores pointing to a possible link to increased Hg values with depth. Although previous reports indicate higher levels of Hg in sulphidic black slates there is no evidence to support that in the limited number of samples for this study. Hg values are the highest in the samples containing the most sulphide minerals (pyrrhotite and pyrite) but the values are extremely low (2.3 ppb to3.4 ppb) to conclude that there is a correlation.

The total field ground magnetic survey and geologic mapping indicate that the geologic contact between the Goldenville Group and Halifax Group is 500 to 1000m

north of that reported on recent maps. Clast identification and counts indicate that the areal extent of the Halifax Group within the study area is smaller than portrayed on the most recent maps.

5.2 Recommendations for Further Work

The source(s) of Hg in the till is still not known. Further work is required to identify sources of Hg in the till possibly through investigations of size fractions most importantly to see if the clay size fraction contains the majority of the Hg in tills or is it within clastic grains. Spatial variance needs to be investigated to identify spatial error variations in Hg distribution in the till to provide important information about precision during sampling. Abundance of Hg with depth needs to be investigated including mineral identification through mineral probing. Future research can expand its scope by investigating a possible correlation of Hg with carbon in the slates as indicated in previous reports. Further sampling programs throughout the province would be beneficial to determine if Hg values within the Kejimkujik National Park are actually higher than values throughout the province.

Previous studies by Sangster *et al.* (2001) indicate that surface bedrock sampling might not be an accurate procedure to determine Hg values of the rock. The low Hg values found in the rock during this study could be an example of this. Future bedrock sampling should determine how Hg concentrations vary with depth.

References

Azzaria, L.M. 1992. Mercury in soil associated with faults, Charlevoix seismic zone, Quebec, Canada, Iraqi Geological Journal. **25**: 18-28.

Beauchamp, S., Tordon, R., Schroeder, B., Witte, J., Ecological Monitoring and Assessment Network, and New Brunswick Department of the Environment. 1998a. Total Gaseous Mercury. *In* Mercury in Atlantic Canada – A Progress Report. *Edited by* The Mercury Team. Chapter 3, Mercury in the Atmosphere. Environment Canada. p. 17-30.

Binnet, W.P., Jenner, K.A., Sangster, A.L., and Zentilli, M. 1986. A Stratabound zinc-lead deposit in Meguma Group Metasediments as Eastville, Nova Scotia. Maritime Sediments and Atlantic Geology. v. **22**:65-68.

Boner, F.J., Finck, P.W. and Graves, r.M. 1990. Trace element analysis of till, South Mountain Batholith. Nova Scotia Department of Mines and Energy. Open File Report 90-006. p. 108.

Boyle, R.W. and Garrett, R.G. 1970. Geochemical prospecting; a review of its status and future. Earth Science Reviews. **6**: 51-75

Branfireun, B. A., Roulet, N. T., Kelly, C. A., and Rudd, W. M. 1999. In Situ Sulphate Stimulation of Mercury Methylation in a Boreal Peatland: Toward a Link Between Acid Rain and Methylmercury Contamination in Remote Environments. Global Biogeochemical Cycles. **13**: 743-750.

Burgess, N. (1996, January). [Online]. High Mercury Levels in Common Loons Breeding in the Maritimes. Canadian Wildlife Services. <http://www.cciw.ca/eman-temp/reports/meetings/national96/burgessn.html> [2001, January 16].

Burgess, N. (March 1996). [Online] Monitoring Mercury Levels in Maritime Common Loons. The Effects Monitor Newsletter. Environment Canada. Vol. 2 #3, March 1996 http://www.atl.ec.gc.ca/epb/eem/em_v2n3e.html

Burgess, N., Beauchamp, S., Brun, G., Clair, T., Roberts, C., Rutherford, L., Tordon, R., and Vaidya, O. 1998. Mercury in Atlantic Canada - A Progress Report. Environment Canada – Atlantic Region.

Burgess, N. M., Evers, D.C., and Kaplan, J.D. 1998. Mercury Levels in the Blood of Common Loons Breeding in the Maritimes and Their Prey. *In* Mercury in Atlantic Canada – A Progress Report. *Edited by* N. M. Burgess. Environment Canada. Chapter 6, Mercury in Biota. p. 96-100.

Burns, C.G. 1997. Stratigraphy of the Goldenville Group-Halifax Group Transition (GHT) of the Meguma Supergroup at Caribou Gold District (Drillcore LL81-5A), Nova Scotia. BSC thesis at Department of Earth Science, Dalhousie University.

Cameron, E.M. and Jonasson, I.R. 1972. Mercury in Precambrian shales of the Canadian Shield. Geological Survey of Canada. Geochimica et Cosmochimica Acta 36: 985-1005.

Cameron, G.W. and Hood, P.J. 1975. Residual aeromagnetic anomalies associated with the Meguma Group of Nova Scotia and their relationship to gold mineralization. Geological Survey of Canada Paper 75-1C, p 197-211.

Carpi, A. 1997. Mercury from Combustion Sources: A Review of the Chemical Species Emitted and their Transport in the Atmosphere. Water, Air, and Soil Pollution. 98: 241-254.

CCME (1998, December 07) [online] Canada Wide Standards for Mercury. CCME

http://www.ccme.ca/3e_priorities/3ea_harmonization/3ea2_cws/3ea2i_overviews/3ea2i3.html>[2002, March 9]

Chesterman, C.W. 1998. National Audubon Society Field Guide to North American Rocks and Mineral. Chanticleer Press Inc. New York. P. 370.

Clair, T.A., Burgess, N., Brun, G.L., and Leger, D. 1998. Mercury in Aquatic Environments. *In* Mercury in Atlantic Canada – A Progress Report. *Edited by* N. M. Burgess. Environment Canada. Chapter 6, Mercury in Biota. p. 54-62.

Clarke, D.B., Barr, S.M. and Donahoe, H.V. 1980. Granitoid and other plutonic rocks of Nova Scotia; Canadian Journal of Earth Sciences. **4**: 2858-2864.

Clarke, D.B., Muecke, G.K. and Chatterjee, A.K. 1985. The South Mountain Batholith: geology, petrology, and geochemistry. *In* Guide to the Granites and Mineral Deposits of Southwestern Nova Scotia. *Edited by* A.K. Chatterjee and D.B. Clarke. Nova Scotia Department of Mines and Energy, Paper 85-3, p. 1-14.

Cockling, D., King, M. L., Ritchie, L., and Hayes, R. 1994. Earthworm Bioaccumulation of Mercury from Contaminated Flood Plain Soils. *In* Mercury Pollution Integration and Synthesis. *Edited by* C. J. Watras and J. W. Huckabee. Lewis Publishers. p. 381-396.

Corey, M.C. 1994. Diamond-Drilling in the Tobeatic Shear Zone of Southwestern Nova Scotia and the Potential for Epithermal-Style Base and Precious Metals. Minerals and Energy Branch, Report of Activities 1994, 95-1. p. 27-42.

d'Entremont, A.A., Carter, J.A., Burgess, N.M., Drysdale, C., and Brun, G.L. 1998. Mercury in Brook Trout and White Perch in Kejimkujik National Park. *In* Mercury in Atlantic Canada – A Progress Report. *Edited by* The Mercury Team. Environment Canada. Chapter 6, Mercury in Biota. p. 77-80.

DiLabio R.N.W. 1990. Glacial dispersal trains. *In* Kujansuu, R. and Saarnisto, M. (eds), Glacial indicator tracing. A. A. Balkema, Rotterdam. p. 109-122.

Dreimanis, A. and Vagners, U.J. 1971. Bimodal Distribution of Rock and Mineral Fragments in Basal Till. *In* Till-A Symposium. *Edited by* R.P. Goldwaith. Ohio State University Press, Columbus Ohio. p. 237-250.

Ebinghaus, R., Tripaht, R. M., Wallschläger, D., and Lindberg, S. E. 1999. Natural and Anthropogenic Mercury Sources and Their Impact n the Air-Surface Exchange of Mercury on Regional and Global Scales. *In* Mercury Contaminated Sites: Characterization, Risk Assessment, and Remediation. *Edited by* R. Ebinghaus. p. 3-50.

Evers, D.C., Kaplan, J.D., Meyer, M.W., Reaman, P.S., Braselton, W.E., Major, A., Burgess, N., and Scheuhammer, A.M. 1998. Geographic Trend in Mercury Measured in Common Loon Feathers and Blood. Environmental Toxicology and Chemistry. **17**: 173-183.

Finck, P. W., Boner, F. J., and Graves, R. M. 1994. Glacial and Till Clast Geology of Kejimkujik Lake, Nova Scotia. South Mountain Batholith Project. NTS Sheets 21A/06 and part of 21A/07. Nova Scotia Department of Natural Resources. Department of Mines and Energy. Map 94-12. Scale 1: 50 000.

Fox, D, Robinson,C. and Zentilli, M. 1997. Pyrrhotite and associated sulphides and their relationship to acid rock drainage in the Halifax Formation, Meguma Group, Nova Scotia. Atlantic Geology. v. **33**:2:87-103.

Goodwin, T.A, Nickel, R.J. and Page, K.D. 2000. Mercury in till and soil gas, Kejimkujik National Park, Nova Scotia [abstract]. Department of Natural Resources Publications Report ME 2000-2. p. 15

Goodwin, T. A., Smith, P. K and Culgin, B. M. 2002: Mercury in Till, Kejimkujik National Park Area, Nova Scotia (NTS 21A/06), Nova Scotia Department of Natural Resources, Minerals and Energy Branch, Report of Activities 2001, Report ME 2002-1, in press.

Godbold, D. L. 1994. Mercury in Forest Ecosystems: Risk and Research Needs. *In* Mercury Pollution Integration and Synthesis. *Edited by* C. J. Watras and J. W. Huckabee. Lewis Publishers. p. 295-304

Graves M.C. and Zentilli, M. 1988. The lithochemistry of metal enriched coticules in the Goldenville-Halifax transition zone of the Meguma Group, Nova Scotia. *In* Current Research, Part B, Geological Survey of Canada, Paper 88-1B, p. 251-261.

Horne, R. J. and Corey, M. C. 1994. Geological Map of Kejimkujik Lake, Nova Scotia. Nova Scotia Department of Natural Resources. Mines and Energy Branches. Map Sheet 21A/06 and part of 21A/07. Map 94-05. Scale 1:50 000.

Internationella Miljoinstitutet. Septmeber 1997. Lund, Sweden <http://www1.ldc.lu.se/iiiee/ EMISSIONS/ MERCURY/MERCURY1.HTML> [November 15, 2001]

Jonasson, I.R. and Boyle, R.W. 1971. Geochemistry of mercury. *In* Watkin JE (ed) Mercury in mans environment. Proceedings of the Royal Society of Canada Symposium, Ottawa, Ont., p. 5-21.

Jonasson, I.R. and Boyle, R.W. 1972. Geochemistry of Mercury and Origins of Natural Contamination of the Environment. (CIM) Bulletin: Canadian Institute of Mining and Metallurgy. **65**: 32-39.

Keppie, J. D. 1979. Geological Map of the Province of Nova Scotia. Department of Mines and Energy, Nova Scotia. Scale 1: 50 000.

Keppie, J. D. 2000. [Online]. Digital Geological Map of the Province of Nova Scotia. Version 1. Nova Scotia Department of Natural Resources. Map D00-01. Scale 1: 500 000. <http://www.gov.ns.ca/natr/meb/pubs3.htm#maps>. [2001, May 20].

Keen, C. E., Kay, W. A., Keppie, D., Marillier, F., Pe-Piper, G., Waldron, J. W. F. 1991. Deep Seismic Reflection Data from the Bay of Fundy and Gulf of Maine: Tectonic Implications for the Northern Appalachian. Canadian Journal of Earth Sciences. **28**: 1096-1111.

Kerekes, J., Duggan, M., Tordon, R., Boros, G., and Bronkhorst, M. 1995. Abundance and distribution of fish-eating birds in Kejimkujik National Park, Nova Scotia (1988-1995). Lake and Reservoir Management. **11**: 156.

King, M.S. 1994a. Magnetic mineralogy and susceptibility f the north-central Meguma Group: Implications for the interpretation of aeromagnetic total field, first derivative and second derivative. Nova Scotia Department of Natural Resources, Open File Report 94-004.

King, M.S. 1994b. Magnetic signature of the Goldenville-Halifax transition zone:North Beaverbank. Nova Scotia Department of Natural Resources, Open File Report 94-015.

King, M.S. 1995. Interpretation of magnetic data from the Meguma Group of Nova Scotia: magnetic mineralogy. *In* Minerals and Energy Branch, Report of Activities 1994. *Edited by* D.R. MacDonald and K.A. Mills Nova Scotia Department of Natural Resources, Minerals and Energy Report, 95-1, p 63-72.

King, M.S. 1997. Magnetic susceptibility mapping; applications for the Meguma Group, central Nova Scotia. *In* Geology and mineralogy of the Meguma Group and their importance to environmental problems in Nova Scotia. Atlantic Geology. **33**: 121-131.

Kujansuu, R. and Saarnisto, M. 1990. Glacier Indicator Tracing. A.A. Balkema. Rotterdam, Netherlands.

Krabbenhoft, D.P. and Rickert, D.A. (1997 April 01) [online] . Mercury Contamination of Aquatic Ecosystems. USGS. < http://water.usgs.gov/wid/FS_216-95/FS_216-95.html>[2002, March 9].

Lee, Y., Borg, G. C., Iverfeldt, Å., and Hultberg, H. 1994. Fluxes and Turnover of Methylmercury: Mercury Pools in Forest Soils. *In* Mercury Pollution Integration and Synthesis. *Edited by* C. J. Watras and J. W. Huckabee. Lewis Publishers. p. 137-152.

Lepeltier, C. 1969. A simplified statistical treatment of geochemical data by graphical representation. Economic Geology **64**: 538-550.

Loukola-Ruskeeniemi, K. 1990. Metalliferous black shales – a probable source of mercury in pike in Lake Kolmisoppi, Sotkamo, Finland. Bulletin of Geologic Society of Finland **62**: 167-175.

MacDonald, M. A. 1994. Geological Map of the South Mountain Batholith. Nova Scotia Department of Natural Resources. Map 94-01. Scale 1: 250 000.

Mason, B. and Moore, C.B. 1982. Principles of Geochemistry. Fourth Edition. John Wiley and Sons Inc. Toronto. P. 47.

McKenzie, C. B. and Clarke, D. B. 1975. Petrology of the South Mountain Batholith, Nova Scotia. Canadian Journal of Earth Sciences. **12**: 1209-1218.

Mercury: Chapter 2 - Forms, Fate & Effects. (1996, August, 8). [Online]. *In* Mercury in Massachusetts: An Evaluation of Sources, Emissions, Impacts and Controls. Department of Environmental Protection, Massachusetts. <http://www.state.ma.us/dep/files/mercury/hgch2.htm>. [2001, November 15].

Moore, D. S. and McCabe, G. P. 1993. Introduction to the Practice of Statistics. 2nd Edition. W.H. Freeman and Company, New York.

Nadakavukaren, A. 2000. Our Global Environment: A Health Perspective. 5th Edition. Waveland Press, Inc. Prospect Heights, Illinois.

National Pollutant Inventory: Mercury and Compounds. (1999). [Online]. Environment Australia. <http://www.environment.gov.au/cgi-bin/epg/npi/database/npi3/report.pl?name=substance_context;substance=53;mode=>. [2000, May 20].

Nikkarinen, M., Kallio, E., Lestinen, P. and Ayras, M. 1984. Mode of occurrence of copper and zinc in till over three mineralized areas in Finland. Journal of Geochemical Exploration. 21: 239-247.

Nova Scotia Department of Natural Resources. 1957. Aeromagnetic map of Whiteburn, Nova Scotia (Sheet 21-A-6-A). OFM 57-033.

O'Driscoll, N., Rencz, A., and Clair, T. A. 2000. Multi-Disciplinary Study of Metal Cycling, Primarily Hg, in Aquatic and Terrestrial Environments. First Workshop Proceedings of Kejimkujik Toxic Substance Research Initiative Work Group Environment Canada-Atlantic Region, Occasional Report no. 15. Environment Canada. Sackville, New Brunswick.

O'Reilly, G. A. 1988. South Mountain Batholith Project: Mineral Deposit Studies. *In* Mines and Minerals Branch. Report of Activities. *Edited by* D. R. MacDonald and Y. Brown. Nova Scotia Department of Mines and Energy. Report 88-3, Part A. p. 105-107.

Page, K.D. 2001. An Examination of Mercury (HG) Contamination in Kejimkujik National Park: The Role of Geologic Sources. M.Sc. thesis. Dalhousie University. Halifax, Nova Scotia.

Parkman, H., Östlund, P., Samuelsson, M., and Iverfeldt, Å. 1994. Methylmercury in a Permanently Stratified Fiord. *In* Mercury Pollution Integration and Synthesis. *Edited by* C. J. Watras and J. W. Huckabee. Lewis Publishers. p. 107-118.

Plouffe, A. 1995. Glacial dispersal of Mercury from Bedrock Mineralization along Pinchi Fault, North Central British Columbia. Water, Air, Soil Pollution. 80: 1109-1112.

Plouffe, A. 1998. Detrital transport of metals by glaciers, an example from the Pinchi Mine, central British Columbia. Environmental Geology. p. 183-193.

Plouffe, A. 1997. Physical partitioning of mercury in till: an example from central British Columbia, Canada. Journal of Geochemical Exploration. **59**:219-232.

Rassmussen, P.E. 1993. The environmental significance of geological sources of mercury: a Precambrian Shield watershed study. PhD. Thesis, University of Waterloo, Waterloo, Ont.

Rasmussen, P. E. 1996. Trace Elements in the Environment: A Geological Perspective. Geological Survey of Canada Bulletin 429, p. 1-26

Rasmussen, P.E., Friske, P.W.B., Azzaria, L.M., and Garrett, R.G. 1998. Mercury in the Canadian Environment: Current Research Challenges. Geoscience Canada. **25**: 1-13

Rencz, A. 2000. Introduction to the Study. *In* Multi-Disciplinary Study of Metal Cycling, Primarily Hg, in Aquatic And Terrestrial Environments. *Edited by* N. O'Driscoll, A. Rencz, and T.A. Clair. First Workshop Proceedings of Kejimkujik Toxic Substance Research Initiative Work Group. Environment Canada-Atlantic Region, Occasional Report no. 15. Environment Canada. Sackville, New Brunswick. p. 1-3.

Rencz, A., Hall, G.E.M., Telmer, K., Sangster, A. and Smith, P. 2000. Introduction to the Study. *In* Multi-Disciplinary Study of Metal Cycling, Primarily Hg, in Aquatic And Terrestrial Environments. *Edited by* N. O'Driscoll, A. Rencz, and T.A. Clair. First Workshop Proceedings of Kejimkujik Toxic Substance Research Initiative Work Group. Environment Canada-Atlantic Region, Occasional Report no. 15. Environment Canada. Sackville, New Brunswick. p. 24-33

Reynolds, P. H. and Muecke, G. K. 1978. Age Studies on Slates: Applicability of the $^{40}Ar/^{39}Ar$ Stepwise Outgassing Method. Earth and Planetary Science Letters. **40**: 111-118.

Rodgers, M.C. and Berger, B.R. 1995. Precambrian geology Adrian, Marks, Sackville, Aldina and Duckworth Townships: Ontario Geological Survey, Report 289. **66**: 5

Rose, A.W., Hawkes, H.E. and Webb, J.S. 1979. Geochemistry in Mineral Exploration. Academic Press, New York.

Rogers, R. D. 1976. Methylation of Mercury in Agricultural Soils. Journal of Environmental Quality. **7**: 440.

Rutherford, L.A., Brun, G., Julien, G.R.J., Hebert, F., and Mroz, R.E. 1998. Mercury in Yellow Perch Study. *In* Mercury in Atlantic Canada – A Progress Report. *Edited by* The Mercury Team. Environment Canada. Chapter 6, Mercury in Biota. p. 81-84.

Ryan, R.J. and Smith P.K. 1998. A review of the mesothermal gold deposits of the Meguma Group, Nova Scotia, Canada. Ore Geology Reviews **13**: 1-5: 153-183

Sangster, A., Smith, P. and Goodwin, T. 2001. Mercury Content of Bedrock and Drill Core. *In* Cycling of mercury in Kejimkujik National Park, Toxic Substance Research Initiative Project #124 Summary. Environment Canada-Atlantic Region, Occasional Report no. 18. Environment Canada. Sackville, New Brunswick. P. 49-51

Schenk, P.E. 1995a Meguma zone (Chapter 3). *In* Geology of the Appalachian-Caledonian Orogen in Canada and Greenland. *Edited by* H. Williams. Geological Survey of Canada. Geology of Canada, no. 6. p. 261-277.

Schenk, P.E. 1995b Annapolis Belt (Chapter 4). *In* Geology of the Appalachian-Caledonian Orogen in Canada and Greenland. *Edited by* H. Williams. Geological Survey of Canada. Geology of Canada, no. 6. p. 367-383.

Schwartz, E.J. and McGrath, P.H. 1974. Aeromagnetic anomalies related to pyrrhotite occurrences in the Canadian Appalachian Region. Geological Survey of Canada Paper 74-1, B, Current Research, p. 107-108.

Shilts, W.W. 1975. Principles of geochemical exploration for sulphide deposits using shallow samples of glacial drift. Can Inst Min Metall Bull. **68**: 73-80.

Shilts, W.W. 1973. Till indicator train formed by glacial transport of nickel and other ultrbasic components: a model for drift prospecting. *In*: Report of Activities Part A. Geological Survey of Canada Paper. 73-1A: 213-218.

Shilts, W.W. 1984. Till geochemistry in Finland and Canada. Journal of Geochemical Exploration. **21**: 95-117.

Shilts, W.W. 1995. Geochemical partitioning in till. In Bobrowsky, P.T., Sibbick, S.J., Newell, J.M., Matysek, P.F. (Eds.). Drift Exploration in the Canadian Cordillra. B.C. Minist. Energy, Mines Pet. Resour. Paper. 2:149-163

Shilts, W.W. and Coker, W.B. 1995. Mercury anomalies in lake water and commercially harvested fish, Kaminak lake area, District of Keewatin, Canada. Water air Soil Pollution. **80**: 881-884.

Sinclair, A.J. 1976. Applications of Probability Graphs in Mineral Exploration. The Association of Exploration Geochemists, Special Volume 4. p 7-24.

Sinclair, A.J. 1990. A fundamental approach to threshold estimation in exploration geochemistry: probability plots revisited. Journal of Geochemical Exploration. **41**:1-22

Smith, P. K. 2000. Mercury and Trace Element Geochemistry of Selected Bedrock Lithologies in the Kejimkujik National Park, Southern Nova Scotia. *In* Multi-Disciplinary Study of Metal Cycling, Primarily Hg, in Aquatic And Terrestrial Environments. *Edited by* N. O'Driscoll, A. Rencz, and T.A. Clair. First Workshop Proceedings of Kejimkujik Toxic Substance Research Initiative Work Group. Environment Canada-Atlantic Region, Occasional Report no. 15. Environment Canada. Sackville, New Brunswick. p. 37-45.

Statpoint (2002, January 1) [online] Statpoint Corporate Center: Internet Statistical ComputingCentre. Englewood Cliffs, N.J.<http://www.sgcorp.com/probability_ plots.htm>[2002,February 19]

Stea, R.R. 1982. Pleistocene geology and till geochemistry of south central Nova Scotia (sheet 6). Nova Scotia Department of Mines and Energy. Map 82-1. Scale 1:100 000.

Stea, R. R. (2002, January 16). [Online]. A Virtual Field Trip of the Landscapes of Nova Scotia. Nova Scotia Natural Resources Minerals and Energy Branch. <http://www. gov.ns.ca/natr/meb/field/start.htm>. [2002, February 16].

Stea, R.R. 1983. Till geochemistry of southwestern Nova Scotia (sheet 5). Nova Scotia Department of Mines and Energy. Open File Report 555, scale 1:100 000.

Stea, R. R. and Grant, D. R. 1982. Pleistoncene geology and till geochemistry of southwestern Nova Scotia (sheets 7 and 8). Nova Scotia Department of Mines and Energy. Map 82-10. Scale 1:100 000.

Stea, R. R. and Grant, D. R. 1988. The Succession and Extent of Wisconsinan Ice Flows in Nova Scotia, Canada. *In* Mines and Minerals Branch. Report of Activities. *Edited by* D. R. MacDonald and Y. Brown. Nova Scotia Department of Mines and Energy. Report 88-1, Part B. p. 254.

Stea, R. R., Piper, D. J. W., Fader, G. B. J. & Boyd, R. 1998: Wisconsinan glacial and sea-level history of Maritime Canada, a correlation of land and sea events. Geological Society of America Bulletin 110, no. 7, 821-845

Stern, R.A. and Henderson, J.R. 1983. Observations on the nature and origin of magnetic total field and vertical gradient anomalies over the Goldenville Formation in Nova Scotia. Geological Survey of Canada Paper 83-1, B, Current Research, p. 92-101.

Taylor F.C. and Schiller, E.A. 1966. Metamorphism of the Meguma Group of Nova Scotia; Canadian Journal of Earth Science. v. 3, p959-974.

Teldford, W.M., Geldart, L.P. and Sheriff, R.E. 1990. Applied Geophysics. Second Edition. Cambridge University Press, Cambridge, New York.

Toxiclogical Profile of Mercury. June 22, 2001. http://www.atsdr.cdc.gov/toxprofiles /tp46.html ATSDR [December 3, 2001]

Wheater, C.P. and Cook, P.A. 2000. Using Statistics to Understand the Environment. Routledge Introduction to Environment Series. Routledge Publishing, London.

Williams, G.L., Fyffe, L.R., Wardle, R. J., Colman-Sadd, S.P., and Boehner, R.C. 1985. Lexicon of Canadian Stratigraphy Vol. VI. Atlantic Region. Canadian Society of Petroleum Geologists. Sentinel Printing, Yarmouth, Nova Scotia.

Appendix A: Geophysical Data

Figure A-1 Magnetic Data transect 1

PROJECT: Keji Mags | **LOCATION: Keji River Rd and Mill Rd** | **MAP SHEET: 21A06**
DATE: July 4,5, 2001 | **STATION DISTANCE: 12.5m** | **MAGNETOMETER MODEL:Scintrex MP-2**
Operator :Terry Goodwin | **SENSOR DIRECTION: North** | **GPS MODEL:Garmin12**
Operator :Belinda Culgin

Base Station

Station	UTME (NAD27)	UTMN (NAD 27)	Reading	Adjustment Time
BS1	329999	4905055	53080	11:00AM
	329999	4905055	52950	1:12PM

Station	UTME (NAD27)	UTMN (NAD 27)	Reading	Correction	Final Reading	AdjustmentTime	Comments
1	329999	4905055	53080	0	53080	11:00AM	*diurnal correction method
2	329990	4905049	53291	215	53506		Determine difference between base
3	329976	4905038	53290	214	53504		stations and time adjustments
4	329965	4905045	53293	217	53510		to calculate slope
5	329956	4905053	53296	220	53516	11:07AM	53080-52950 = 130
6	329944	4905048	53296	220	53516		11:00 - 1:12 = 132 min.
7	329934	4905050	53304	229	53533		130/132 = 0.98
8	329918	4905060	53299	223	53522		53080 is y- intercept
9	329904	4905064	53305	230	53535		y=0.98X+53080
10	329894	4905070	53305	230	53535	11:10AM	Solve for X (see column F)
11	329885	4905080	53283	207	53490		
12	329873	4905081	53295	219	53514		
13	329859	4905086	53300	224	53524		
14	329855	4905089	53301	226	53527		
15	329840	4905099	53299	223	53522	11:13AM	
16	329835	4905103	53298	222	53520		
17	329823	4905110	53294	218	53512		
18	329815	4905116	53297	221	53518		
19	329803	4905117	53296	220	53516		
20	329791	4905121	53296	220	53516	11:16AM	
21	329774	4905112	53297	221	53518		
22	329768	4905120	53299	223	53522		
23	329755	4905135	53300	224	53524		
24	329746	4905144	53296	220	53516		
25	329727	4905154	53307	232	53539	11:18AM	
26	329715	4905162	53314	239	53553		
27	329704	4905164	53315	240	53555		
28	329697	4905169	53309	234	53543		
29	329686	4905170	53305	230	53535		
30	329671	4905176	53308	233	53541	11:20AM	
31	329661	4905181	53309	234	53543		
32	329651	4905193	53312	237	53549		
33	329639	4905201	53307	232	53539		
34	329631	4905207	53310	235	53545		
35	329622	4905209	53312	237	53549	11:23AM	
36	329612	4905215	53317	242	53559		
37	329596	4905213	53319	244	53563		
38	329589	4905221	53317	242	53559		
40	329564	4905233	53309	234	53543	11:28AM	
41	329555	4905236	53312	237	53549		
42	329544	4905244	53314	239	53553		
43	329532	4905249	53314	239	53553		
44	329522	4905253	53313	238	53551		
45	329512	4905260	53317	242	53559	11:30AM	
46	329500	4905265	53321	246	53567		
47	329490	4905270	53329	254	53583		
48	329481	4905270	53340	265	53605		
49	329465	4905278	53359	285	53644		
50	329452	4905288	53485	413	53898	11:33AM	

Figure A-1 Magnetic Data transect 1

51	329444	4905291	53391	317	53708
52	329433	4905296	53333	258	53591
53	329419	4905298	53559	489	54048
54	329408	4905307	53325	250	53575
55	329396	4905308	53333	258	53591 11:35AM
56	329382	4905317	53319	244	53563
57	329369	4905324	53317	242	53559
58	329365	4905325	53313	238	53551
59	329354	4905328	53312	237	53549
60	329344	4905333	53310	235	53545 11:38AM
61	329334	4905330	53311	236	53547
62	329324	4905343	53314	239	53553
63	329316	4905351	53315	240	53555
64	329305	4905355	53315	240	53555
65	329293	4905368	53320	245	53565 11:41AM
66	329287	4905374	53327	252	53579
67	329278	4905389	53331	256	53587
68	329265	4905402	53341	266	53607
69	329254	4905412	53340	265	53605
70	329245	4905423	53332	257	53589 11:44AM
71	329237	4905433	53342	267	53609
72	329229	4905446	53356	282	53638
73	329217	4905455	53362	288	53650
74	329206	4905457	53358	284	53642
75	329199	4905456	53366	292	53658 11:46AM
76	329192	4905469	53395	321	53716
77	329183	4905473	53475	403	53878
78	329170	4905482	53530	459	53989
79	329157	4905484	53350	276	53626
80	329140	4905490	53375	301	53676 11:49AM
81	329133	4905491	53302	227	53529
82	329124	4905488	53291	215	53506
83	329113	4905487	53311	236	53547
84	329100	4905487	53327	252	53579 11:52AM (time at 85 deleted for culvert)
86	329077	4905500	53299	223	53522
87	329060	4905503	53283	207	53490
88	329051	4905501	53296	220	53516
89	329037	4905499	53297	221	53518
90	329022	4905499	53322	247	53569 11:54AM
91	329015	4905500	53445	372	53817
92	329003	4905504	53377	303	53680
93	328997	4905510	53297	221	53518
94	328986	4905512	53280	204	53484
95	328972	4905521	53289	213	53502 11:57AM
96	328961	4905529	53288	212	53500
97	328953	4905531	53290	214	53504
98	328944	4905537	53290	214	53504
99	328925	4905547	53285	209	53494
100	328920	4905551	53293	217	53510 12:01PM
101	328908	4905558	53292	216	53508
103	328877	4905566	53292	216	53508
104	328872	4905569	53301	226	53527
105	328864	4905573	53309	234	53543 12:04PM
106	328850	4905574	53314	239	53553
107	328841	4905579	53302	227	53529
108	328831	4905587	53299	223	53522
109	328820	4905596	53301	226	53527
110	328808	4905598	53307	232	53539 12:07PM
111	328795	4905612	53304	229	53533
112	328787	4905625	53301	226	53527

Figure A-1 Magnetic Data transect 1

113	328773	4905622	53309	234	53543	
114	328766	4905628	53301	226	53527	
115	328760	4905634	53310	235	53545 12:09PM	across from Georges Rd
116	328746	4905639	53307	232	53539	
117	328737	4905644	53320	245	53565	
118	328721	4905648	53312	237	53549	
119	328704	4905652	53315	240	53555	
120	328694	4905654	53323	248	53571 12:14PM	
121	328680	4905659	53327	252	53579	
122	328663	4905659	53338	263	53601	
123	328652	4905661	53359	285	53644	
124	328640	4905667	53372	298	53670	
125	328627	4905671	53374	300	53674 12:17PM	
126	328614	4905671	53321	246	53567	
127	328603	4905670	53312	237	53549	
128	328591	4905674	53309	234	53543	
129	328579	4905676	53311	236	53547	
130	328566	4905677	53318	243	53561 12:19PM	
131	328555	4905681	53320	245	53565	
132	328542	4905687	53343	268	53611	
133	328532	4905693	53365	291	53656	
134	328521	4905699	53355	281	53636	
135	328512	4905707	53355	281	53636 12:22PM	
136	328503	4905712	53355	281	53636	
137	328492	4905720	53321	246	53567	
138	328484	4905726	53321	246	53567	
139	328477	4905733	53322	247	53569	
140	328468	4905737	53340	265	53605 12:25PM	
141	328455	4905749	53357	283	53640	
142	328447	4905755	53408	335	53743	
143	328433	4905766	53420	347	53767	
144	328421	4905774	53381	307	53688	
145	328413	4905786	53355	281	53636	1 D. Veinot clearcut
146	328404	4905795	53353	279	53632	
148	328387	4905803	53329	254	53583	
149	328376	4905805	53349	274	53623	
150	328368	4905804	53371	297	53668 12:30PM	
151	328356	4905811	53421	348	53769	
152	328345	4905815	53470	398	53868	
153	328334	4905817	53402	329	53731	
154	328325	4905820	53322	247	53569	
155	328310	4905824	53286	210	53496	#25 Rd.
156	328300	4905831	53293	217	53510	
157	328283	4905832	53296	220	53516	
158	328272	4905830	53299	223	53522	
159	328263	4905835	53302	227	53529	
160	328246	4905831	53309	234	53543 12:35PM	
161	328240	4905829	53309	234	53543	
162	328230	4905824	53314	239	53553	
163	328220	4905834	53315	240	53555	
164	328209	4905831	53318	243	53561	
165	328199	4905827	53329	254	53583 12:37PM	
166	328186	4905827	53317	242	53559	
167	328168	4905827	53323	248	53571	
168	328153	4905831	53328	253	53581	
169	328143	4905842	53335	260	53595	
170	328124	4905842	53348	273	53621 12:40PM	Maple Rd.
171	328117	4905853	53356	282	53638	
172	328107	4905859	53365	291	53656	
173	328100	4905863	53380	306	53686	
174	328089	4905874	53393	319	53712	
175	328078	4905878	53412	339	53751 12:43PM	
176	328065	4905880	53424	351	53775	

Figure A-1 Magnetic Data transect 1

234	327731	4906468	53347	272	53619	
235	327732	4906481	53313	238	53551	
236	327734	4906494	53312	237	53549 2:27PM	
237	327733	4906505	53368	294	53662	
238	327732	4906516	53390	316	53706	
239	327735	4906528	53334	259	53593	
240	327733	4906542	53320	245	53565	
241	327737	4906553	53358	284	53642 2:29PM	
242	327739	4906565	53441	368	53809	
243	327739	4906580	53371	297	53668	
244	327741	4906595	53289	213	53502	
245	327743	4906610	53261	185	53446	
246	327747	4906619	53067	-13	53054 2:31PM	
247	327743	4906628	53119	40	53159	
248	327736	4906630	53131	52	53183	
249	327731	4906640	53275	199	53474	
250	327730	4906651	53184	106	53290 2:33PM	
251	327719	4906675	53225	148	53373	
252	327712	4906691	53127	48	53175	slate outcrop, rock sample TG2001-1
253	327702	4906698	53193	115	53308	
254	327689	4906705	53292	216	53508	
255	327674	4906707	53256	180	53436 2:35PM	
256	327664	4906717	53165	87	53252	
257	327663	4906722	53093	13	53106	
258	327665	4906731	53165	87	53252	
259	327661	4906748	53197	119	53316	
260	327659	4906761	53142	63	53205 2:37PM	
261	327657	4906773	53199	121	53320	
262	327650	4906790	53240	163	53403	
263	327644	4906799	53202	124	53326	
264	327642	4906811	53175	97	53272	
265	327637	4906827	53172	94	53266 2:39PM	
266	327636	4906838	53209	132	53341	
267	327633	4906847	53258	182	53440	

Figure A-1 Magnetic Data transect 2

PROJECT: Keji Mags | **LOCATION: Boyle Rd and Hemlock Hill Rd** | **MAP SHEET: 21A06**
DATE: July 4,5, 2001 | **STATION DISTANCE: 12.5m** | **MAGNETOMETER MODEL:Scintrex MP-2**
Operator :Terry Goodwin | **SENSOR DIRECTION: North** | **GPS MODEL:Garmin12**
Operator :Belinda Culgin

Base Station

Station	UTME (NAD27)	UTMN (NAD 27)	Reading	Time
BS1	330557	4905934	53285	2:25PM
			53327	3:06PM
			53330	5:10PM

Station	UTME (NAD27)	UTMN (NAD 27)	Reading	Correction	Final Reading	Time	Comments
1	331052	4905722	53308	224	53084	2:40PM	beside gwke subcrop, rock sample TG2001-4
2	331045	4905725	53314	229	53085		
3	331037	4905732	53315	230	53085		
4	331026	4905738	53312	227	53085		
5	331014	4905745	53314	229	53085		
6	331001	4905752	53332	247	53085	2:42PM	
7	330993	4905761	53302	218	53084		
8	330980	4905765	53314	229	53085		
9	330967	4905769	53315	230	53085		
10	330955	4905770	53311	226	53085	2:44PM	
11	330946	4905770	53312	227	53085		
12	330933	4905770	53313	228	53085		
13	330916	4905766	53315	230	53085		
14	330903	4905762	53319	234	53085		
15	330887	4905758	53315	230	53085	2:46PM	
16	330875	4905755	53311	226	53085		
17	330863	4905751	53311	226	53085		by garbage
18	330846	4905755	53313	228	53085		
19	330830	4905756	53311	226	53085		
20	330823	4905755	53322	237	53085	2:47PM	
21	330813	4905760	53318	233	53085		
22	330801	4905763	53318	233	53085		
23	330782	4905767	53385	299	53086		
24	330772	4905773	53320	235	53085		
25	330765	4905779	53333	248	53085	2:51PM	
26	330755	4905788	53331	246	53085		
27	330748	4905793	53329	244	53085		
28	330736	4905802	53325	240	53085		
29	330724	4905809	53321	236	53085		
30	330714	4905820	53324	239	53085	2:53PM	
31	330701	4905827	53325	240	53085		
32	330695	4905835	53327	242	53085		
33	330690	4905844	53328	243	53085		
34	330682	4905854	53330	245	53085		
35	330677	4905863	53325	240	53085	2:55PM	
36	330669	4905871	53329	244	53085		
37	330657	4905879	53325	240	53085		
38	330648	4905888	53325	240	53085		
39	330640	4905900	53320	235	53085		
40	330623	4905909	53343	258	53085	3:01PM	
41	330619	4905914	53337	252	53085		
42	330608	4905919	53329	244	53085		
43	330589	4905923	53177	95	53082		
45	330569	4905925	53325	240	53085	3:04PM	
46	330556	4905934	53328	243	53085		
47	330546	4905945	53332	247	53085		South edge of Mersey River Rd.
48	330669	4906225	53160	78	53082		North side Mersey river Rd.
49	330659	4906229	53302	218	53084	3:42PM	(at 50, deleted metal gate)
51	330641	4906252	53342	257	53085		
52	330627	4906259	53346	261	53085		
53	330618	4906265	53349	264	53085		
54	330610	4906282	53342	257	53085		
55	330602	4906291	53340	255	53085	3:44PM	
56	330594	4906300	53342	257	53085		
57	330588	4906307	53346	261	53085		
58	330581	4906322	53348	263	53085		
59	330571	4906330	53342	257	53085		
60	330564	4906340	53332	247	53085	3:46PM	

Figure A-1 Magnetic Data transect 2

61	330554	4906349	53358	272.55	53085.45	
62	330543	4906361	53361	275.49	53085.51	
63	330533	4906370	53361	275.49	53085.51	
64	330524	4906378	53360	274.51	53085.49	
65	330518	4906383	53357	271.57	53085.43 3:49PM	
66	330512	4906390	53359	273.53	53085.47	
67	330505	4906398	53368	282.35	53085.65	
68	330493	4906404	53369	283.33	53085.67	
69	330483	4906420	53381	295.10	53085.90	
70	330471	4906435	53408	321.57	53086.43 3:51PM	
71	330463	4906443	53442	354.90	53087.10	
72	330457	4906454	53436	349.02	53086.98	
73	330447	4906459	53369	283.33	53085.67	
74	330436	4906475	53347	261.76	53085.24	
75	330427	4906489	53343	257.84	53085.16 3:54PM	
76	330419	4906501	53343	257.84	53085.16	
77	330410	4906513	53342	256.86	53085.14	by Fire Pond (0.4 Km from Rd
78	330405	4906528	53338	252.94	53085.06	
79	330397	4906532	53294	209.80	53084.20	
80	330387	4906543	53356	270.59	53085.41 3:55PM	
81	330379	4906550	53345	259.80	53085.20	
82	330373	4906557	53338	252.94	53085.06	
83	330366	4906568	53323	238.24	53084.76	
84	330355	4906577	53317	232.35	53084.65	
85	330346	4906589	53324	239.22	53084.78 3:58PM	
86	330341	4906600	53321	236.27	53084.73	
87	330332	4906611	53322	237.25	53084.75	
88	330323	4906619	53321	236.27	53084.73	
89	330314	4906631	53320	235.29	53084.71	
90	330308	4906641	53320	235.29	53084.71 4:00PM	
91	330300	4906653	53325	240.20	53084.80	
92	330293	4906663	53325	240.20	53084.80	
93	330287	4906675	53327	242.16	53084.84	
94	330282	4906688	53326	241.18	53084.82	
95	330276	4906700	53325	240.20	53084.80 4:02PM	
96	330272	4906712	53324	239.22	53084.78	
98	330256	4906732	53325	240.20	53084.80	
99	330252	4906745	53329	244.12	53084.88	
100	330246	4906755	53328	243.14	53084.86 4:04PM	
101	330243	4906768	53329	244.12	53084.88	
102	330238	4906781	53331	246.08	53084.92	
103	330233	4906793	53330	245.10	53084.90	
105	330221	4906816	53374	288.24	53085.76 4:07PM	
106	330215	4906827	53334	249.02	53084.98	
107	330206	4906837	53330	245.10	53084.90	
108	330198	4906848	53353	267.65	53085.35	
109	330190	4906858	53385	299.02	53085.98	
110	330182	4906868	53380	294.12	53085.88 4:10PM	
111	330172	4906878	53380	294.12	53085.88	
112	330163	4906888	53361	275.49	53085.51	
113	330155	4906900	53342	256.86	53085.14	
114	330148	4906911	53343	257.84	53085.16	
115	330142	4906919	53333	248.04	53084.96 4:12PM	
117	330127	4906942	53347	261.76	53085.24	
118	330119	4906952	53343	257.84	53085.16	
119	330114	4906966	53348	262.75	53085.25	
120	330111	4906979	53358	272.55	53085.45 4:14PM	
121	330116	4906981	53358	272.55	53085.45	
122	330112	4906992	53360	274.51	53085.49	
123	330107	4907003	53388	301.96	53086.04	
124	330104	4907013	53439	351.96	53087.04	
125	330103	4907027	53420	333.33	53086.67 4:17PM	
126	330100	4907038	53397	310.78	53086.22	
127	330096	4907051	53338	252.94	53085.06	
128	330089	4907062	53263	179.41	53083.59	
129	330085	4907072	53278	194.12	53083.88	
130	330077	4907085	53290	205.88	53084.12 4:21PM	
131	330069	4907094	53305	220.59	53084.41	
132	330060	4907104	53323	238.24	53084.76	

202	329525	4907795	53974	876.47	53097.53	
203	329516	4907806	53546	456.86	53089.14	
204	329508	4907818	53561	471.57	53089.43	
205	329496	4907826	53093	12.75	53080.25 3:32PM	
206	329484	4907835	52864	-211.76	53075.76	
207	329476	4907823	53227	144.12	53082.88	
208	329466	4907835	52887	-189.22	53076.22	
209	329450	4907842	52553	-516.67	53069.67	
210	329444	4907845	52426	-641.18	53067.18 3:34PM	
211	329428	4907840	53440	352.94	53087.06	
212	329413	4907841	53861	765.69	53095.31	
213	329400	4907845	53801	706.86	53094.14	
214	329389	4907850	53537	448.04	53088.96	
215	329381	4907864	53298	213.73	53084.27 3:36PM	
217	329371	4907889	53253	169.61	53083.39	
218	329361	4907897	53145	63.73	53081.27	
219	329354	4907907	53154	72.55	53081.45	
220	329345	4907918	53144	62.75	53081.25 3:38PM	
221	329334	4907926	53125	44.12	53080.88	
222	329324	4907935	53130	49.02	53080.98	
223	329315	4907938	53139	57.84	53081.16	slate outcrop, rock sample TG2001-3
224	329302	4907946	53143	61.76	53081.24	
225	329295	4907955	53140	58.82	53081.18 3:40PM	bottom of slate pit
226	329284	4907962	53136	54.90	53081.10	
227	329274	4907969	53122	41.18	53080.82	
228	329266	4907981	53135	53.92	53081.08	
229	329259	4907991	53133	51.96	53081.04	
230	329255	4908004	53118	37.25	53080.75 3:42PM	
231	329248	4908015	53148	66.67	53081.33	
232	329240	4908026	53175	93.14	53081.86	
233	329233	4908038	53155	73.53	53081.47	
234	329223	4908046	53138	56.86	53081.14	
235	329216	4908052	53138	56.86	53081.14 3:44PM	
236	329207	4908063	53139	57.84	53081.16	top of slate pit,rock sample TG2001-2
237	329196	4908071	53140	58.82	53081.18	
238	329186	4908080	53141	59.80	53081.20	
239	329176	4908085	53142	60.78	53081.22	intersection of Boyle Rd and Pulpwood

Figure A-1 : Magnetic Data Transect 3

PROJECT: Keji Mags | **LOCATION: Grassy Lake Rd.** | **MAP SHEET: 21A06**
DATE: July 16, 2001 | **STATION DISTANCE: 12.5m** | **MAGNETOMETER MODEL:Scintrex MP-2**
Operator :Terry Goodwin | **SENSOR DIRECTION: North** | **GPS MODEL:Garmin12**
Operator :Belinda Culgin

Base Station

Station	UTME (NAD27)	UTMN (NAD 27)	Reading	Time
BS1	329601	4909121	53209	2:42pm
	329601	4909121	53209	4:01pm
BS161	331280	4908058	53225	1:50pm
		4908058	53240	2:42pm

adjustment	Station		UTME (NAD27)	UTMN (NAD 27)	Reading	Correction	Final Reading	Time	Comments
	195	1	329601	4909121	53209			53209 2:24PM	* no diurnal correction
	194	2	329611	4909106	53238			53238	needed for stations
	193	3	329620	4909098	53239			53239	1 to 160
	192	4	329632	4909089	53241			53241	
	191	5	329640	4909081	53240			53240 2:26PM	
	190	6	329651	4909083	53235			53235	
	189	7	329659	4909075	53235			53235	
	188	8	329669	4909064	53236			53236	
	187	9	329680	4909060	53229			53229	
	186	10	329691	4909053	53234			53234 2:28PM	
	185	11	329704	4909043	53233			53233	
	184	12	329715	4909034	53230			53230	
	183	13	329725	4909028	53227			53227	
	182	14	329744	4909013	53222			53222	
	181	15	329752	4909007	53215			53215 2:30PM	
	180	16	329763	4909008	53210			53210	
	179	17	329774	4909001	53210			53210	
	178	18	329783	4909001	53212			53212	
	177	19	329794	4908999	53215			53215	
	176	20	329805	4908987	53215			53215 2:32PM	
	175	21	329815	4908975	53216			53216	
	174	22	329828	4908966	53211			53211	
	173	23	329841	4908966	53206			53206	
	172	24	329850	4908964	53199			53199	
	171	25	329863	4908954	53198			53198 2:34PM	
	170	26	329874	4908949	53200			53200	
	169	27	329887	4908947	53205			53205	
	168	28	329900	4908938	53200			53200	
	167	29	329912	4908933	53201			53201	
	166	30	329924	4908931	53200			53200 2:36PM	
	165	31	329933	4908923	53190			53190	
	164	32	329944	4908920	53187			53187	
	163	33	329957	4908922	53178			53178	
	162	34	329969	4908926	53180			53180	
	161	35	329983	4908930	53182			53182 2:38PM	
	160	36	329995	4908927	53185			53185	
	159	37	330011	4908921	53196			53196	
	158	38	330020	4908914	53186			53186	
	157	39	330034	4908911	53176			53176	
	156	40	330049	4908904	53175			53175 2:40PM	
	155	41	330059	4908896	53170			53170	
	154	42	330072	4908890	53169			53169	slate outcrop,
	153	43	330081	4908886	53168			53168	rock sample TG2001-5
	152	44	330091	4908883	53170			53170	
	151	45	330101	4908875	53155			53155 2:42PM	
	150	46	330110	4908867	53149			53149	slate outcrop
	149	47	330121	4908858	53135			53135	
	148	48	330132	4908854	53148			53148	
	147	49	330143	4908847	53136			53136	
	146	50	330153	4908836	53137			53137 2:44PM	slate outcrop
	145	51	330162	4908828	53126			53126	slate outcrop,
	144	52	330172	4908821	53120			53120	rock sample TG2001-6
	143	53	330181	4908810	53116			53116	
	142	54	330192	4908808	53118			53118	
	141	55	330202	4908797	53116			53116 2:46PM	Delory Rd.

Figure A-1 : Magnetic Data Transect 3

140	56	330211	4908799	53111	53111	slate outcrop,
139	57	330222	4908790	53103	53103	rock sample
138	58	330230	4908771	53111	53111	TG2001-7
137	59	330239	4908764	53112	53112	
136	60	330252	4908760	53122	531222:48PM	
135	61	330260	4908752	53119	53119	
134	62	330275	4908740	53004	53004	Grassy Rd C
133	63	330283	4908738	53150	53150	
132	64	330295	4908736	53159	53159	
131	65	330305	4908735	53198	531982:51PM	
130	66	330314	4908723	53195	53195	
129	67	330321	4908709	53168	53168	
128	68	330330	4908700	53148	53148	
127	69	330341	4908686	53200	53200	
126	70	330353	4908669	53340	533402:53PM	
125	71	330365	4908666	53360	53360	
124	72	330378	4908656	53348	53348	
123	73	330388	4908650	53359	53359	
122	74	330400	4908642	53372	53372	
121	75	330408	4908634	53392	533922:55PM	
120	76	330417	4908626	53480	53480	
119	77	330432	4908620	53533	53533	
118	78	330446	4908614	53511	53511	
117	79	330456	4908599	53465	53465	Grassy Rd B
116	80	330466	4908592	53492	534922:57PM	
115	81	330478	4908587	53419	53419	
114	82	330490	4908580	53396	53396	
113	83	330503	4908576	53299	53299	
112	84	330515	4908573	53216	53216	
111	85	330527	4908566	54046	540462:59PM	
110	86	330535	4908558	53306	53306	
109	87	330549	4908555	54318	54318	
108	88	330561	4908547	54240	54240	
107	89	330571	4908542	54451	54451	
106	90	330577	4908540	53970	539703:03PM	
105	91	330590	4908534	53566	53566	
104	92	330603	4908535	54025	54025	
103	93	330617	4908524	53818	53818	
102	94	330631	4908520	53810	53810	
101	95	330643	4908516	53835	538353:05PM	
100	96	330656	4908515	53870	53870	
99	97	330671	4908511	53880	53880	
98	98	330683	4908505	53870	53870	
97	99	330695	4908500	53855	53855	
96	100	330706	4908497	53885	538853:07PM	Grassy Rd A
95	101	330720	4908493	53897	53897	
94	102	330728	4908492	53903	53903	
93	103	330744	4908490	53930	53930	
92	104	330756	4908493	53920	53920	
91	105	330766	4908484	53889	538893:09PM	
90	106	330777	4908487	53852	53852	
89	107	330791	4908492	53845	53845	
88	108	330799	4908488	53825	53825	
87	109	330813	4908485	53790	53790	
86	110	330828	4908482	53761	537613:12PM	
85	111	330843	4908477	53749	53749	
84	112	330856	4908472	53728	53728	
83	113	330868	4908463	53788	53788	
82	114	330887	4908459	53836	53836	
81	115	330891	4908447	53785	537853:14PM	
80	116	330899	4908439	53804	53804	
79	117	330906	4908426	53869	53869	
78	118	330913	4908415	53813	53813	
77	119	330923	4908402	53799	53799	
76	120	330927	4908397	53778	537783:15PM	
75	121	330937	4908385	53937	53937	
74	122	330947	4908370	53799	53799	

Figure A-1 : Magnetic Data Transect 3

73	123	330954	4908357	53734		53734	
72	124	330961	4908347	53790		53790	
71	125	330965	4908339	53905		53905 3:17PM	
70	126	330972	4908328	53927		53927	
68	128	330987	4908303	54012		54012	
67	129	330995	4908291	53889		53889	
66	130	331001	4908281	53827		53827 3:19PM	
65	131	331008	4908269	53728		53728	
64	132	331016	4908260	53738		53738	slate outcrop,
63	133	331020	4908250	53680		53680	rock sample TG2001-8
62	134	331027	4908236	53647		53647	
61	135	331023	4908222	53578		53578 3:21PM	
60	136	331036	4908209	53498		53498	
59	137	331044	4908199	53482		53482	
58	138	331052	4908189	53452		53452	
57	139	331059	4908179	53435		53435	slate outcrop,
56	140	331067	4908169	53405		53405 3:23PM	rock sample TG2001-9
55	141	331074	4908160	53377		53377	
54	142	331082	4908150	53351		53351	
53	143	331093	4908140	53336		53336	
52	144	331103	4908132	53315		53315	
51	145	331112	4908125	53326		53326 3:26PM	
50	146	331124	4908121	53323		53323	
49	147	331136	4908116	53292		53292	
47	149	331157	4908102	53295		53295	
46	150	331166	4908097	53297		53297 3:28PM	
45	151	331176	4908091	53288		53288	
44	152	331190	4908083	53285		53285	
43	153	331204	4908079	53274		53274	
42	154	331217	4908077	53266		53266	
41	155	331229	4908072	53270		53270 2:31PM	
40	156	331242	4908070	53234		53234	
38	158	331267	4908064	53260		53260	
36	160	331287	4908058	53260		53260 2:34PM	S ditch Mersey River Rd.
35	161	331280	4908058	53225	0	53225 1:50PM	
34	162	331298	4908056	53234	15	53219	
33	163	331303	4908051	53236	18	53218	
32	164	331309	4908042	53242	28	53214	
31	165	331318	4908032	53241	27	53214	
30	166	331320	4908019	53249	40	53209 1:57pm	
29	167	331329	4908017	53251	43	53208	
28	168	331339	4908018	53258	55	53203	
27	169	331349	4908017	53254	48	53206	
26	170	331361	4908008	53268	72	53196	
25	171	331368	4908004	53275	83	53192 1:59pm	
24	172	331370	4908001	53281	93	53188	
23	173	331384	4907997	53295	117	53178	
22	174	331392	4907987	53296	118	53178	
21	175	331397	4907974	53286	102	53184	
20	176	331406	4907958	53291	110	53181 2:03pm	
19	177	331410	4907951	53287	103	53184	
18	178	331417	4907940	53289	107	53182	
17	179	331422	4907925	53291	110	53181	
16	180	331421	4907919	53277	87	53190	
15	181	331420	4907906	53283	97	53186 2:05pm	
14	182	331420	4907891	53281	93	53188	
13	183	331423	4907878	53284	98	53186	
12	184	331431	4907869	53288	105	53183	
11	185	331438	4907863	53277	87	53190	
10	186	331452	4907853	53284	98	53186 2:08pm	
9	187	331460	4907839	53285	100	53185	
8	188	331467	4907832	53285	100	53185	
7	189	331475	4907825	53282	95	53187	
6	190	331481	4907817	53279	90	53189 2:11pm	
5	191	331488	4907808	53288	105	53183	
4	192	331493	4907797	53277	87	53190	
3	193	331497	4907786	53295	117	53178	
2	194	331505	4907782	53291	110	53181	
1	195	331516	4907778	53283	97	53186 2:13pm	in clearing by road

Appendix B: Till and Rock Geochemical Data

Figure B-1 Till description sheet

SOIL/TILL SAMPLE SHEET

PROJECT: Keji TSRI
DATE: 01/08/2001
SAMPLER: Terry Goodwin
SAMPLER: Belinda Culgin

PROPERTY: Kejimkujik National Park
LOCATION: South of Kejimkujik National Park
MAP SHEET: 21A/06

CO-ORD CONTROL: GPS
GPS MODEL: GARMIN 12
SAMPLE TOOL: auger/shovel

SAMPLE #	Utm-E27	Utm-N27	CODE	C DEPTH	C COLOR	S%	S%	C%	O%	HCL	QUALITY	CLAST %	SHAPE	TYPE	COMPACT	MOISTURE	COMMENTS	Surficial Geology	Bedrock
K2000-47	331349	4908141	1	150	ol. grn brn	4	4	2	0	N	good	20	angular		hard	dry	mixed hard wood, roadcut	SLB	cog
K2000-48	330918	4908405	1	100	ol. grn brn	4	4	2	0	N	good	20	angular		moderate	dry	mixed hard wood, roadcut	SLB	coh
K2000-49	330437	4908563	1	100	ol. grn brn	4	4	2	0	N	good	20	angular		moderate	dry	mixed hard wood, roadcut	SLB	coh
K2000-50	329820	4908982	1	80	ol. grn brn	4	4	2	0	N	good	20	angular		moderate	dry	mixed soft wood	SLB	coh
K2000-51	329445	4909320	1	130	ol. grn brn	4	4	2	0	N	good	20	angular		moderate	dry	mixed mature wood	SLB	coh
K2000-52			5														standard		
K2000-53	329265	4909721	1	140	ol. grn brn	4	4	2	0	N	good	20	angular		moderate	dry	mixed mature wood	GSRT	coh
K2000-54	328649	4910934	1	130	ol. grn brn	4	4	2	0	N	good	10	angular		moderate	dry	mixed soft wood, few gwke boulders	GSRT	coh
K2000-64	330352	4906588	1	80	ol. grn brn	4	4	2	0	N	good	20	angular		moderate	dry	mixed mature wood	SLB	cog
K2000-65	330680	4906260	1	80	ol. grn brn	4	4	2	0	N	good	30	angular		moderate	dry	mixed mature wood	SLB	cog
K2000-66	331024	4905754	1	150	ol. grn brn	5	3	2	0	N	good	30	angular		hard	dry	mixed mature wood, old french	GWB	cog
K2000-67	331285	4905289	1	100	ol. grn brn	5	3	2	0	N	good	40	angular		moderate	dry	mixed mature wood road cut	GWB	cog
K2000-68	331754	4905289	1	150	ol. grn brn	5	3	2	0	N	good	35	angular		moderate	dry	mixed mature wood road cut	GWB	cog
K2001-69	329215	4907950	1	100	ol. grn brn	4	3	3	0	N	good	40	angular	slate	moderate	dry	slate gravel pit , Boyle Rd.	SLB	coh
K2001-70			2														dup of 69, 2m apart	SLB	coh
K2001-71	329612	4907561	1	90	ol. grn brn	4	3	3	0	N	good	40	angular	slate	moderate	dry	road cut, Boyle Rd.	SLB	coh
K2001-72	330065	4907086	1	100	ol. grn brn	4	3	3	0	N	good	40	angular	slate	moderate	dry	road cut, Boyle Rd.	SLB	coh
K2001-73	329922	4907278	1	90	gry brn	4	3	3	0	N	good	30	angular	slate	moderate	dry	road cut, Boyle Rd.	SLB	coh
K2001-74	330147	4906896	1	100	ol. grn brn	4	3	3	0	N	good	40	angular	slate	moderate	dry	road cut, Boyle Rd.	SLB	coh
K2001-75			5														STEA-1 standard		
K2001-76	330267	4906702	1	80	ol. grn brn	4	3	3	0	N	good	30	angular	slate	moderate	dry	road cut, Boyle Rd.	SLB	coh
K2001-77	330403	4906517	1	90	ol. grn brn	5	3	2	0	N	good	25	angular	slate	moderate	dry	road cut, Boyle Rd.	SLB	coh
K2001-78	330537	4906334	1	100	ol. grn brn	5	3	2	0	N	good	30	angular	slate	moderate	dry	road cut, Boyle Rd. slightly oxidized	SLB	coh
K2001-79	330691	4906286	1	100	ol. grn brn	5	3	2	0	N	good	20	angular	slate, gwke	moderate	dry	road cut, intersection Boyle Rd. and Mersey River Rd, oxidized	SLB	coh
K2001-80	327678	4906710	1	100	tan brn	3	4	3	0	N	good	20	angular	slate	moderate	dry	mixed soft wood, North end Mill Rd	SLB	coh
K2001-81	327817	4906254	1	150	ol. grn brn	4	4	2	0	N	good	30	angular	slate	moderate	dry	mixed soft wood, old pit Mill Rd	SLB	coh
K2001-82	328054	4905892	1	120	ol. grn brn	3	4	3	0	N	good	30	angular	slate	moderate	dry	mixed mature wood, intersection south end Mill Rd/ Keji River Rd.	SLB	coh
K2001-83			3														split of #91		
K2001-84	328335	4905879	1	130	ol. grn brn	3	4	3	0	N	good	30	angular	slate	moderate	dry	mixed mature wood, intersection of #25 Rd and Keji River Rd	SLB	coh
K2001-85	328523	4905692	1	90	org. olv	4	3	3	0	N	moderate	40	sub-round, sub-angular		moderate	wet	recent clearcut, Keji River Rd, granite ablation, abundant granite erratics	SLB	coh
K2001-86	328780	4905609	1	120	ol. grn brn	5	3	1	0	N	good	40	sub-angular		moderate	dry	roadcut, intersection of George Rd and Keji River Rd	SLB	coh
K2001-87	328948	4905580	1	80	ol. grn brn	5	3	2	0	N	good	30	sub-angular		moderate	dry	mixed mature wood, Keji River Rd	GWB	coh
K2001-88	329152	4905502	1	80	org. olv	5	3	2	0	N	good	20	sub-angular	more gwke	moderate	dry	mixed mature wood, Keji River Rd, mottled slightly oxidized, more gwke clasts	GWB	cog
K2001-89	329260	4905425	1	100	ol. grn brn	5	3	2	0	N	good	15	sub-angular		loose	dry	mixed mature wood, Keji River Rd	GWB	cog
K2001-90			2														Field dup of 89, 2m apart		
K2001-91	329460	4905292	1	100	ol. grn brn	3	4	3	0	N	good	15	sub-angular		loose	dry	mixed mature wood, Keji River Rd	GWB	cog
K2001-92	330000	4905052	1	70	ol. grn brn	5	3	2	0	N	good	20	sub-angular	gwke	moderate	dry	mixed mature wood, intersection Keji River Rd and Rossignol Lake Rd, gwke clasts	GWB	cog

Code	Moisture	s=%sand x 10	Color		HCl
1 ... field sample	D ... dry	s=%silt x 10	blk	black	n : none
2 ... field duplicate	W ...wet	c=%clay x 10	brn	brown	w: weak
3 ... analytical replicate	NV ... not visible	0=%organics x 10	red	red	m: moderate
4 ... prep blank			org	orange	s: strong
5 ... standard			yel	yellow	vs: very strong
6 ... analytical blank			grn	green	*
a ... minus 80 mesh/acid digestion			lt	light	
			dk	dark	

Figure B-2 Analytical Methods

ANALYTICAL METHODS FROM BONDAR CLEGG LABORATORIES (AU)

SCOPE:

This method is suitable for the semi-quantitative analysis of gold in geochemical samples within the defined analytical ranges where the limitations of a fire assay preconcentration are acceptable.

PRINCIPLE:

The sample (either 30 gram or 50 gram) is weighted into the fire assay pot. Litharge is added to the sample and the mixture is fluxed in a furnace. The precious metals are collected with lead. The lead button is cupelled to an Ag/Au bead. The bead is hot digested with 50% HNO3 followed by concentrated HCl. The sample is bulked to the final volume and analyzed by Induced Coupled Plasma Atomic Emissions Spectrometer (ICP-AES).

APPLICABLE ANALYTE RANGES FOR ICP-ATOMIC EMISSION SPECTROSCOPY:

Element Code	Unit	Detection Limit	Upper Limit
Au	ppb	1	2000

PRECISION:

The tolerance criteria for variation of analytical data result from all stages of the analysis and are subject to the sample matrix and the specific technique used. Expected tolerance criteria at various concentrations for this method are as follows:

Element Code	Standard Value	Tolerance
Au	Detection Limit 1	+/- 100%
	2 - 4	50%
	5 - 10	25%
	11 - 15	20%
	16 - 100	15%
	101 - 1000	10%
	>1000	15%

This table is intended as a guideline in the absence of repeatability and reproducibility data.

ANALYTICAL METHODS FROM BONDAR CLEGG LABORATORIES

(TRACE ELEMENTS)

SCOPE:

This method is suitable for the semi-quantitative analysis of geological samples within the defined analytical ranges where the limitation of strong mineral acid apply.

PRINCIPLE:

The sample (0.5 grams) is digested with a mixture of hydrochloric and nitric acids. The samples are heated in a hot water bath (90 °C). After the digestion step the samples are cooled, bulked to the final volume and mixed well. The resulting solution is analyzed by ICP-AES. A slightly modified version of this method has been set up for clients with sample matrices containing high total dissolved solids (i.e. high Iron (Fe) concentrations >10%).

APPLICABLE ANALYTE RANGES FOR ICP-AES:

Element	Ag	Bi	Cr	K	Mn	Ni	Sn	Ti	Zr	Al	Ca
Detection Limit	0.2	5	1	0.01	1	1	20	0.01	1	0.01	0.01
Upper Limit	200.0	2000	20000	10.00	20000	20000	2000	10.00	5000	10.00	10.00
Units	ppm	ppm	ppm	%	ppm	ppm	ppm	%	ppm	%	%
Element	Cu	La	Mo	Pb	Sr	V	Zn	As	Cd	Fe	Li
Detection Limit	1	1	1	2	1	1	1	5	0.2	0.01	1
Upper Limit	10000	2000	10000	10000	2000	20000	10000	10000	2000.0	10.00	20000
Units	ppm	ppm	ppm	ppm	ppm	ppm	ppm	ppm	ppm	%	ppm
Element	Na	Sb	Ta	W	Ba	Co	Ga	Mg	Nb	Sc	Te
Detection Limit	0.01	5	10	20	1	1	2	0.01	1	5	10
Upper Limit	10.00	2000	1000	2000	2000	20000	10000	10.00	10000	2000	2000
Units	%	ppm	ppm	ppm	ppm	ppm	ppm	%	ppm	ppm	ppm

Element	Y
Detection Limit	1
Upper Limit	2000
Units	ppm

PRECISION:

The tolerance criteria for variation of analytical data result from all stages of the analysis and are subject to the sample matrix and the specific technique used.

Expected tolerance criteria at various concentrations for this method are as follows:

Element	Duplicate of Reference Value		Tolerance
Ag, Cd	Detection Limit	0.2	+/- 100%
(ppm)	0.4	1.0	50%
	1.2	5.0	25%
	5.2	50.0	15%
	50.2	200.0	10%
		>200.0	15%
Bi, Sb, Sc, As, Ce	Detection Limit	5	+/- 100%
(ppm)	10	25	50%
	30	50	25%
	55	500	15%
	505	2000	10%
		>2000	15%
Cr, V, Zn, Li, Y,	Detection Limit	1	+/- 100%
Nb, Ba, La, Sr, Zr	2	10	50%
(ppm)	11	20	25%
	21	200	15%
	201	2000	10%
		> 2000	15%
K, Ti, Al, Ca, Fe,	Detection Limit	0.01	+/- 100%
Na, Mg, S	0.02	0.05	50%
(%)	0.06	0.10	25%
	0.11	1.00	15%
	1.01	10.00	10%
		>10.00	15%
Sn, W	Detection Limit	20	+/- 100%
(ppm)	40	100	50%
	120	200	25%
	220	2000	10%
		>2000	15%
Ni, Cu, Co, Mn,	Detection Limit	1	+/- 100%
Mo, Sr(ppm)	2	5	50%
	6	10	25%
	11	100	15%
	101	1000	10%
		>1000	15%
Pb, Ga	Detection Limit	2	+/- 100%
(ppm)	4	10	50%
	12	20	25%
	22	200	15%
	202	2000	10%
		> 2000	15%
Te, Ta, P, Se	Detection Limit	10	+/- 100%
(ppm)	20	50	50%
	60	100	25%
	110	1000	10%
		>1000	15%
Be, Hg	Detection Limit	0.5	+/- 100%
(ppm)	1.0	2.5	50%
	2.0	25.0	25%
	25.5	500.0	10%
		>500.0	15%

This table is intended as a guideline in the absence of repeatability and reproducibility data.

Analytical Methods From ACME Laboratories - HG

Analytical Process

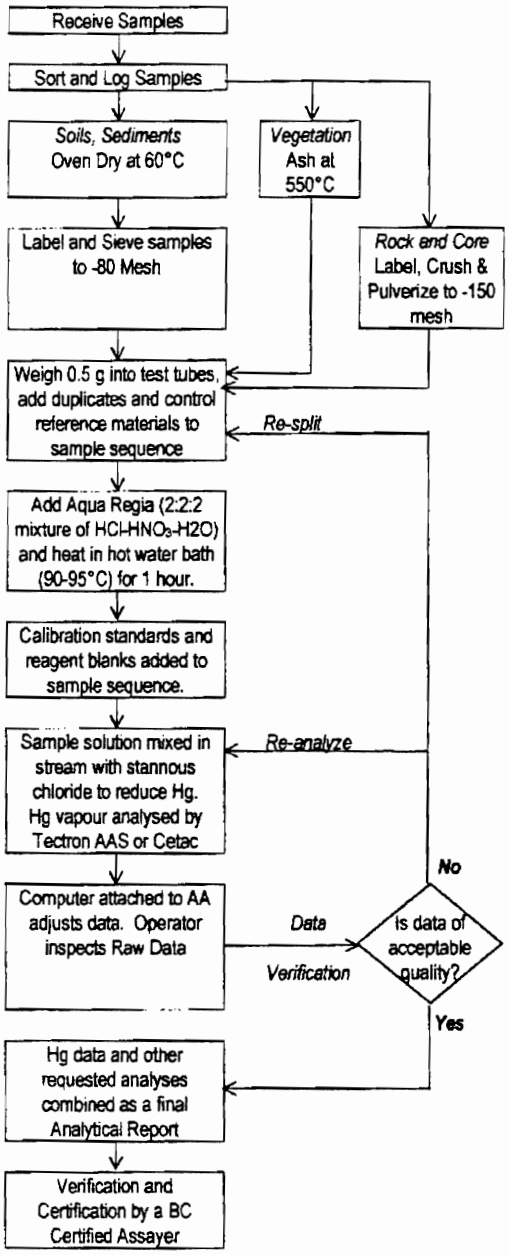

Comments

Sample Preparation

Samples are dried (default is 60°C unless specified otherwise by client). Soil, sediments and moss mats are pounded to disaggregate the fine grained material then screened (default is -80 mesh ASTM [-177 microns]). Rocks and drill core are crushed and pulverized (default is 95% -150 mesh ASTM [-100 microns]). Sample splits are weighed (0.5 g) into test tubes. Duplicate splits of crushed (rejects) and pulverized (pulp) fractions are included with every 34 rock samples to define sample homogeneity (reject split) and analytical precision (pulp split). Duplicate pulp splits are included in each batch of 34 soil or sediment samples. A blank and standard STD C3 are included in each batch of samples to monitor accuracy.

Sample Digestion

The Aqua regia mixture of 2:2:2 H_2O-HCl-HNO_3 (ACS grade) is added to each sample. Solutions are then heated in a hot water (90-95°C) bath for 60 minutes.

Sample Analysis

The sample solution is mixed on stream with a 5% stannous chloride solution which is then swept by a carrier gas into the cold vapour cell of a Tectron atomic absorption spectrometer or a Cetac Hg Analyser. Results are adjusted based on standards included in each batch. Quality is evaluated at three separate levels based on results of reference materials, duplicates and prep and analytical blanks included in each batch.

Data Evaluation

Raw and final data undergoes a final verification by a British Columbia Certified Assayer who then signs the Analytical Report before it is released to the client. Chief Assayer is Clarence Leong, other certified assayers are Dean Toye and Jacky Wang.

Figure B-3: Clast Identification and Counts

Clast Identification and Count

No.	Sample	#Slate	#Greywacke	#Granite	#Other	Total	Notes
1	K2000-54	26	44	1	4	75	
2	K2000-53	74	44	0	3	121	rare staining
3	K2000-51	128	55	1	0	184	rare staining
4	K2000-50	104	51	3	0	158	some with rust staining
5	K2000-49	21	10	0	1	32	slate clasts dominate <1cm
6	K2000-48	78	32	0	1	111	
7	K2000-64	19	14	2	1	36	
8	K2000-65	55	67	11	3	136	
9	K2000-66	38	67	7	0	112	
10	K2000-67	37	180	1	0	128	
11	K2000-68	39	81	9	0	129	
					TOTAL	1222	

Clast Identification and Count: Percentage

No.	Sample	%Slate	%Greywacke	%Granite	%Other	Notes
1	K2000-54	35	59	1	5	
2	K2000-53	61	37	0	2	
3	K2000-51	70	29	1	0	
4	K2000-50	66	32	2	0	
5	K2000-49	66	31	0	1	
6	K2000-48	70	29	0	1	CONTACT ?
7	K2000-64	53	39	5	3	
8	K2000-65	40	49	8	3	
9	K2000-66	34	60	6	0	
10	K2000-67	16	83	1	0	
11	K2000-68	30	63	7	0	

B-4 Till geochemical results

Samples	utm-E27	utm-N27	type	Hg-ppb	Au-ppb	Ag-ppm	Cu-ppm	Pb-ppm	Zn-ppm	Mo-ppm	Ni-ppm	Co-ppm	Cd-ppm	Bi-ppm
K2000-47	331349	4908141	slate	20.3	3	0.1	22	12	71	3	18	8	0.1	2.5
K2000-48	330918	4908405	slate	49	4	0.1	24	11	77	3	22	9	0.1	2.5
K2000-49	330437	4908563	slate	20.6	10	0.1	19	11	77	2	21	9	0.1	2.5
K2000-50	329820	4908982	slate	52.9	5	0.1	29	18	87	2	27	11	0.1	2.5
K2000-51	329445	4909320	slate	53.8	2	0.1	29	18	80	3	25	11	0.1	2.5
K2000-53	329285	4909721	slate	53.8	4	0.1	20	11	70	3	22	8	0.1	2.5
K2000-54	328649	4910934	greywacke	28.4	9	0.1	12	6	57	0.5	21	10	0.1	2.5
K2000-64	330352	4906588	slate	35.2	7	0.1	13	9	55	2	13	6	0.1	2.5
K2000-65	330680	4906260	slate	151.5	2	0.1	6	17	71	0.5	4	3	0.1	2.5
K2000-66	331024	4905754	greywacke	6.6	3	0.1	22	16	61	3	16	9	0.1	2.5
K2000-67	331285	4905289	greywacke	71.2	2	0.1	45	282	191	2	35	15	0.2	2.5
K2000-68	331754	4905289	greywacke	7.3	4	0.1	14	14	53	1	16	8	0.1	2.5
K2001-69	329215	4907950	slate	60	3	0.1	29	13	56	2	20	11	0.3	2.5
K2001-71	329612	4907561	slate	24.5	1	0.1	26	16	55	3	19	12	0.3	2.5
K2001-72	330065	4907086	slate	27.7	1	0.1	18	10	48	3	14	9	0.1	2.5
K2001-73	329922	4907278	slate	13.2	27	0.1	14	12	47	3	16	9	0.2	2.5
K2001-74	330147	4906896	slate	59	5	0.1	18	16	45	4	16	10	0.4	2.5
K2001-76	330267	4906702	slate	27.3	0.5	0.1	17	9	43	2	18	8	0.2	2.5
K2001-77	330403	4906517	slate	16.5	7	0.1	12	7	35	2	12	7	0.2	2.5
K2001-78	330537	4906334	slate	17.3	2	0.1	12	9	42	2	12	9	0.3	2.5
K2001-79	330691	4906286	slate/greywacke	25.5	1	0.1	11	8	34	2	12	7	0.1	2.5
K2001-80	327678	4906710	slate	44.2	1	0.1	11	9	22	0.5	11	6	0.1	2.5
K2001-81	327817	4906254	slate	15.8	2	0.1	35	13	36	3	13	11	0.5	2.5
K2001-82	328054	4905892	slate	64.1	0.5	0.1	17	11	50	6	12	8	0.4	2.5
K2001-84	328335	4905879	slate	37.9	0.5	0.1	17	10	30	3	10	7	0.3	2.5
K2001-85	328523	4905692	slate	20.9	3	0.1	58	18	46	3	17	18	0.4	2.5
K2001-86	328780	4905609	slate	20.4	2	0.1	13	14	28	1	12	7	0.1	2.5
K2001-87	328948	4905580	greywacke	44.5	0.5	0.1	11	7	25	1	11	6	0.1	2.5
K2001-88	329152	4905502	greywacke	44.6	0.5	0.1	11	8	30	1	10	7	0.1	2.5
K2001-89	329260	4905425	greywacke/slate	46	8	0.1	13	7	31	1	11	6	0.3	2.5
K2001-91	329460	4905292	greywacke	15.5	2	0.1	15	7	44	2	16	11	0.1	2.5
K2001-92	330000	4905052	greywacke	30	2	0.1	22	9	44	2	25	10	0.3	2.5

B-4 Till geochemical results

As-ppm	Sb-ppm	Fe-pct	Mn-ppm	Te-ppm	Ba-ppm	Cr-ppm	V-ppm	Sn-ppm	W-ppm	La-ppm	Al-pct	Mg-pct	Ca-pct	Na-pct	K-pct
33	2.5	4.14	1063	5	53	27	24	10	10	23	2.52	0.74	0.005	0.01	0.12
32	2.5	4.02	1058	5	52	30	24	10	10	24	2.79	0.68	0.005	0.01	0.11
40	2.5	4.35	1396	5	51	28	23	10	10	33	2.63	0.8	0.005	0.01	0.1
43	2.5	4.76	1364	5	45	32	25	10	10	30	3.49	0.78	0.01	0.01	0.09
50	2.5	4.78	1588	5	46	30	25	10	10	30	2.98	0.8	0.01	0.01	0.08
46	2.5	4.16	1394	5	38	28	22	10	10	24	2.61	0.7	0.005	0.01	0.07
43	2.5	2.45	1047	5	32	20	18	10	10	23	2.01	0.51	0.02	0.005	0.07
21	2.5	3.22	836	5	50	22	19	10	10	23	2.27	0.54	0.01	0.01	0.1
2.5	2.5	2.1	87	5	28	13	29	10	10	14	6.14	0.08	0.01	0.005	0.05
32	2.5	4.13	1185	5	66	22	21	10	10	34	2.38	0.65	0.01	0.01	0.11
76	2.5	3.51	978	5	45	30	22	10	10	26	2.85	0.71	0.03	0.005	0.07
27	2.5	2.94	948	5	47	18	16	10	10	33	1.66	0.56	0.03	0.01	0.09
27	2.5	4.07	892	5	38	33	22	10	10	30	2.58	0.54	0.01	0.005	0.06
32	2.5	4.36	1027	5	55	31	20	10	10	32	2.33	0.65	0.005	0.005	0.09
28	2.5	4.02	767	5	43	28	19	10	10	19	2.22	0.58	0.005	0.005	0.08
42	2.5	3.69	834	5	56	28	18	10	10	43	2.01	0.62	0.005	0.01	0.08
45	2.5	4.1	671	5	39	29	21	10	10	22	2.44	0.5	0.005	0.005	0.06
22	2.5	3.52	720	5	44	27	18	10	10	22	2.13	0.54	0.005	0.005	0.07
12	2.5	2.39	644	5	33	20	14	10	10	22	1.67	0.44	0.01	0.005	0.05
30	2.5	3.63	722	5	31	26	18	10	10	17	1.89	0.53	0.01	0.005	0.06
16	2.5	2.58	587	5	36	21	15	10	10	21	1.89	0.42	0.01	0.005	0.06
15	2.5	1.82	417	5	19	14	12	10	10	14	1.77	0.25	0.01	0.005	0.03
54	2.5	5.4	512	5	25	22	16	10	10	19	1.63	0.39	0.005	0.005	0.04
35	2.5	4.58	510	5	25	29	19	10	10	23	2.37	0.49	0.005	0.005	0.04
31	2.5	3.07	465	5	23	20	15	10	10	18	1.59	0.38	0.005	0.005	0.05
55	2.5	4.92	849	5	44	23	20	10	10	27	2.1	0.47	0.01	0.005	0.07
16	2.5	2.26	637	5	24	16	11	10	10	22	1.47	0.36	0.005	0.005	0.04
11	2.5	1.84	525	5	21	15	12	10	10	17	1.38	0.3	0.005	0.005	0.03
11	2.5	2.3	532	5	26	16	13	10	10	25	1.59	0.32	0.01	0.005	0.03
15	2.5	2.26	547	5	29	16	14	10	10	21	1.59	0.35	0.005	0.005	0.04
16	2.5	3.14	936	5	41	23	18	10	10	32	1.87	0.55	0.02	0.005	0.08
22	2.5	2.95	627	5	28	23	17	10	10	24	1.95	0.49	0.02	0.005	0.04

B-4 Till geochemical results

Sr-ppm	Y-ppm	Ga-ppm	Li-ppm	Nb-ppm	Sc-ppm	Ta-ppm	Ti-pct	Zr-ppm	S-pct
5	6	4	53	0.5	2.5	5	0.042	14	0.005
5	5	3	57	0.5	2.5	5	0.035	12	0.02
6	5	3	61	0.5	2.5	5	0.041	12	0.02
4	5	4	67	0.5	2.5	5	0.041	14	0.02
5	5	3	65	0.5	2.5	5	0.044	11	0.02
5	5	3	56	0.5	2.5	5	0.038	10	0.03
3	6	2	39	0.5	2.5	5	0.052	5	0.01
6	5	2	39	0.5	2.5	5	0.049	5	0.02
3	4	14	37	3	2.5	5	0.053	4	0.1
10	7	2	43	0.5	2.5	5	0.058	13	0.05
3	8	3	47	1	2.5	5	0.127	8	0.02
14	6	1	36	0.5	2.5	5	0.069	9	0.06
7	6	3	52	2	2.5	5	0.034	7	0.04
11	5	1	50	0.5	2.5	5	0.046	13	0.08
5	4	2	42	1	2.5	5	0.046	12	0.03
15	7	1	45	1	2.5	5	0.038	12	0.1
5	5	1	42	1	2.5	5	0.031	7	0.03
7	4	1	39	1	2.5	5	0.038	7	0.03
6	4	1	32	0.5	2.5	5	0.046	5	0.005
4	4	1	39	0.5	2.5	5	0.036	6	0.02
4	4	1	32	1	2.5	5	0.038	5	0.01
1	4	1	22	1	2.5	5	0.053	6	0.02
3	5	1	29	0.5	2.5	5	0.044	7	0.03
4	4	1	40	1	2.5	5	0.033	11	0.02
3	4	1	29	0.5	2.5	5	0.051	8	0.02
6	6	1	36	0.5	2.5	5	0.055	5	0.03
6	4	1	25	0.5	2.5	5	0.052	5	0.03
3	4	1	23	1	2.5	5	0.052	4	0.01
6	5	1	28	2	2.5	5	0.03	2	0.02
4	4	1	28	0.5	2.5	5	0.047	4	0.02
10	7	1	43	0.5	2.5	5	0.049	10	0.02
3	6	1	35	2	2.5	5	0.069	6	0.01

Figure B-5 Hand plotted log probability graph

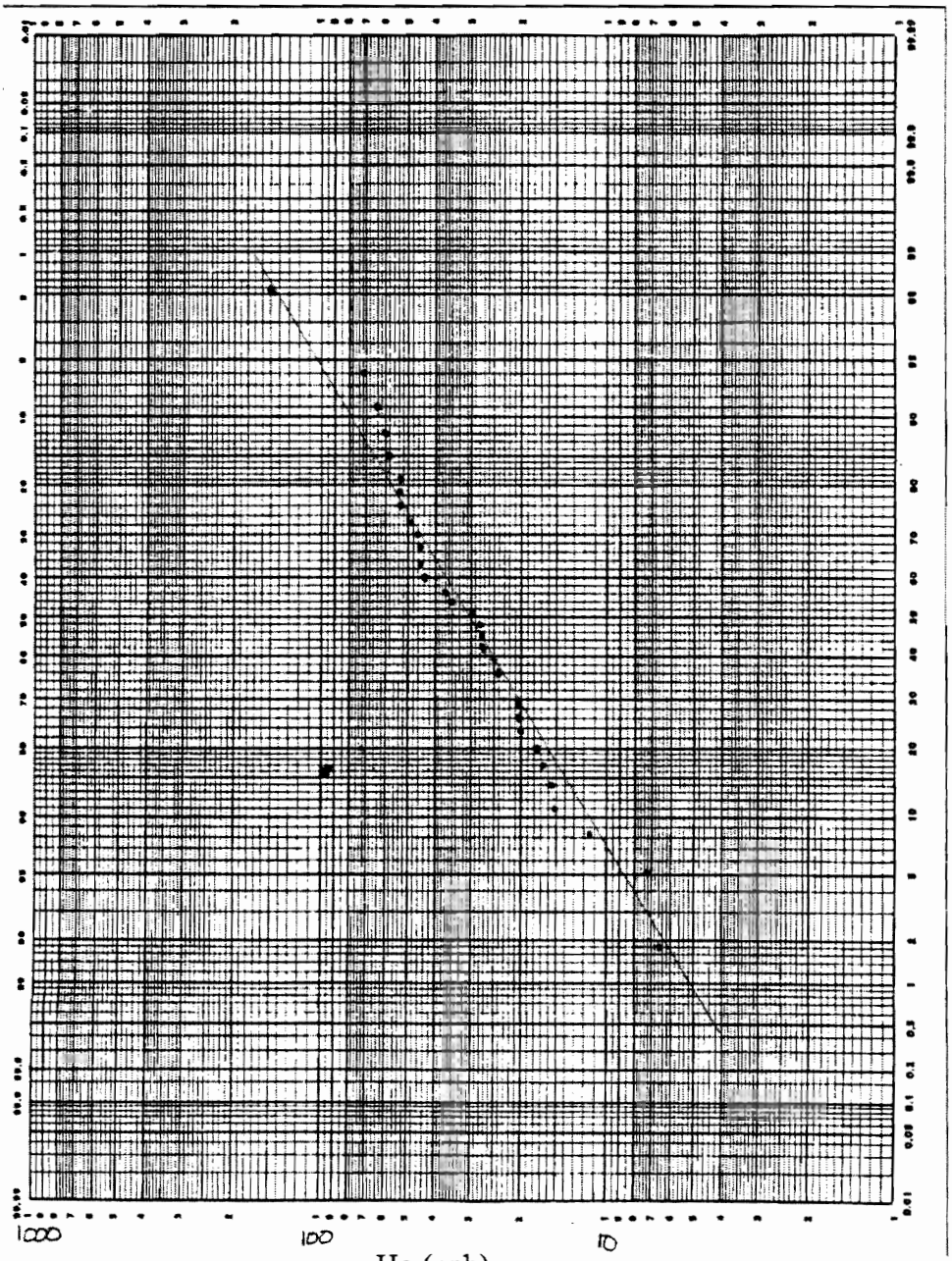

Figure B-6 Rock sample descriptions

ROCK SAMPLE SHEET

PROJECT PROPERTY:Kejimkujik National Park **CO-ORD. CONTROL:GPS**
DATE:Au LOCATION:South of Kejimkujik National Park **GPS MODEL:GARMIN 12**
SAMPLE MAP SHEET:21A/06 **Sample Tool: rock hammer, shovel**
SAMPLER:Belinda Culgin

SAMPLE	utm-E27	utm-N27	Hg_ppb	Magline #	Station #	Rock Typ	Comments
TG2001-1	327719	4906675	2.5	1	251	slate	outcrop on road, Mill Road (Coleman Member)
TG2001-2	329207	4908063	2.8	2	236	slate	top of slate pit, Boyle Rd. (Coleman Member)
TG2001-3	329315	4907938	2.9	2	223	slate	bottom of slate pit, Boyle Rd. (Coleman Member)
TG2001-4	331052	4905722	2.8	2	1	greywack	beside gwke subcrop, Hemlock Hill Rd. (Goldenville)
TG2001-5	330072	4908890	2.5	3	42	slate	slate outcrop in road, Grassy Lake Rd. (Coleman Member)
TG2001-6	330162	4908828	0.2	3	51	slate	roadside slate outcrop, Grassy Lake Rd (Coleman Member)
TG2001-7	330211	4908799	1.9	3	56	slate	roadside slate outcrop at intersection of Delory Rd. & Grassy Lk Rd (Coleman Member)
TG2001-8	331016	4908260	2.3	3	132	slate	roadside slate outcrop on Grassy Lake Rd (Cunard Member)
TG2001-9	331059	4908179	3.4	3	139	slate	roadside slate outcrop on Grassy Lake Rd (Cunard Member)

Figure B-7 Rock geochemical results

Rock Samples												
Sample#	utm-E27	utm-N27	Hg-ppb	AU	Ag	Cu	Pb	Zn	Mo	Ni	Co	Cd
TG-2001-1	327719	4906675	2.5	2	-0.2	17	7	44	2	4	7	-0.2
TG-2001-2	329207	4908063	2.8	1	-0.2	17	4	78	1	13	11	0.2
TG-2001-3	329315	4907938	2.9	1	-0.2	9	-2	74	1	23	13	0.2
TG-2001-4	331052	4905722	2.8	2	-0.2	13	4	34	1	22	10	-0.2
TG-2001-5	330072	4908890	2.5	1	-0.2	14	5	71	-1	22	13	-0.2
TG-2001-6	330162	4908828	0.2	1	-0.2	9	2	86	2	26	18	-0.2
TG-2001-7	330211	4908799	1.9	1	-0.2	15	3	77	-1	29	16	-0.2
TG-2001-8	331016	4908260	2.3	2	-0.2	19	12	47	5	9	8	0.3
TG-2001-9	331059	4908179	3.4	1	-0.2	16	8	53	6	12	11	-0.2

Bi	As	Sb	Fe	Mn	Te	Ba	Cr	V	Sn	W	La	Al
-5	-5	-5	4.35	320	-10	23	35	16	-20	-20	14	1.48
-5	15	-5	5.82	2346	-10	29	38	22	-20	-20	19	2.71
-5	7	-5	5.02	1546	-10	21	36	18	-20	-20	27	2.62
-5	-5	-5	3.12	507	-10	49	47	30	-20	-20	21	1.41
-5	8	-5	4.81	875	-10	20	36	18	-20	-20	40	2.26
-5	6	-5	5.73	1607	-10	16	35	20	-20	-20	49	2.74
-5	10	-5	5.12	1414	-10	23	35	18	-20	-20	63	2.53
-5	30	-5	3.73	264	-10	31	32	17	-20	-20	12	1.78
-5	14	-5	4.31	559	-10	32	38	19	-20	-20	23	1.94

Mg	Ca	Na	K	Sr	Y	Ga	Li	Nb	Sc	Ta	Tl	Zr	S
0.71	0.01	0.04	0.09	7	7	-2	42	-1	-5	-10	-0.01	18	0.03
1	0.03	0.03	0.13	8	6	3	68	-1	-5	-10	0.044	22	0.01
0.97	0.07	0.03	0.1	6	7	-2	81	-1	-5	-10	0.034	22	0.01
0.59	0.25	0.02	0.31	28	9	-2	26	2	-5	-10	0.121	3	-0.01
0.81	0.03	0.03	0.09	6	7	-2	65	-1	-5	-10	0.031	20	0.01
1.02	0.05	0.02	0.08	6	7	3	83	-1	-5	-10	0.033	25	-0.01
0.87	0.02	0.03	0.11	11	9	-2	77	-1	-5	-10	0.028	18	-0.01
0.89	-0.01	0.04	0.12	7	5	-2	56	-1	-5	-10	-0.01	18	0.44
0.87	0.01	0.05	0.12	10	10	-2	58	-1	-5	-10	-0.01	19	0.55

Figure B-8 Polished thin section descriptions

Rock Descriptions									
Sample #	utm-E27	utm-N27	Hg	ock Typ	Pyrite	Pyrrhotit	Marcasite	halcopyri	Notes
1	327719	4906675	2.5						Layering have ilmenite grains and other unidentifiable grains; Fluid has moved along fractures
2	329207	4908063	2.8						sulphides corroded; < 1 % visible along fractures; in association with ilmenite.
3	329315	4907938	2.9						
4	331052	4905722	2.8						
5	330072	4908890	2.5						
6	330162	4908828	0.2						
7	330211	4908799	1.9						
8	331016	4908260	2.3		C	C		R	Pyrite and marcasite (?) grains are in close relation to each other
9	331059	4908179	3.4		C	VR	C ?	VR	marcasite corroded with brownish-yellow mottled appearance
									Pyrite grains well structured, definite shape
Codes									Pyrrhotite grains blob shaped, holes, light yellow to bronze; chalcopyrite within grains darker yellow
VR = < 0.5 %									sulphides seemed to be associated with lighter coloured coarser grained layers.
R = < 1%									need XRD to identify marcasite
C = < 2 %									
A = < 5 %									